2021

Research on Advanced Control Strategies for Vehicle Active Seat Suspension Systems

Wenxing Li

UNIVERSITY
OF WOLLONGONG
AUSTRALIA

Research on Advanced Control Strategies for Vehicle Active Seat Suspension Systems

Wenxing Li

This thesis is presented as part of the requirements for the conferral of the degree:

PhD of Automation and Control Engineering

Supervisor:
Professor Haiping Du

Co-supervisor:
Professor Weihua Li

The University of Wollongong
School of Electrical, Computer and Telecommunications Engineering

05, 2021

This research has been conducted with the support of an Australian Government Research Training Program Scholarship.

Declaration

I, *Wenxing Li*, declare that this thesis is submitted in partial fulfilment of the requirements for the conferral of the degree *PhD of Automation and Control Engineering*, from the University of Wollongong, is wholly my own work unless otherwise referenced or acknowledged. This document has not been submitted for qualifications at any other academic institution.

Wenxing Li

May 12, 2021

Abstract

Vehicle seat suspensions play a very important role in vibration reduction for vehicle drivers, especially for some heavy vehicles. Compared with small vehicles, these heavy vehicle drivers suffer much more from vibrations, which influence driving comfort and may cause health problems, so seat suspensions are necessary for those heavy vehicle drivers to reduce vibrations and improve driving comfort. Advanced control systems and control strategies are investigated for vehicle seat suspensions in this project. Firstly, for an active single-degree of freedom (single-DOF) seat suspension, a singular system-based approach for active vibration control of vehicle seat suspensions is proposed, where the drivers' acceleration is augmented into the conventional seat suspension model together with seat suspension deflection and relative velocity as system states to make the suspension model as a singular system. Then, an event-triggered H_∞ controller is designed for an active seat suspension, where both the continuous and discrete-time event-triggered schemes are considered, respectively. The proposed control method can reduce the workload of data transmission of the seat suspension system and work as a filter to remove the effect of noise, so it can decrease the precision requirement of the actuator, which can help to reduce the cost of the seat suspension. For complicated seat suspension systems, a singular active seat suspension system with a human body model is also established and an output-feedback event-triggered H_∞ controller is designed. The accelerations of each part are considered as part of the system states, which makes the system a singular system. The seat suspension deflection, relative velocity, the accelerations of the seat frame, body torso, and head are defined as the system outputs. At last, to deal with whole-body vibration, a control system and a robust H_∞ control strategy are designed for a 2-DOF seat suspension system. Two H_∞ controllers are designed to reduce vertical and rotational vibrations simultaneously. All the proposed seat suspension systems and control methods are verified by simulations and some are also tested by experiments. These simulation and experimental results show their effectiveness and advantages of the proposed methods to improve the driving comfort and some can reduce the workload of data transmission.

Publications

Journal

Li, Wenxing, Du, Haiping, Feng, Zhiguang, Ning, Donghong, Li, Weihua, Sun, Shuaishuai, Wei, Jumei. (2020). Singular System-Based Approach for Active Vibration Control of Vehicle Seat Suspension. *Journal of Dynamic Systems, Measurement, and Control*, 142(9). (Chapter 3)

Li, Wenxing, Du, Haiping, Ning, Donghong, Li, Weihua, Sun, Shuaishuai, Wei, Jumei. (2021) Event-triggered H_∞ control for active seat suspension systems based on relaxed conditions for stability. *Mechanical Systems and Signal Processing*, 149, 107210, DOI: 10.1016/j.ymssp.2020.107210. (Chapter 4)

Ning, Donghong, Sun, Shuaishuai, Du, Haiping, Li, Weihua, **Li, Wenxing** (2018). Control of a multiple-DOF vehicle seat suspension with roll and vertical vibration. *Journal of Sound and Vibration*, 435, 170-191.

Tu, Lixin, Ning, Donghong, Sun, Shuaishuai, **Li, Wenxing**, Huang, Hua, Dong, Mingming, Du, Haiping. (2020). A novel negative stiffness magnetic spring design for vehicle seat suspension system. *Mechatronics*, 68, 102370.

Tu, Lixin, Du, Haiping, Dong, Mingming, Ning, Donghong, Wu, Yang, **Li, Wenxing**, Huang, Hua. (2020). Semi-actively Controllable Vehicle Seat Suspension System with Negative Stiffness Magnetic Spring. *IEEE/ASME Transactions on Mechatronics*, 2020, DOI: 10.1109/TMECH.2020.3006619.

Li, Wenxing, Wei, Jumei, Du, Haiping, Ning, Donghong, Li, Weihua, Zhu, Xunlin. Event-triggered H_∞ control for active seat suspension systems with state delay. *Transactions of the Institute of Measurement and Control*, under review, 2020. (Chapter 5)

Li, Wenxing, Du, Haiping, Feng, Zhiguang, Ning, Donghong, Li, Weihua. Dynamic output-feedback event-triggered H_∞ control for singular active seat suspension systems with a human body model. *IET Control Theory & Applications*, 2020, DOI: 10.1049/cth2.12064. (Chapter 6)

Conference

Li, Wenxing, Du, Haiping, Ning, Donghong, Li, Weihua. (2019). Robust adaptive sliding mode PI control for active vehicle seat suspension systems. *In 2019 Chinese Control And Decision Conference (CCDC)*. IEEE, 2019: 5403-5408.

Acknowledgements

First of all, I want to express my sincere thanks and appreciation to my supervisor, Prof. Haiping Du, who always provides his inspirational guidance and a great help to me during my whole PhD career. At the beginning of my research work, I met a lot of difficulties because of different working circumstances and some culture shock in Australia. The PhD research work to me was like the Himalayas, the highest peak in the world, of which I could never climb to the top. My supervisor always encourages me and gives me much useful advice, which gives me the confidence to pursue my PhD degree. Whenever I met a challenging problem, he could provide some possible solutions or some innovative ideas quickly like a lighthouse to my voyage. His extensive knowledge and serious responsible work attitude have had a very positive impact on me and will also benefit me in the future.

I also want to thank my co-supervisor, Prof. Weihua Li, who is very kind and considerate to me. I would like to thank visiting scholars, Zhiguang Feng and Jumei Wei, who offered me some creative ideas and a great help to finish some journal papers. Special thanks are extended to my colleagues and friends, Donghong Ning and Shuaishuai Sun, who are excellent researchers and gave me a lot of precious comments and suggestions, and helped me a lot to learn some lab equipment/software and do experiments. I also want to express my gratitude to all my colleagues and friends, Huan Zhang, Wenfei Li, Lei Deng, Lixin Tu, Chao Huang, Qianbin Zhao, Dan Yuan, and Boyuan Li for your help and our great research time together. I also appreciate the help of the UOW staff in the workshop and the IT department who gave me a lot of help to deal with hardware and software problems and guarantee the safety of the Lab.

I also want to thank China Scholarship Council and University of Wollongong, which provided me a united scholarship to cover my tuition and living fees, so I got this great chance to pursue my PhD degree in Australia without worrying about financial issues.

Last but not the least, I want to thank my parents and other family members, who care about me a lot despite the far distance between us. They stand by me no matter what happens, which greatly comforts me when I feel upset.

Contents

List of Tables

List of Figures

List of Abbreviations and Notations

S-DOF	single degree of freedom
M-DOF	multiple degrees of freedom
2-DOF	two degrees of freedom
DOF	degree(s) of freedom
GA	genetic algorithm
WBV	whole body vibration
CCL	cone complementarity linearization
LMI	linear matrix inequality
RMS	root mean square
FWRMS	frequency-weighted root mean square
SEAT	seat effective amplitude transmissibility
ISO 2631-1	international standard to evaluate human exposure to whole-body vibration
I	identity matrix of appropriate dimensions
$*$	symmetric index in a symmetric matrix
$\mathrm{sym}(A)$	$A+A^T$
$\mathrm{diag}\{...\}$	diagonal matrix
$\mathbf{R}$	real number
$\mathbf{N}$	natural number
$\mathbf{R}^{m\times n}$	set of $m\times n$ real matrices

Chapter 1

Introduction

1.1 Background and Motivation

Vibrations of vehicles, caused by rough road surfaces or vehicle operations, are harmful to vehicle drivers, which may influence the vehicle operators' driving comfort, fatigue, health, and safety. Such vibrations are even severer for heavy vehicle drivers, such as drivers of trucks, buses, vans, agricultural vehicles, mining vehicles, and industrial vehicles, because these heavy vehicles with large masses, always face harsh working circumstances or special operations. In general, tires and vehicle suspensions are capable to isolate the most common vibrations for light vehicles, like cars, because of their small masses and relatively better running road surfaces. However, for most heavy vehicles, seat suspensions are necessary to reduce vibrations and improve driving comfort for drivers.

Generally, there are three main types of seat suspensions: passive, semi-active, and active seat suspensions. Passive seat suspensions have the simplest structures and the lowest cost, but they have a very limited performance to reduce vibrations. Semi-active seat suspensions have better performance to reduce vibrations with small energy cost, but their control performance has many constraints. Active seat suspensions have the best control performance among the three types of seat suspensions, but they also consume much more energy. There are both advantages and disadvantages of these three types of seat suspensions, but this study mainly focuses on the active seat suspensions to achieve better control performance to reduce vibration and improve driving comfort.

There have been many research outcomes of the study of active seat suspensions during the past decades. Drivers' accelerations have a close relationship with the driving comfort, but in most previous seat suspension studies, this signal is not directly applied in modeling the seat suspension system or designing controllers, while the acceleration signal can be easily measured in real time by acceleration sensors. This motivates the author to design a seat suspension system and controllers by considering the acceleration signals.

With the fast development of network communication and big data analysis technol-

ogy, network control methods have been applied in many areas, such as intelligent transportation systems, smart homes, autonomous driving technology, etc. The application of network control in active seat suspension control also gains the author's interest.

Most of the previous active seat suspension research focuses on vertical vibrations because it is easy to design seat suspension model systems and control strategies with one degree of freedom (vertical direction). However, the actual vibrations are not only from the vertical direction but also from the lateral direction and rotational directions. Besides, the human body is also a very complicated system, so the design of the seat suspension system with a human body and the whole body vibration are good research topics for the study of active seat suspensions.

Overall, there are a lot of worthy studying issues for active seat suspensions for heavy vehicles. This thesis is motivated to design novel seat suspension systems and control strategies for vehicle seat suspension systems to better reduce drivers' vibration and improve their driving comfort.

1.2 Research Objectives

The main aim of this thesis is to design novel seat suspension systems and controllers for heavy vehicle seat suspension systems to reduce drivers' vibrations and improve driving comfort. Some simulations and experimental tests are done to validate the effectiveness of the proposed methods.

Some specific objectives of this thesis are listed as follows:

1. A novel singular active seat suspension and an H_∞ controller are designed for an active seat suspension system with a time-delay actuator.

2. Network could control is applied to seat suspension systems based on continuous and discrete event-triggered scheme, which can reduce both drivers' vibration and the workload of data transmission.

3. A dynamic output-feedback event-triggered H_∞ controller is designed for a singular active seat suspension system with a human body model.

4. A two-DOF seat suspension system is established and the H_∞ control strategy is designed for this system to reduce both vertical and rotational vibrations.

1.3 Thesis Outline

The thesis outline is listed as follows:

Chapter 1 introduces the background and motivation, research objectives, and thesis outline of this research.

Chapter 2 gives a literature review of previous studies of seat suspensions, including the simple introduction of three main types of seat suspension, their advantages and disadvantages, control strategies, and future direction of development.

In Chapter 3, a novel singular active seat suspension system is established where the acceleration signal is considered as one of the system states. All state variables are measurable in real time, so it is more practical for industrial application.

In Chapter 4, an H_∞ controller based on a continuous event-triggered scheme is designed for active seat suspension systems, which can reduce the data transmission load and drivers' vibration simultaneously.

In Chapter 5, a discrete event-triggered H_∞ controller is designed for active seat suspension systems, which is more practical to deal with the issues of the discrete-time data collection and control input with time delay.

In Chapter 6, a novel singular active seat suspension system with a human body in the loop is built and a dynamic output-feedback event-triggered H_∞ controller is designed for this system.

In Chapter 7, a 2-DOF seat suspension system is established to deal with the whole body vibration, and two H_∞ controllers are designed to reduce vertical and rotational vibrations.

Chapter 8 concludes the main contributions of this thesis and discusses some possible future research work.

Chapter 2

Literature Review

2.1 Introduction

The previous chapter gives some introduction to this thesis, which briefly describes the background of the seat suspensions and what motivates the author to do some research about active seat suspensions. The research objectives and thesis outlines are also given to show the aim of this research and the structure of this thesis. In this chapter, some literature reviews about the vehicle or seat suspensions are presented to realize the development of seat suspensions and the present research issues.

Vehicle vibrations, caused by uneven road surfaces or other disturbances, damage not only vehicles and cargos but also the health of drivers and passengers [1]. Suspension systems are one of the important parts of the vehicles, which can protect the vehicle and cargos from damage and improve drivers' comfort [2]. The vehicle suspension comprises tires, tire air, dampers, springs, linkages, and sensors. In the past decades, a lot of research has been done to improve the performance of vehicle suspensions and many good results have come out. However, the heavy vehicle drivers, such as truck, SUV, crane, agricultural vehicle drivers, still suffer a lot from vehicle vibrations [3]. And some industrial vehicles often do some special work digging, dumping, shoveling, excavating or loading, etc. The vibrations of those heavy vehicles are much more severe than light cars because of their large masses or special working operation and situations [4]. Therefore, a seat suspension is necessary for those heavy vehicles to improve driving comfort. Moreover, many research results of the vehicle suspensions can be used in the research of seat suspensions, because the mechanical structures of those two types of suspension are very similar.

Figure 2.1 shows some seat suspension products from different companies. The exterior design of these seat suspensions is different, but their mechanism principles have many similarities. According to their structure and working methods, there are three main types of seat suspensions: passive seat suspensions, semi-active seat suspensions, and ac-

Figure 2.1: Some seat suspension products

tive seat suspensions [5]. Passive seat suspensions are the simplest and cheapest because they only contain springs and dampers. The springs and dampers have fixed parameters, which makes them only suitable for certain disturbances [6]. Most research about passive seat suspension concentrates on the optimization of spring stiffness and damper coefficients. Semi-active seat suspensions are one kind of controllable seat suspension because they contain controllable dampers which can adjust coefficients of dampers according to external disturbances [7]. Therefore, semi-active seat suspensions can improve smooth and stable driving performance for drivers compared with passive seat suspensions. They have simple structures, low cost, and good performance, but most time the output forces of controllable dampers are nonlinear and constrained, so it is not easy to control them. The main research topics of semi-active seat suspension are to design better controllable dampers and reduce the energy cost. Generally, active seat suspensions have the best control performance among the three types of seat suspensions, because active suspensions have an additional control force device (actuator). The input force of the actuator can be changed online to make seat suspension systems always stay in optimum vibration reduction state with fewer constraints. However, active seat suspensions also consume more power [8]. The main research topics of active seat suspensions are to design better control strategies.

In the past decades, most researchers have paid their effect to investigate seat suspensions only for vertical (single-degree-of-freedom, S-DOF) vibration control, but there are

still a few researchers who consider the vibrations from other directions, such as rotational vibrations [9, 10]. Some previous research results of three types of seat suspensions and multiple-degrees-of-freedom (M-DOF) seat suspensions are presented to show the research history and directions of seat suspensions in the following sections.

2.2 Passive seat suspension

Springs were firstly used in suspension systems to reduce vibration and still play an important role in suspension systems now. In general, springs are chosen according to the vehicles' mass where the upper limited weight of vehicles equals approximately the spring stiffness multiplying its maximum deflection [11]. If the springs are selected irrelevantly (too hard or too soft), suspensions become invalid or even causing oscillation, which will be harmful to vehicles and drivers.

Dampers are a kind of device to provide kinetic resistance and dissipate kinetic energy into thermal energy. The characteristics of dampers are beneficial to oscillation attenuation, so they are widely used in suspension systems. Dampers can absorb vibration energy from vibration systems and damper force is generally in direct proportion to velocities of vibration systems.

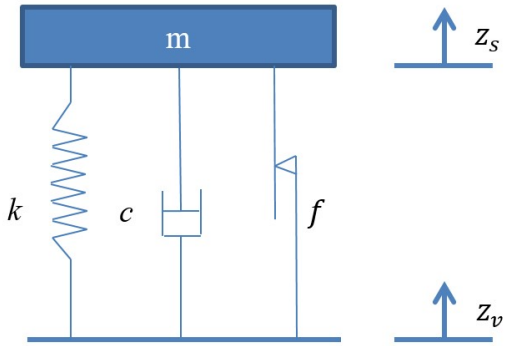

Figure 2.2: Passive seat suspension model

Passive seat suspensions are the most conventional seat suspensions, which mainly contain springs and dampers. A passive seat suspension model is shown in Figure 2.2. According to Newton's Second Law, the dynamic equation of the passive seat suspension system can be written as

$$m\ddot{z}_s + k(z_s - z_v) + c(\dot{z}_s - \dot{z}_v) + f = 0 \tag{2.1}$$

where z_s and z_v are the suspension upper and base displacement, respectively; m is the sprung mass including the masses of a driver's body, cushion, and seat suspension top

platform; k and c are constants representing the spring stiffness and the damping coefficient, respectively; f denotes the internal resistant force like friction, which is often ignored in some theoretical research papers, but in practical or experimental situations, it should be taken into consideration.

Most of the passive seat suspension research focuses on the optimization of damping coefficients c and springs stiffness k without external inputs. An optimal vehicle and seat suspension are designed by using Genetic Algorithm (GA) in [12] to select the best pattern of the spring stiffness and the damping coefficient. Negative-stiffness structures are designed and investigated in [13, 14] for passive seat suspension to isolate the effectiveness from disturbance of low excitation frequencies. Passive seat suspensions have easy structures and don't need a power source, which makes them suitable for vehicle seats with low cost and low demand to isolate vibrations. However, because of their characteristics, passive seat suspensions can only deal with vibrations from particular road disturbances. For various road circumstances, the performance of passive seat suspension is not good enough, so semi-active and active seat suspensions are investigated by many researchers.

2.3 Semi-active seat suspension

Semi-active seat suspensions are one kind of controllable seat suspensions, which are able to adjust coefficients of dampers according to road surface conditions and vehicle body posture perceived by sensors, in order to improve the smooth and stable driving performance of vehicles [15]. Semi-active seat suspensions can change damper coefficients or spring stiffness based on practical situations. Because of simple structures, low cost, and good performance, semi-active seat suspensions have extensive application prospects. A semi-active seat suspension model is shown in Figure 2.3. The dynamic equation of the semi-active seat suspension system can be written as

$$m\ddot{z}_s + F_k + F_c + f = 0 \tag{2.2}$$

where m and f are defined the same as equation (2.1); F_k is the output controllable force of the adjustable spring; F_c is the output controllable force of the adjustable damper.

For the damper coefficients changing semi-active seat suspension, there are two main types: switchable and continuously adjustable seat suspensions as shown in Figure 2.4. Switchable damping seat suspensions are commonly set up 2-3 levels. Damping coefficients can switch among several levels quickly according to relative and absolute velocities of seats. Damping coefficients of continuously adjustable seat suspensions are able to change continuously in a certain range. There are two basic implementations of continuously adjustable suspensions. One is aperture setting by adjusting the area of damper throttle valves to change damping coefficients, which is realized by electromag-

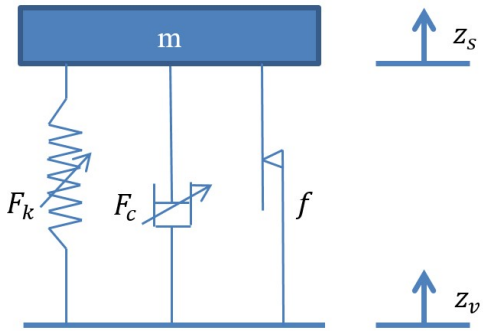

Figure 2.3: Semi-active seat suspension model

netic valves or other similar electromechanical drive valves. The other is electrorheological (ER) or magnetorheological (MR) adjustable damping seat suspensions, which can change damping coefficients by changing electric or magnetic field intensity. The main research topic of semi-active seat suspensions is to design better adjustable dampers.

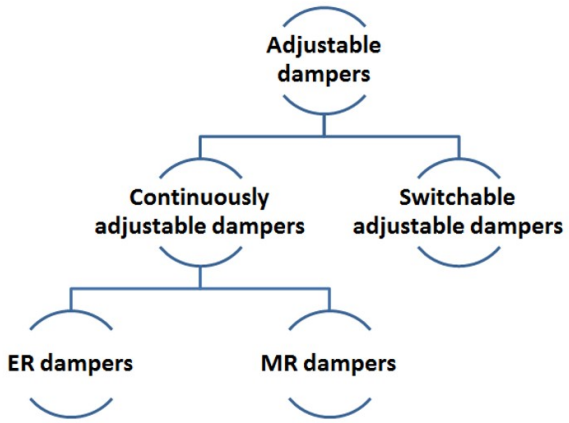

Figure 2.4: The main types of adjustable dampers for semi-active seat suspension systems

Many control methods have been proposed since semi-active seat suspensions were presented, such as skyhook algorithm [7], acceleration-driven damping, fuzzy control, and sliding mode control, etc, according to driving conditions of vehicles (such as road conditions and motion state of vehicles) in order to make seat suspension systems always stay in optimum vibration reduction state. Seung-Bok Choi is one outstanding semi-active seat suspension researcher who designed some kinds of magneto-rheological dampers [16–18] and electrorheological dampers [19] for semi-active seat suspensions, and developed many good control methods for these suspensions for vibration control, such as skyhook controller [19], sliding mode controller [20], fuzzy sliding mode controller [21], adaptive sliding mode controller [22], adaptive fuzzy sliding- mode controller [23, 24], etc.

2.4 Active seat suspension

Active seat suspensions are based on passive seat suspensions (elastic component, shock absorber, guide mechanism) by attaching an additional control force device [25]. It consists of springs, dampers, actuators, measuring system, feedback control system, and energy system as shown in Figure 2.5. The function of an actuator is to execute the command of the control system, which generally is a force or torque generator, such as hydraulic cylinder, air cylinder, servo motor, electromagnet, etc. The function of measuring systems, including various sensors, is to measure system states and provide a basis for control systems [26]. The function of control systems, whose core component is a computer, is to process data and issue various control instructions. The function of energy systems is to provide energy for the above systems. Active seat suspensions have many advantages over passive seat suspensions, such as controlling the height of the driver's body, improving passing ability and riding comfort [27]. Therefore, many researchers have done a lot of work to investigate active seat suspensions and many control strategies have been put forward to improve the performance of active seat suspensions.

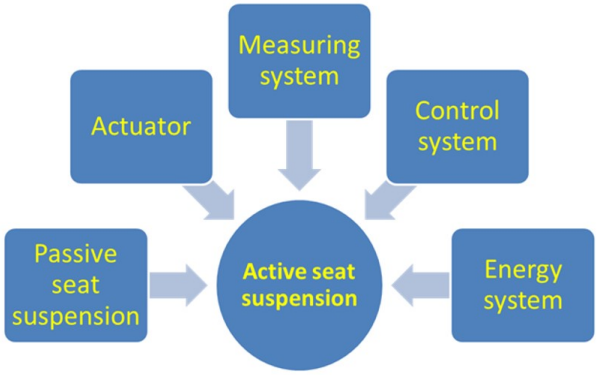

Figure 2.5: The main components of active seat suspension systems systems

The model of the active seat suspension is shown in Figure 2.6 and the dynamic equation of the active seat suspension system can be written as follows.

$$m\ddot{z}_s + k(z_s - z_v) + c(\dot{z}_s - \dot{z}_v) + u + f = 0 \tag{2.3}$$

where m, k, c, z_s, z_v, and f are defined the same as equation (2.1); u is the output force of the actuator whose value is defined by the controller.

Actuators and control strategies are the two main parts of active suspensions [28]. Actuators output control force according to control strategies, so selecting a proper control strategy is the key to the design of active seat suspensions to provide good driving comfort for drivers [29].

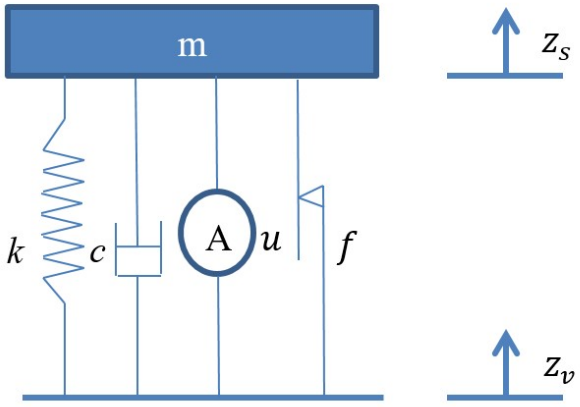

Figure 2.6: Active seat suspension model

2.5 Some control strategies for seat suspensions

Semi-active and active seat suspensions are both controllable seat suspensions. The performance of these two types of seat suspension systems can be adjusted appropriately according to the actual situation so that a better vibration absorption effect can be achieved. Therefore, the research of the control strategies for these controllable seat suspensions has become a hot topic for many seat suspension researchers. In this section, some commonly used control methods for suspensions are introduced and the advantages and disadvantages of these methods are discussed.

2.5.1 Optimal control

Optimal control theory has been applied in the research of suspension systems since the 1960s. A resultant frequency-shaping optimal control is used to design an active seat suspension controller in order to improve ride comfort in [30]. Linear quadratic regulator controller and linear quadratic Gaussian controller are designed in [31] and [32] for vehicle suspensions. The optimal control method can greatly improve the performance of seat suspensions and have a large stability margin, but the active seat suspension based on optimal control is not robust to the model perturbation. It's also difficult for the optimal control theory to tackle the vibration reduction problem in the frequency domain.

2.5.2 Adaptive control

Adaptive control is a real-time control method whose research subjects are systems with limited uncertainty like some unknown or random factors [33]. In the design of the active seat suspension system, adaptive control is able to detect the change of the system parameters and adjust the control strategies in real time in order to make the system perform better [34]. An adaptation mechanism is used in [35] to recognise the actual suspended

mass which can improve the performance of vibration isolation of the active seat suspension. However, the adaptive control is just suitable for the slow change of the suspension parameters in a limited range [36]. When the suspension system parameters are beyond this specific range or change too fast, the control performance of the system gets worse [27, 28].

2.5.3 Fuzzy control

Fuzzy control is a typical intelligent control method that can mimic human control to some extent [37]. It doesn't need the accurate mathematical model but needs a great amount of control experience and knowledge as the main basis [38]. Fuzzy control can be used for seat suspension control to deal with some nonlinear characteristics of the control system [39]. A disturbance observer based on a Takagi-Sugeno (TS) fuzzy controller which is used to consider the variation of driver's weight, is proposed for an active seat suspension to enhance the control performance in [40]. However, many factors of fuzzy control like fuzzy rules, membership functions, fuzzy subsets, and fuzzy inference systems need experts' experience [41]. And in many cases, the experts' experience is incomplete or mutually contradictory [42].

2.5.4 Genetic algorithm

Genetic algorithm (GA) is one kind of evolutionary algorithm, which searches for the optimal solution by imitating the natural selection and genetic mechanism [6]. GA has three basic operators: selection, intersection, and variation. Compared with general iterative operations, GA is effective to deal with the local minimax trap problem and get the global optimal solution. GA control strategy for an active seat suspension is proposed in [43]. Seat suspension with a quarter vehicles model is considered and only the seat suspension has an actuator to output control force.

2.5.5 Robust control

Robust control is a control method to maintain some characteristics of the performance under limited parameters perturbation of the control system [44]. The robust controller is a fixed controller that is obtained from the target design for the robustness of the closed-loop system and robust control aims at dealing with the uncertainties of the control systems by a fixed controller to make the uncertain control objective satisfy the control quality [45]. A robust H_∞ controller with friction compensation is designed for an innovative active seat suspension for heavy-duty vehicles in [46]. However, the robust control is a relatively conventional control method, so the fixed controller cannot achieve the best control effect in the face of different external disturbances [47, 48].

2.5.6 Sliding mode control

Sliding mode control is a kind of nonlinear control method with a discontinuous controller [49]. The structure of the control system is not fixed, which can modify in purpose according to the states of the control system in dynamics in order to force the system to move by the state track of 'sliding mode surface' [50]. A terminal sliding mode controller is designed for an active seat suspension in [51] and disturbance and state observers are proposed for the nonlinear friction and uncertainties in the suspension system. Sliding mode control can deal with the uncertainties of the control systems, but for active seat suspension systems, it needs the absolute displacement signals in real time, which is not possible to measure in practice.

2.5.7 Other control methods

There are many other control strategies for active seat suspensions (like preview control, neural network control). Many researchers may combine two or more of those control methods together to unite the advantages of every control method to get better control performance like [29, 52].

2.6 M-DOF seat suspension

The seat suspension research mentioned before is all about S-DOF vibration control. The study of M-DOF seat suspension is still at an initial stage, just for the structure design of the M-DOF seat suspension. Several papers are also caring about the control of seat suspensions with multiple degrees of freedom like [53–55]. A 4-DOF seat suspension is built on a spherical surface architecture in [56] which can reduce the roll (rotation around X-axis), pitch (rotation around Y-axis), and yaw (rotation around Z-axis) acceleration by gravity, but vertical body acceleration is only partially damped by the vehicle suspension system, so this M-DOF seat suspension is only a passive seat suspension. An active seat suspension with two DOF is designed for military vehicles in [53], which can provide vibration reduction in vertical and lateral directions by a hybrid Skyhook and Groundhook-Principle controller. An innovative two-layer M-DOF seat suspension is proposed in [9] for reducing the whole-body vibration (WBV) of heavy-duty vehicle drivers and a control strategy of roll and vertical vibration of this M-DOF seat suspension is proposed in [10]. However, the research of M-DOF seat suspension control is still little until now and the control strategy for M-DOF seat suspension is not mature, so some control strategies from other research areas like robot control, aircraft posture control may be considered as references.

2.7 Conclusion

Suspension systems are an important part of vehicles, which help to isolate vibration caused by road surface conditions, protect vehicles and cargo from damage, and to improve driving comfort. Among the three main types of seat suspension systems (passive, semi-active, active), passive seat suspensions are the simplest but only suitable for certain disturbances because of their fixed parameters. Semi-active seat suspensions are able to change damper coefficients online and don't need too much power, but the output force has many constraints. Although with high cost, active seat suspensions are able to adjust the output force of actuators online, so they have better control performance than passive and semi-active suspensions. A lot of research has been done to improve the performance of active seat suspension, but most conventional active control methods need the absolute displacement or velocity signals of the seat suspensions in real time, which is not possible to measure in practice. This motivates the author to design novel seat suspension systems and control strategies only based on measurable signals. Besides, most of the previous research results just care about vertical vibrations. Vibrations from other dimensions, like roll, pitch, and yaw rotation, also affect drivers' health a lot, so these vibrations should also be taken into consideration. Therefore, the research of M-DOF seat suspension may become one promising research topic, which also attracts the author's attention. The next chapter introduces a singular system based control strategy for active seat suspensions.

Chapter 3

Singular System Based Control Strategy

3.1 Introduction

The previous chapter introduces some literature review of seat suspension systems. Three main types of seat suspensions and their characteristics are shown and some control strategies for controllable seat suspensions and their advantages/disadvantages are discussed. In this chapter, a novel singular active seat suspension system is established and a H_∞ controller is proposed.

Generally, there are three main types of seat suspensions (passive, semi-active, and active seat suspensions) and active seat suspensions have the best control performance among the three types of seat suspensions [41]. During the past years, a lot of researchers did a lot of work to improve the driving comfort for active seat suspensions [28, 35, 46]. An active seat suspension is designed for heavy-duty vehicles by applying a rotary motor as an actuator and static output feedback H_∞ controller with friction compensation in [46]. Genetic algorithm PID and fuzzy self-tuning PID controllers are designed for active seat suspension systems to improve pregnant women's driving comfort in [57]. However, two main issues make those control methods very difficult for industrial applications [58]. The first one is that most of those control methods need absolute seat displacement and velocity, which cannot be measured in practice. The other one is that drivers' acceleration is often defined as the output of seat suspension systems because it is closely related to driving comfort. However, most controllers of the previous works still use Newton's Second Law to calculate drivers' acceleration, even though it can be measured easily by accelerometers. Because of the uncertainties of the parameters and some other internal disturbance (such as friction), the acceleration calculation is unprecise and unnecessary.

In the aim of solving the above two main issues, singular systems are introduced here to describe seat suspension systems [59]. Different from regular systems, singular systems are a class of systems comprehensively described by differential and algebraic equations [60]. For seat suspension systems, singular systems can substitute acceleration vari-

ables into system state variables and use an algebraic equation to describe the relationship among the state variables by Newton's Second Law. To the authors' best knowledge, a singular system based approach is firstly proposed for active vibration control of vehicle seat suspension. In the singular seat suspension system, the drivers' acceleration, together with the deflection and relative velocity of the seat suspension, is defined as one of the state variables. The deflection can be measured by a laser ranging sensor; the relative velocity can be obtained by calculating the derivation of the deflection signal; the acceleration can be measured by an accelerometer. Therefore, the singular seat suspension system can make full use of all easily measured system signals in practice, which does not lead to a waste of useful data.

Some other issues also affect the control performance of the active seat suspensions, like parameter uncertainties, friction, actuator saturation, and time delay problem [61]. Robust control is one of the most commonly used control methods to deal with uncertainty, which is designed to apply in some situations provided that uncertain parameters or disturbances are found within some set [62]. It can achieve robust performance and stability when bounded modeling errors are present. H_∞ control is one of the most important methods in robust control, which optimizes control index by using the H_∞ norm of the transfer function matrix [63]. In this chapter, to solve parameter uncertainties and friction problems, a friction observer is designed to estimate the friction value in real-time. Then the observed friction value is added into the H_∞ controller to compensate for the friction influence. Time delay is an inevitable problem for actuators because it needs time to deal with data collection, transmission, and computer operation [64, 65]. Time delay value may be little, but neglect of time delay may cause a bad control performance or even make a system unstable, so it is necessary to take the time delay of the actuator into consideration [66]. blueA modified inequality of the inequality in [67] is used as a lemma to deal with the time delay of the actuator and the cone complementarity linearization (CCL) [68] is applied to solve the nonlinear constraints. The actuator saturation problem is also taken into consideration. Then, an H_∞ controller will be designed by using all easily measurable state signals by considering parameter uncertainties, friction, time-delay problems of the input, and actuator saturation.

The main contributions of this chapter can be listed as follows:

1) To the authors' best knowledge, a singular system based approach is firstly proposed in this chapter for active vibration control of vehicle seat suspensions, where the acceleration signal of the seat suspension is also considered as a state variable, together with the deflection and relative velocity. The system output is defined as drivers' acceleration, which will be one of the system states and can be measured by an accelerometer instead of calculating it as previous works.

2) All three state variables are measurable in practice. The proposed H_∞ controller

makes full use of the measurable signals which helps to get better control performance.

3) A friction observer is applied to compensate for the internal disturbance and the actuator saturation is also considered, which helps to get better control performance.

4) The time delay of the actuator is considered in this chapter. A less conservative inequality is applied to reduce the conservatism of the seat suspension system.

3.2 Singular seat suspension system model

An active singular seat suspension model system is shown in Figure 2.6 in Chapter 2 and according to Newton's Second Law, the dynamic equation of the seat suspension system can be denoted as:

$$m\ddot{z}_s(t) + c(\dot{z}_s(t)) - \dot{z}_v(t)) + k(z_s(t)) - z_v(t)) + f_r(t) = u(t) \tag{3.1}$$

where m is the sprung mass; z_s and z_v represent the suspension upper and base displacements, respectively; $\dot{z}_s$ and $\dot{z}_v$ represent the suspension upper and base velocities, respectively; $\ddot{z}_s$ is the body acceleration; k and c are the stiffness and the damping coefficient of the seat suspension, respectively; f_r is the internal friction of the seat suspension; u is the control input.

Define the state variables as follows:

$$x_1 = z_s - z_v, x_2 = \dot{z}_s - \dot{z}_v, x_3 = \ddot{z}_s,$$

where x_1 is the suspension deflection, x_2 is the relative seat velocity. The body acceleration has a close relationship with the ride comfort, so $\ddot{z}_s$ is chosen as one performance output. Define the state vector as $x = \begin{bmatrix} x_1 & x_2 & x_3 \end{bmatrix}^T$ and the disturbance as $\upsilon = \begin{bmatrix} \ddot{z}_v & f_r \end{bmatrix}^T$, so the dynamic equation of the seat suspension system can be rewritten as:

$$\begin{aligned} E\dot{x}(t) &= Ax(t) + Bu(t) + D\upsilon(t), \\ z(t) &= Cx(t), \end{aligned} \tag{3.2}$$

where

$$E = \begin{bmatrix} 1 & 0 & 0 \\ 0 & 1 & 0 \\ 0 & 0 & 0 \end{bmatrix}, A = \begin{bmatrix} 0 & 1 & 0 \\ 0 & 0 & 1 \\ k & c & m \end{bmatrix}, B = \begin{bmatrix} 0 \\ 0 \\ -1 \end{bmatrix}, D = \begin{bmatrix} 0 & 0 \\ -1 & 0 \\ 0 & 1 \end{bmatrix}, C = \begin{bmatrix} 0 \\ 0 \\ 1 \end{bmatrix}^T.$$

If we do not consider the disturbance and control force, the singular seat suspension

system can be written as:

$$E\dot{x}(t) = Ax(t). \tag{3.3}$$

Definition 3.1 *[69, 70]*

1. *The pair* (E,A) *is said to be regular if* $\det(sE-A)$ *is not identically zero, where s is a complex variable.*

2. *The pair* (E,A) *is said to be impulse free if* $\deg(\det(sE-A))=\text{rank}(E)$.

Remark 3.1 *Based on Definition 3.1, the regularity and impulse-freeness of system (3.2) is equivalent to the matrix pair* (E,A)*. If we do not consider the controller, we have*

$$sE-A = \begin{bmatrix} s & -1 & 0 \\ 0 & s & -1 \\ -k & -c & -m \end{bmatrix}.$$

Then we have $\det(sE-A) = -ms^2-cs-k$*, which is not identically zero and* $\deg(\det(sE-A)) = \text{rank}(E)=2$ *since* $m \neq 0$*, so the system (3.11) is regular and impulse free.*

3.3 Friction observer

In equation (3.2), the seat suspension deflection x_1 and the body acceleration x_3 can be measured and observed in real-time by a displacement sensor and an accelerometer. The relative seat velocity x_2 can be obtained by differentiating x_1. However, the internal friction f_r cannot be observed directly, which makes it not easy to design a proper controller. Hence, a friction observer $\hat{f}_r$ is needed to get better control performance.

From equations (3.1) and (3.2), we can get

$$f_r = -kx_1 - cx_2 - mx_3 + u, \tag{3.4}$$

where $f_r \in [f_{r\min}, f_{r\max}]$.

A friction observer is designed as

$$\dot{\hat{f}}_r = l(f_r - \hat{f}_r), \tag{3.5}$$

where $l > 0$. Then, the friction observer error can be defined as

$$e_f = f_r - \hat{f}_r. \tag{3.6}$$

Because the friction value varies slowly compared with the observer dynamics, it is reasonable to assume $\dot{f}_r = 0$. Hence, the derivative of the friction observer error can be

obtained as

$$\dot{e}_f = \dot{f}_r - \dot{\hat{f}}_r = -l(f_r - \hat{f}_r) = -le_f. \tag{3.7}$$

By solving the differential equation (3.7), we can get $e_f = e^{-l(t-t_0)}e(t_0)$. Because $l > 0$, the friction observer error e_f will exponentially converged to zero.

In experimental conditions, we need to use an integrator to calculate the estimated friction in real-time. However, because of the measuring error and computing time delay, it is easy to accumulate the error and get a too large friction value, which will make the seat suspension system have bad control performance or even unstable. To solve this problem, a projecting algorithm is adapted here to bound the estimated friction value and to strengthen the robustness of the seat suspension system. Hence, the friction observer can be modified as follows:

$$\begin{aligned} \dot{\hat{f}}_r =& \text{Proj}_{\hat{f}_r}(l(f_r - \hat{f}_r)), \\ \text{Proj}_{\hat{f}}(\bullet) =& \begin{cases} 0 & \text{if } \hat{f}_r \geq f_{r\max} \text{ and } \dot{\hat{f}}_r > 0 \\ 0 & \text{if } \hat{f}_r \leq f_{r\min} \text{ and } \dot{\hat{f}}_r < 0 \\ \bullet & \text{otherwise} \end{cases} \end{aligned} \tag{3.8}$$

When $\hat{f}_r$ surpasses the maximum (or minimum) value and tends to keeping increasing (or decreasing), set $\hat{f}_r$ unchangeable by setting $\dot{\hat{f}}_r = 0$. Therefore, this projecting algorithm can bound $\hat{f}_r \in [f_{r\min}, f_{r\max}]$, which will reduce observing friction error because of the accumulating error.

Remark 3.2 *The real seat suspension systems are much more complicated than the linear seat suspension system with friction proposed in this chapter. The real friction during the performance of the seat suspension system is unknown (or uncertain) and cannot be obtained in practice, which brings a lot of difficulties when we do the friction compensation. Equation (3.4) can calculate the friction values of the simplified seat suspension system based on data collected at the last moment, while the value of the friction force at this moment is not available, so a friction observer (3.5) is needed to observe the friction in real time. However, this observer works based on the assumption of slowly changing friction ($\dot{f}_r = 0$). The rate at which friction changes cannot be ignored but the friction is also bounded in a limited area, so here we use the projecting algorithm to bound the estimated friction value. This friction observer may not estimate the real friction very well, but it still makes a big difference in the robust control of the seat suspension system.*

3.4 H_∞ controller design

From the above section, we can see that the friction observer can estimate the real friction. Data collection by sensors, data transmission, and computer operation to get the control

force by calculating the measured data cause the time-delay problems for the actuator. Define the time delay of the actuator is $\tau(t)$, where $\tau(t) \in [\tau_m, \tau_M]$ and $\mid \dot{\tau}(t) \mid \leq \bar{\tau}$. In order to get better control performance, the H_∞ controller is designed by considering the friction compensation as the following form:

$$u(t) = Kx(t-\tau(t)) + \hat{f}_r. \tag{3.9}$$

Considering the saturation problem of the actuator, the output of the controller should satisfy the following conditions:

$$\bar{u} = \text{sat}(u) = \begin{cases} -u_{\max}, & \text{if } u \leq -u_{\max}, \\ u, & \text{if } -u_{\max} < u < u_{\max}, \\ u_{\max}, & \text{if } u \geq u_{\max}. \end{cases} \tag{3.10}$$

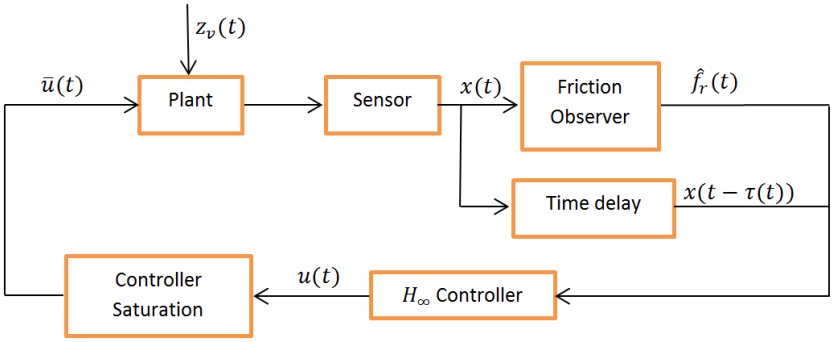

Figure 3.1: Diagram of the active singular seat suspension system

Figure 3.1 shows the working diagram of the active singular seat suspension system with H_∞ controller considering the friction compensation and input time delay. Substituting equation (3.9) into system (3.2), we can get the closed-loop controlled seat suspension system as:

$$\begin{aligned} E\dot{x}(t) &= Ax(t) + BKx(t-\tau(t)) + D\omega(t), \\ z(t) &= Cx(t), \end{aligned} \tag{3.11}$$

where $\omega(t) = \begin{bmatrix} \ddot{z}_v(t) & e_f(t) \end{bmatrix}^T$.

Definition 3.2 *[71]*

1. *The singular delay system (3.11) is said to be regular and impulse free if the pair (E,A) is regular and impulse free.*

2. *The singular delay system (3.11) is said to be stable if for any* $\varepsilon > 0$ *there exists a scalar* $\delta(\varepsilon) > 0$*, such that, for any compatible initial condition* $\phi(t)$ *which satisfies* $\sup_{-\tau(t)<t\leq 0} \| \phi(t) \| \leq \delta(\varepsilon)$*, the solution* $x(t)$ *of system (3.11) satisfies* $\| x(t) \| \leq \varepsilon$*, and a scalar* $\delta > 0$ *can be chosen such that* $\sup_{-\tau(t)<t\leq 0} \| \phi(t) \| \leq \delta$ *implies* $x(t) \to 0$*, when* $t \to \infty$*.*

3. *The singular system (3.11) is said to be admissible if it is regular, impulse free and stable.*

An H_∞ controller designed for the active singular seat suspension system should satisfy some conditions as follows [72].

1. For $\omega = 0$, the active singular seat suspension system (3.11) is asymptotically stable.

2. Under zero initial conditions, the system (3.11) satisfies

$$\|z(t)\| < \gamma \|\omega(t)\|,$$

where $\|\bullet\|$ stands for the Euclidean norm of $\bullet$, $\omega(t) \neq 0$ and γ is a postive scalar. Since $\ddot{z}_v(t)$ is bounded in a limited area and $e_f(t)$ will exponentially converged to zero, so we have $\omega(t) \in L_2[0,\infty)$.

To design an H_∞ controller for the system (3.11), the following lemma will introduce a relaxed inequality, which is essential for the calculation of the controller.

Lemma 3.1 *Let x be a differentiable function:* $[\alpha,\beta] \to \boldsymbol{R}^n$*. For symmetric matrices* $R \in \boldsymbol{R}^{n\times n}$ *and* Z_1*,* $Z_3 \in \boldsymbol{R}^{3n\times 3n}$*, and any matrices* $Z_2 \in \boldsymbol{R}^{3n\times 3n}$*,* $N_1, N_2 \in \boldsymbol{R}^{3n\times n}$ *and* $E \in \boldsymbol{R}^{n\times n}$ $(\text{rank}(E) = g \leq n)$ *satisfying*

$$\Theta = \begin{bmatrix} Z_1 & Z_2 & N_1 \\ * & Z_3 & N_2 \\ * & * & R \end{bmatrix} > 0,$$

the following inequality holds:

$$-\int_\alpha^\beta \dot{x}^T(t) E^T R E \dot{x}(t) ds < \varpi^T(\alpha,\beta) \Psi_1 \varpi(\alpha,\beta),$$

where

$$\varpi(\alpha,\beta) = \begin{bmatrix} x^T(\beta) & x^T(\alpha) & \frac{1}{\beta-\alpha}\int_\alpha^\beta (Ex(s))^T ds \end{bmatrix}^T,$$

$$\Psi_1 = (\beta-\alpha)\left(Z_1 + \frac{1}{3}Z_3\right) + \text{sym}\left\{N_1 \begin{bmatrix} E & -E & 0 \end{bmatrix} + N_2 \begin{bmatrix} -E & -E & 2I \end{bmatrix}\right\}.$$

Proof. Define a function and a vector as

$$f(s)=\frac{\beta+\alpha-2s}{\beta-\alpha},\zeta(s)=\left[\begin{array}{ccc}\varpi^T & f(s)\varpi^T & (E\dot{x}(s))^T\end{array}\right]^T.$$

Because of $\Theta>0$, we can easily get

$$\zeta^T(t)\Theta\zeta(t)>0. \tag{3.12}$$

By considering the following equations

$$\int_\alpha^\beta f(s)ds=0,\int_\alpha^\beta f^2(s)ds=\frac{\beta-\alpha}{3},$$

$$\int_\alpha^\beta f(s)E\dot{x}(s)ds=(2e_3-Ee_1-Ee_2)\varpi,$$

$$\int_\alpha^\beta \dot{x}(s)ds=(e_1-e_2)\varpi,$$

where

$$e_i=\left[\begin{array}{ccc}0_{n\times n(i-1)} & I_n & 0_{n\times n(3-i)}\end{array}\right],i=1,2,3,$$

integrating the left-hand side of (3.12) from α to β, we have

$$\begin{aligned}0<&\int_\alpha^\beta \zeta^T(t)\Theta\zeta(t)ds\\ =&(\beta-\alpha)\varpi^TZ_1\varpi+\frac{\beta-\alpha}{3}\varpi^TZ_3\varpi+2\varpi^TN_1E(e_1-e_2)\varpi\\ &+2\varpi^TN_2(2e_3-Ee_1-Ee_2)\varpi+\int_\alpha^\beta \dot{x}^T(t)E^TRE\dot{x}(t)ds.\end{aligned} \tag{3.13}$$

To rearrange inequality (3.13), we have

$$\begin{aligned}&-\int_\alpha^\beta \dot{x}^T(t)E^TRE\dot{x}(t)ds\\ <&(\beta-\alpha)\varpi^TZ_1\varpi+\frac{\beta-\alpha}{3}\varpi^TZ_3\varpi+2\varpi^TN_1E(e_1-e_2)\varpi\\ &2\varpi^TN_2(2e_3-Ee_1-Ee_2)\varpi=\varpi^T\Theta\varpi.\end{aligned}$$

Then we complete the proof of this lemma. ■

Now a new H_∞ controller design conditions will be presented for the active singular seat suspension system (3.11) based on Definition 3.1, 3.2 and Lemma 3.1. When the H_∞ controller is designed, it is difficult to consider the system stability and the controller saturation simultaneously. Therefore, the controller saturation is not taken into consideration when designing the controller, but saturation and admissibility test will be done both in simulation and experiment.

Theorem 3.1 *The singular seat suspension system (3.11) is admissible with H_∞ control performance γ, if there exists an invertible matrix P, positive definite matrices $Q_i > 0$, $(i = 1,2,3)$, $R_j > 0$, $(j = 1,2)$, symmetric matrices Z_l, $(l = 1,2,3,4)$, any matrices Y_j, N_l and the controller K with appropriate dimensions, such that the following inequalities hold,*

$$P^T E = E^T P \geq 0, \tag{3.14}$$

$$\begin{bmatrix} Z_1 & Y_1 & N_1 \\ * & Z_2 & N_2 \\ * & * & R_1 \end{bmatrix} > 0, \begin{bmatrix} Z_3 & Y_2 & N_3 \\ * & Z_4 & N_4 \\ * & * & R_2 \end{bmatrix} > 0, \tag{3.15}$$

$$\Psi = \begin{bmatrix} \Psi_{11} & \Gamma^T & \Gamma^T & e_1^T C^T \\ * & -\frac{1}{\tau_m} R_1^{-1} & 0 & 0 \\ * & * & -\frac{1}{\tau_M - \tau_m} R_2^{-1} & 0 \\ * & * & * & -I \end{bmatrix} < 0, \tag{3.16}$$

where

$$\begin{aligned} \Psi_{11} =& e_1^T P^T \Gamma + \Gamma^T P e_1 + e_1^T (Q_1 + Q_2 + Q_3) e_1 - e_2^T Q_1 e_2 \\ & - \bar{\tau} e_3^T Q_2 e_3 - e_4^T Q_3 e_4 + \eta_1^T \Phi_1 \eta_1 + \eta_2^T \Phi_2 \eta_2 - \gamma^2 e_7^T e_7, \\ \eta_1^T =& \begin{bmatrix} e_1^T & e_2^T & e_5^T \end{bmatrix}, \eta_2^T = \begin{bmatrix} e_2^T & e_4^T & e_6^T \end{bmatrix}, \\ \Gamma =& A e_1 + BK e_3 + D e_7, \end{aligned}$$

$$\begin{aligned} \Phi_1 =& \tau_m \left(Z_1 + \frac{1}{3} Z_2 \right) + \mathrm{sym} \left\{ N_1 \begin{bmatrix} E & -E & 0 \end{bmatrix} + N_2 \begin{bmatrix} -E & -E & 2I \end{bmatrix} \right\}, \\ \Phi_2 =& (\tau_M - \tau_m) \left(Z_3 + \frac{1}{3} Z_4 \right) + \mathrm{sym} \left\{ N_3 \begin{bmatrix} E & -E & 0 \end{bmatrix} + N_4 \begin{bmatrix} -E & -E & 2I \end{bmatrix} \right\}, \\ e_i =& \begin{bmatrix} 0_{3\times(i-1)} & I_3 & 0_{3\times(7-i)} \end{bmatrix}, i = 1,2,...,7. \end{aligned}$$

Proof. Based on Remark 3.1, the singular seat suspension system (3.11) is regular and impulse free. To prove the stability of the closed-loop seat suspension system (3.11), a Lyapunov function is designed as

$$V(t) = V_1(t) + V_2(t) + V_3(t), \tag{3.17}$$

where

$$V_1(t) = x(t)^T P^T E x(t), \tag{3.18}$$

$$V_2(t) = \int_{t-\tau_m}^{t} x(v)^T Q_1 x(v) dv + \int_{t-\tau(t)}^{t} x(v)^T Q_2 x(v) dv + \int_{t-\tau_M}^{t} x(v)^T Q_3 x(v) dv, \tag{3.19}$$

$$V_3(t) = \int_{-\tau_m}^{0} \int_{t+v}^{t} \dot{x}(s)^T E^T R_1 E \dot{x}(s) ds dv + \int_{-\tau_M}^{-\tau_m} \int_{t+v}^{t} \dot{x}(s)^T E^T R_2 E \dot{x}(s) ds dv. \tag{3.20}$$

Define a state vector as

$$\xi^T(t) = \Big[\; x^T(t) \quad x^T(t-\tau_m) \quad x^T(t-\tau(t)) \quad x^T(t-\tau_M) \\ \tfrac{1}{\tau_m}\int_{t-\tau_m}^{t} x^T(s) ds \quad \tfrac{1}{\tau_M-\tau_m}\int_{t-\tau_M}^{t-\tau_m} x^T(s) ds \quad \omega^T(t) \; \Big].$$

Then, we calculate the derivative of $V(t)$ as follows.

$$\dot{V}_1(t) = 2x^T(t) P^T E \dot{x}(t) = \xi^T(t) \mathrm{sym}\{e_1^T P^T \Gamma\} \xi(t), \tag{3.21}$$

$$\begin{aligned} \dot{V}_2(t) =& x^T(t) Q_1 x(t) - x^T(t-\tau_m) Q_1 x(t-\tau_m) + x^T(t) Q_2 x(t) \\ & - \dot{\tau}(t) x^T(t-\tau(t)) Q_2 x(t-\tau(t)) + x^T(t) Q_3 x(t) - x^T(t-\tau_M) Q_3 x(t-\tau_M), \\ \leq& \xi^T(t) \left\{ e_1^T (Q_1 + Q_2 + Q_3) e_1 - e_2^T Q_1 e_2 - \bar{\tau} e_3^T Q_2 e_3 - e_4^T Q_3 e_4 \right\} \xi(t), \end{aligned} \tag{3.22}$$

$$\begin{aligned} \dot{V}_3(t) =& \tau_m \dot{x}(t)^T E^T R_1 E \dot{x}(t) - \int_{t-\tau_m}^{t} \dot{x}(s)^T E^T R_1 E \dot{x}(s) ds \\ & + (\tau_M - \tau_m) \dot{x}(t)^T E^T R_2 E \dot{x}(t) - \int_{t-\tau_M}^{t-\tau_m} \dot{x}(s)^T E^T R_2 E \dot{x}(s) ds. \end{aligned} \tag{3.23}$$

Based on Lemma 3.1, we have

$$-\int_{t-\tau_m}^{t} \dot{x}(s)^T E^T R_1 E \dot{x}(s) ds \leq \eta_1^T \Phi_1 \eta_1, \tag{3.24}$$

$$-\int_{t-\tau_M}^{t-\tau_m} \dot{x}(s)^T E^T R_2 E \dot{x}(s) ds \leq \eta_2^T \Phi_2 \eta_2, \tag{3.25}$$

Then the derivative of $V_3(t)$ can be estimated as

$$\dot{V}_3(t) \leq \xi^T(t) \left\{ \Gamma^T (\tau_m R_1 + (\tau_M - \tau_m) R_2) \Gamma + \eta_1^T \Phi_1 \eta_1 + \eta_2^T \Phi_2 \eta_2 \right\} \xi(t) \tag{3.26}$$

Then, based on the inequalities (3.21) to (3.26), we can get the derivative of $V(t)$ as

$$\dot{V}(t) \leq \xi^T(t) \Phi \xi(t). \tag{3.27}$$

where

$$\begin{aligned}\Phi =& e_1^T P^T \Gamma + \Gamma^T P e_1 + e_1^T (Q_1 + Q_2 + Q_3) e_1 - e_2^T Q_1 e_2 - \bar{\tau} e_3^T Q_2 e_3 \\ & - e_4^T Q_3 e_4 + \Gamma^T (\tau_m R_1 + (\tau_M - \tau_m) R_2) \Gamma + \eta_1^T \Phi_1 \eta_1 + \eta_2^T \Phi_2 \eta_2.\end{aligned}$$

Adding $z^T z - \gamma^2 \omega^T \omega$ into both sides of the equation (3.27), we have

$$\dot{V}(t) + z^T z - \gamma^2 \omega^T \omega \leq \xi^T(t)(\Phi + e_1^T C^T C e_1 - \gamma^2 e_7^T e_7)\xi(t) = \xi^T(t)\Xi\xi(t) \tag{3.28}$$

According to Schur complement, $\Xi < 0$ is equivalent to $\Psi < 0$. Based on inequality (3.15), we have $\dot{V}(t) + z^T z - \gamma^2 \omega^T \omega < 0$, so the singular seat suspension system (3.11) is stable with H_∞ control performance γ. Then the system (3.11) is admissible for any compatible condition. The proof of the Theorem 1 is completed. ■

In inequality (3.16), we cannot solve the controller K directly by the linear matrix inequality (LMI) toolbox of MATLAB, because there exist two variable matrices in one term $P^T BK$ and invertible matrices R_1 and R_2. To solve this problem, we introduce the following theorem.

Theorem 3.2 *The singular seat suspension system (3.11) is admissible with H_∞ control performance γ, if there exists an invertible matrix $\bar{P}$, positive definite matrices $\bar{Q}_i > 0$, $(i = 1,2,3)$, $\bar{R}_j > 0$, $(j = 1,2)$, symmetric matrices $\bar{Z}_l$, $(l = 1,2,3,4)$ and any matrices $\bar{Y}_j$, $\bar{N}_l$, $\bar{U}$, $\bar{K}$ with appropriate dimensions, such that the following inequalities hold*

$$E\bar{P} = \bar{P}^T E^T \geq 0 \tag{3.29}$$

$$\begin{bmatrix} \bar{Z}_1 & \bar{Y}_1 & \bar{N}_1 \\ * & \bar{Z}_2 & \bar{N}_2 \\ * & * & \bar{R}_1^{-1} \end{bmatrix} > 0, \begin{bmatrix} \bar{Z}_3 & \bar{Y}_2 & \bar{N}_3 \\ * & \bar{Z}_4 & \bar{N}_4 \\ * & * & \bar{R}_2^{-1} \end{bmatrix} > 0, \tag{3.30}$$

$$\bar{\Psi} = \begin{bmatrix} \bar{\Psi}_{11} & \bar{\Gamma}^T & \bar{\Gamma}^T & e_1^T \bar{P}^T C^T \\ * & -\frac{1}{\tau_m}\bar{R}_1 & 0 & 0 \\ * & * & -\frac{1}{\tau_M - \tau_m}\bar{R}_2 & 0 \\ * & * & * & -I \end{bmatrix} < 0, \tag{3.31}$$

where

$$
\begin{aligned}
\bar{\Psi}_{11} =& e_1^T\bar{\Gamma}+\bar{\Gamma}^T e_1+e_1^T(\bar{Q}_1+\bar{Q}_2+\bar{Q}_3)e_1-e_2^T\bar{Q}_1e_2\\
&-\bar{\tau}e_3^T\bar{Q}_2e_3-e_4^T\bar{Q}_3e_4+\eta_1^T\bar{\Phi}_1\eta_1+\eta_2^T\bar{\Phi}_2\eta_2-\gamma^2e_7^Te_7,\\
\eta_1^T =& \left[\begin{array}{ccc} e_1^T & e_2^T & e_5^T \end{array}\right], \eta_2^T=\left[\begin{array}{ccc} e_2^T & e_4^T & e_6^T \end{array}\right],\\
\bar{\Gamma} =& A\bar{P}e_1+B\bar{K}e_3+De_7,\\
\bar{\Phi}_1 =& \tau_m\left(\bar{Z}_1+\frac{1}{3}\bar{Z}_2\right)+\mathrm{sym}\left\{\bar{N}_1[\begin{array}{ccc} E & -E & 0 \end{array}]+\bar{N}_2[\begin{array}{ccc} -E & -E & 2I \end{array}]\right\},\\
\bar{\Phi}_2 =& (\tau_M-\tau_m)\left(\bar{Z}_3+\frac{1}{3}\bar{Z}_4\right)+\mathrm{sym}\left\{\bar{N}_3[\begin{array}{ccc} E & -E & 0 \end{array}]+\bar{N}_4[\begin{array}{ccc} -E & -E & 2I \end{array}]\right\},\\
e_i =& \left[\begin{array}{ccc} 0_{3\times(i-1)} & I_3 & 0_{3\times(7-i)} \end{array}\right], i=1,2,...,7.
\end{aligned}
$$

Furthermore, if the inequalities (3.29), (3.30) and (3.31) are feasible, a state feedback controller gain is given by $K=\bar{K}\bar{P}^{-1}$.

Proof. Define $\bar{P}=P^{-1}$, $\bar{R}_j=R_j^{-1}$, $\bar{Q}_i=\bar{P}^TQ_i\bar{P}$, $\bar{Z}_l=\mathrm{diag}\left\{\bar{P}^T,\bar{P}^T,I\right\}Z_l\mathrm{diag}\left\{\bar{P},\bar{P},I\right\}$, $\bar{Y}_j=\mathrm{diag}\left\{\bar{P}^T,\bar{P}^T,I\right\}Y_j\mathrm{diag}\left\{\bar{P},\bar{P},I\right\}$, $\bar{N}_l=\mathrm{diag}\left\{\bar{P}^T,\bar{P}^T,I\right)N_l$. Pre- and post-multiplying (3.14) by $\bar{P}^T$ and $\bar{P}$, we can get inequality (3.29). Similarly, pre- and post-multiplying (3.15) by $\mathrm{diag}(\bar{P}^T,\bar{P}^T,I,\bar{P}^T,\bar{P}^T,I,I)$ and $\mathrm{diag}(\bar{P},\bar{P},I,\bar{P},\bar{P},I,I)$, we can get inequality (3.30). And pre- and post-multiplying (3.16) by $\mathrm{diag}(\bar{P}^T,\bar{P}^T,\bar{P}^T,\bar{P}^T,I,I,I,I,I,I)$ and $\mathrm{diag}(\bar{P},\bar{P},\bar{P},\bar{P},I,I,I,I,I,I)$, we can get inequality (3.31). Then, the H_∞ controller can be solved by $K=\bar{K}\bar{P}^{-1}$. The proof of Theorem 2 is completed. ■

Because the inequality (3.30) is not LMI, the state feedback gains K cannot be solved by the LMI Toolbox of MATLAB. To solve nonlinear inequality (3.30), we design a CCL algorithm. This requires introduction of the real symmetric positive-definite matrices $\widehat{R}_1$, and $\widehat{R}_2$, satisfying

$$\widehat{R}_1\bar{R}_1=I,\widehat{R}_2\bar{R}_2=I. \tag{3.32}$$

The inequalities (3.30) are feasible if equations (3.32) and the following inequalities hold

$$\left[\begin{array}{ccc} \bar{Z}_1 & \bar{Y}_1 & \bar{N}_1 \\ * & \bar{Z}_2 & \bar{N}_2 \\ * & * & \widehat{R}_1 \end{array}\right]\geq 0, \left[\begin{array}{ccc} \bar{Z}_3 & \bar{Y}_2 & \bar{N}_3 \\ * & \bar{Z}_4 & \bar{N}_4 \\ * & * & \widehat{R}_2 \end{array}\right]\geq 0. \tag{3.33}$$

CCL algorithm

Step 1: Choose a sufficiently initial $\tau_M>\tau_m$, such that there exists a feasible solution

to (3.29), (3.31), (3.32), (3.33) and

$$\begin{gathered}\bar{Q}_i > 0, \bar{R}_j > 0, \widehat{R}_j > 0 \\ \begin{bmatrix} \bar{R}_j & I \\ * & \widehat{R}_j \end{bmatrix} > 0 \end{gathered} \tag{3.34}$$

Step 2: Find a feasible set of $\bar{R}_{10}$, $\widehat{R}_{10}$, $\bar{R}_{20}$, $\widehat{R}_{20}$, $\bar{P}_0$, $\bar{Q}_{i0}$, $\bar{Z}_{l0}$, $\bar{Y}_{j0}$, $\bar{N}_{l0}$ and $\bar{K}_0$ satisfying (3.29), (3.31), (3.33) and (3.34). Set $k = 0$.

Step 3: Solve the following LMI problem for the variables $\bar{P}$, $\bar{Q}_i$, $\bar{R}_j$, $\bar{Z}_l$, $\bar{Y}_j$, $\bar{N}_l$, $\bar{K}$ where (3.29), (3.31), (3.33) and (3.34).

$$\min_{\text{subject to (3.29),(3.31),(3.33) and (3.34)}} \text{tr}\Omega_1 + \text{tr}\Omega_2. \tag{3.35}$$

where

$$\Omega_1 = \overline{R}_{1k}\widehat{R}_1 + \overline{R}_1\widehat{R}_{1k}, \Omega_2 = \overline{R}_{2k}\widehat{R}_2 + \overline{R}_2\widehat{R}_{2k}.$$

Set $\bar{P}_{k+1} = \bar{P}$, $\bar{Q}_{i(k+1)} = \bar{Q}_i$, $\bar{R}_{j(k+1)} = \bar{R}_j$, $\widehat{R}_{j(k+1)} = \widehat{R}_j$, $\bar{Z}_{l(k+1)} = \bar{Z}_l$, $\bar{Y}_{j(k+1)} = \bar{Y}_j$, $\bar{N}_{l(k+1)} = \bar{N}_l$, and $\bar{K}_{k+1} = \bar{K}$.

Step 4: If LMIs (3.29), (3.30) and (3.31) are feasible for variables $\bar{P}$, $\bar{Q}_i$, $\bar{R}_j$, $\widehat{R}_j$, $\bar{Z}_l$, $\bar{Y}_j$, $\bar{N}_l$ and $\bar{K}$ obtained in Step 3, or if LMIs in (3.29), (3.30) and (3.31) are infeasible within a specified number of iteration, then stop. Otherwise, set $k = k+1$ and go to Step 3.

3.5 Simulation results

Some simulation results of the proposed control method are shown in this section for the active singular seat suspension system. Firstly, the parameters of the active singular seat suspension system are shown in Table 3.1. Based on the LMI toolbox and CCL algorithm, we can calculate the H_∞ controller as $[3011 \ -102 \ 30]$ according to Theorem 3.2. Here, we assume the friction of the seat suspension system as

$$f_r = \begin{cases} f_{r\min}, & \text{if } x_2 \le -\triangle, \\ \frac{f_{r\max}}{\triangle} x_2, & \text{if } -\triangle < x_2 < \triangle, \\ f_{r\max}, & \text{if } x_2 \ge \triangle. \end{cases}$$

where $\triangle = 0.05$ m/s is a small velocity interval to make the sign change of friction smoothly. The time-varying delay of the suspension system is set as $\tau(t) = 0.006 + 0.004\sin(250t)$.

Table 3.1: The active singular seat suspension system parameters

m(kg)	k(N/m)	c(Ns/m)	$\tau_m(s)$	$\tau_M(s)$
80	4600	500	0.002	0.01
$\bar{\tau}$	l	$f_{r\min}$(N)	$f_{r\max}$(N)	$u_{\max}$(N)
1	120	-80	80	180

Bumpy and random road disturbances are two common kinds of road surfaces, which are chosen to evaluate the vibration control performance of seat suspension systems in the time domain. A bumpy road surface is defined as:

$$z_v(t) = \begin{cases} \frac{a}{2}\left(1-\cos\left(\frac{2\pi v_0 t}{l}\right)\right), & 0 \le t \le \frac{l}{v_0} \\ 0, & t > \frac{l}{v_0} \end{cases} \tag{3.36}$$

where $a = 0.07$ m and $l = 0.8$ m are the height and length of the bumpy [19], respectively; $v_0 = 2.77$ m/s is the vehicle speed. This bumpy road disturbance is firstly transferred to a vehicle suspension and then the output becomes the disturbance to the active seat suspension system.

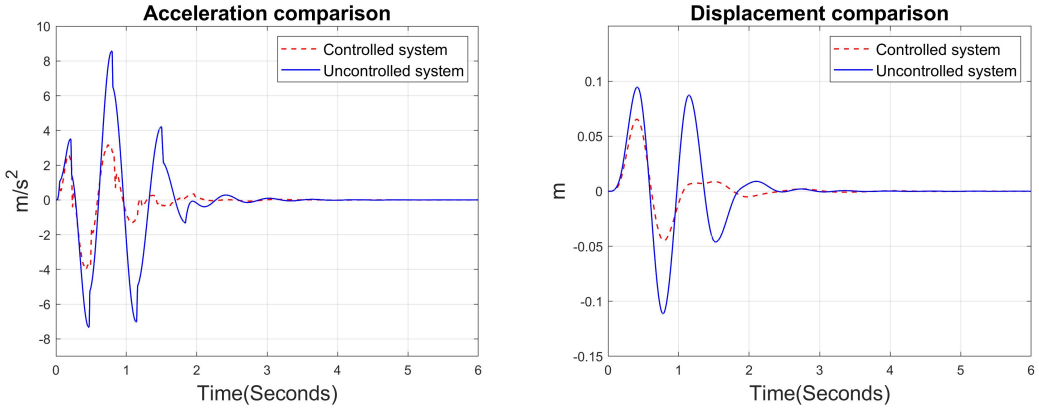

Figure 3.2: The acceleration and absolute displacement comparison for the singular seat suspension system with a bumpy road disturbance

Figures 3.2 shows the acceleration and absolute displacement comparison for the singular seat suspension system with a bumpy road disturbance, where we can see that the proposed controller can both reduce the acceleration and displacement of the upper seat suspension compared with the uncontrolled seat suspension system. Figure 3.3 shows the friction comparison and the input force of the controller. Here we can see the friction observer is able to estimate the real friction in real time, which is helpful to make compensation for the controller. The input force of the controller meets its saturation during this control performance, but it still can help to keep the stability of the system and reduce vibrations.

A random road surface is generated from the simulation. Similarly, as the bumpy road disturbance, it is first transferred to a vehicle suspension and then to the active seat sus-

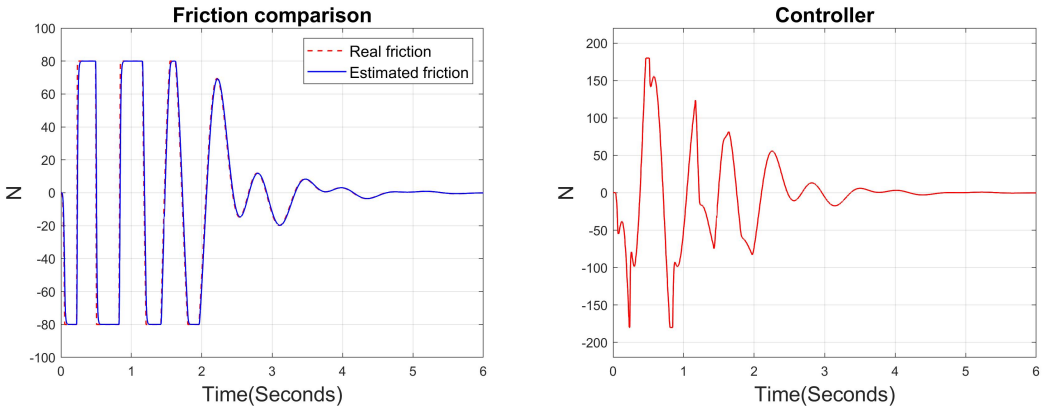

Figure 3.3: The estimated friction and the input force for the singular seat suspension system with a bumpy road disturbance

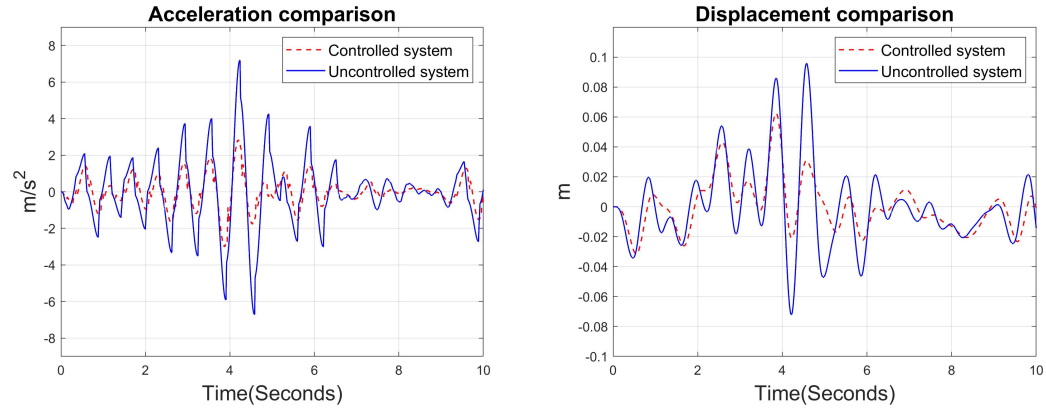

Figure 3.4: The acceleration and absolute displacement comparison for the singular seat suspension system with a random road disturbance

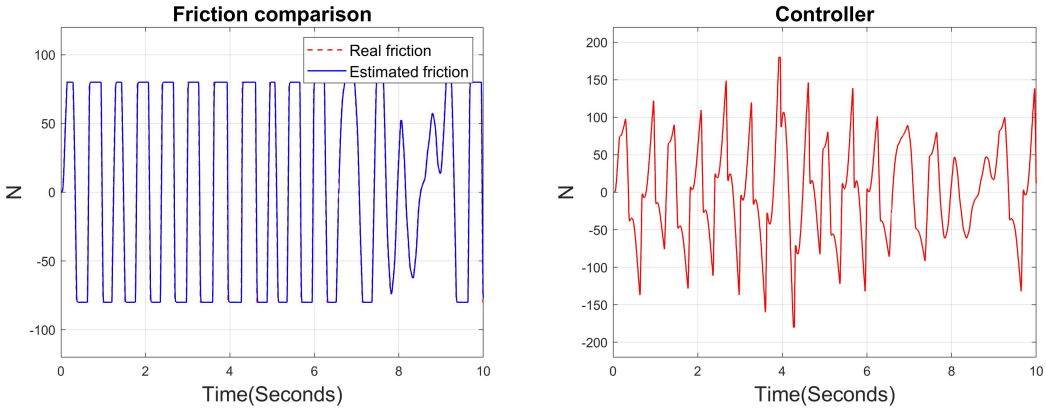

Figure 3.5: The estimated friction and the input force for the singular seat suspension system with a random road disturbance

pension system. Figure 3.4 shows the acceleration and absolute displacement comparison for the suspension system with a random road disturbance. Here we can see that the pro-

posed control method can reduce both the acceleration and the displacement of the upper seat suspension effectively compared with the uncontrolled seat suspension system. Figure 3.5 shows the estimated friction and real friction comparison and the input force of the controller for the suspension system with a random road disturbance. The friction comparison figure shows that the friction observer can estimate the friction properly in real time under a random road disturbance. The controller plot shows that the controller can reduce the seat suspension vibration despite its saturation and time-varying delay issue. The simulation results show that the proposed control method has a good control performance to reduce vibration and improve the driving comfort under bumpy and random road disturbances with the time-varying delay and saturation issues of the actuator.

3.6 Experimental results

In this section, some experimental results of the proposed control method for the active singular seat suspension system will be shown in the time domain and frequency domain. This includes the experimental setup, the comparison of the proposed control method controlled, and the uncontrolled seat suspension system performance.

3.6.1 Experimental setup

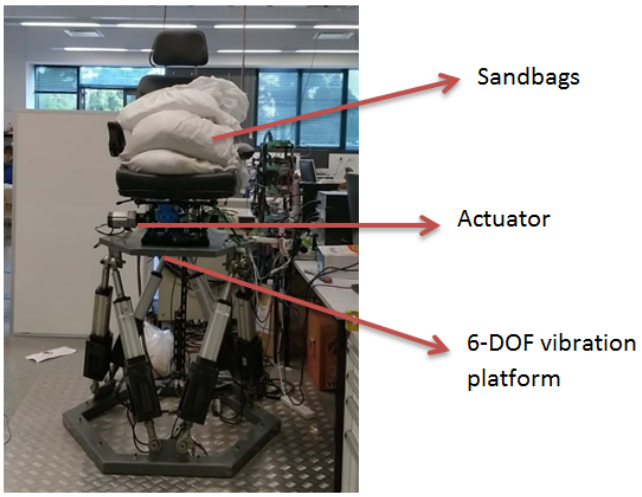

Figure 3.6: The experimental setup

The experimental setup is shown in Figure 3.6 for the active singular seat suspension system. The sandbags (70kg) are put on the seat to simulate a driver's weight. The actuator is set to provide the active input force. The 6-degree-of-freedom platform can generate different kinds of vertical vibration disturbances. Computer 1 with NI CompactRio 9076

implements excitation commandment to the 6-DOF platform according to different requirements. The whole seat suspension is fixed on the platform. Two laser displacement sensors (Micro-Epsilon ILD1302-100 and ILD1302-200) are used here to measure the deflection of the seat suspension and the absolute displacement of the upper seat, while the deflection signal is used for the controller and the absolute displacement signal is used only for comparison. Two accelerometers (ADXL203EB) are used to measure the vertical seat acceleration and the platform excitation acceleration, respectively. Computer 2 with NI CompactRio 9074 is used to obtain the real-time data from these sensors and to implement the control force.

Compared with conventional active seat suspension system models, the active singular seat suspension system model uses the deflection, relative velocity and acceleration signal as the system states, all of which are easily measured. The upper seat acceleration can be easily obtained by the accelerometer sensor, so it does not need to be calculated by Newton's Second Law. Meanwhile, the acceleration signal will be used for friction observation and controller design.

3.6.2 Experiment in the time domain

Similarly, bumpy and random disturbances are chosen as the excitation to test the seat suspension system. The same bumpy road disturbance is used here as the simulation section. These road excitations can be generated by the 6-DOF platform for the seat suspension.

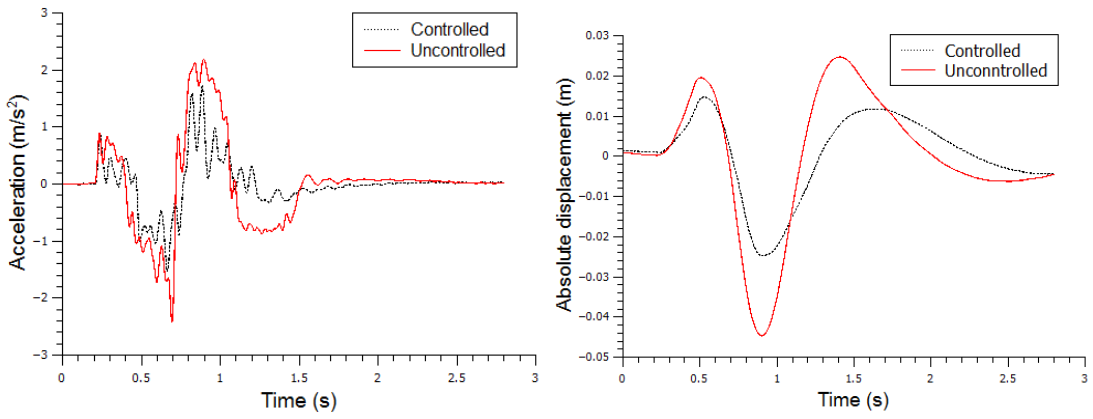

Figure 3.7: The acceleration and absolute displacement comparison for the singular seat suspension system with a bumpy road disturbance

Figure 3.7 shows the acceleration and absolute displacement comparison for the controlled and uncontrolled singular seat suspension system with a bumpy road disturbance. Here we can see that the proposed controller can both reduce the acceleration and absolute displacement for the upper seat suspension, so it can help to improve the driving comfort

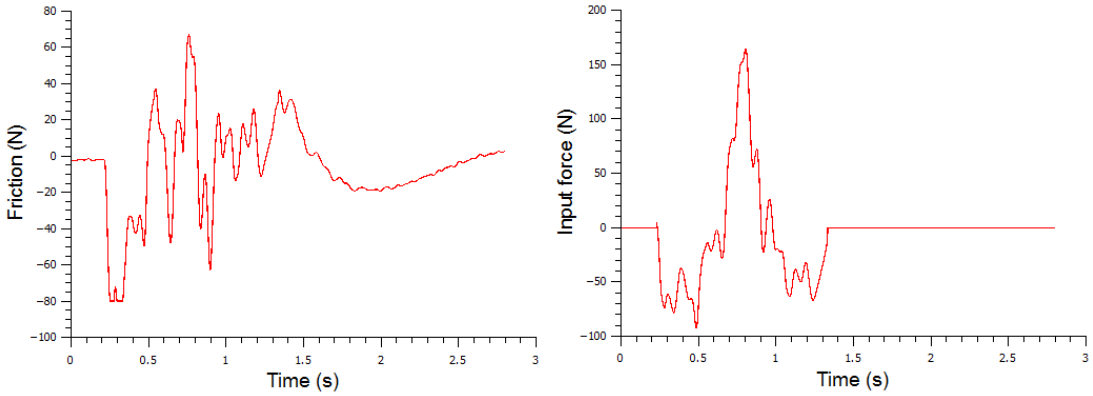

Figure 3.8: The estimated friction and the input force for the singular seat suspension system with a bumpy road disturbance

for drivers. Figure 3.8 shows the estimated friction and the input force for the singular seat suspension with a bumpy road disturbance. The friction figure shows that the friction observer can estimate the friction and bound the friction value among its normal range by the projecting algorithm. The estimated friction is compensated to the controller as (3.9) as shown in Figure 3.8. To save energy for the seat suspension system, we set the input force as zero when there is no excitation or the excitation is very small, so the seat suspension can keep stable or only suffer a small vibration which drivers can bear without harm to their health. This can be realized by measuring the root mean square (RMS) of the acceleration of the cab floor $\ddot{z}_v$ within a small unit of time in real-time, such as $u = 0$, when $\text{RMS}(\ddot{z}_v)_{t_0} \leq c$, where t_0 is the time unit for the measurement of $\text{RMS}(\ddot{z}_v)$ and c is a small constant. The force input figure shows the actuator input force for the singular seat suspension system, where we can see that the actuator only output force during the vehicle passing the bumpy road. The seat suspension can return its stability by itself after the bumpy road disturbance, which can greatly reduce energy consumption.

And a random road surface [19] is defined as

$$\dot{z}_v(t) + \rho V z_v(t) = V W_n \tag{3.37}$$

where $\rho = 0.4\ \text{m}^{-1}$ is the roughness parameter; $V = 20$ m/s is the forward vehicle velocity; W_n is white noise with intensity $2\delta^2\rho V$ and $\delta^2 = 300\ \text{mm}^2$ is the covariance of the random road roughness.

Figure 3.9 shows the acceleration and absolute displacement comparison for the controlled and uncontrolled singular seat suspension system with a random road disturbance. Both the acceleration and the absolute displacement of the upper seat suspension can be reduced by the proposed controller, especially around the resonant frequency of the seat suspension. Therefore, the proposed controller can greatly improve driving comfort. Fig-

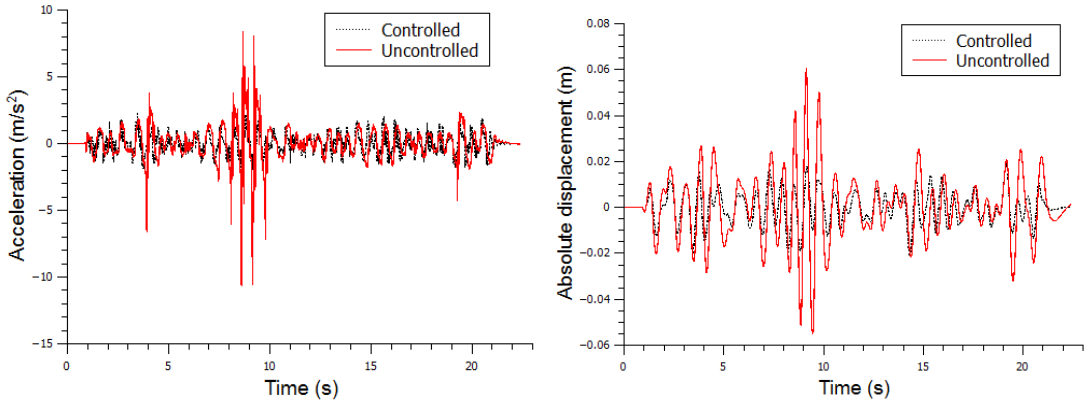

Figure 3.9: The acceleration and absolute displacement comparison for the singular seat suspension system with a random road disturbance

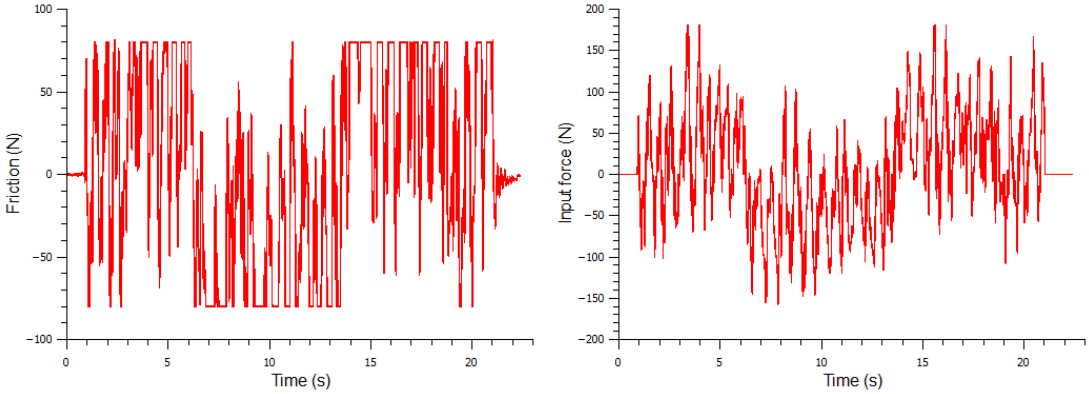

Figure 3.10: The estimated friction and the input force for the singular seat suspension system with a random road disturbance

ure 3.10 shows the estimated friction and the input force for the singular seat suspension system with a random road disturbance. In the friction figure, we can see that the friction observer can estimate the friction and bound it within its normal range according to the projecting algorithm. The input force is compensated by the estimated friction and bounded within its maximum output force as shown in Figure 3.10.

Table 3.2 shows the comparison of the root mean square (RMS) values of drivers' acceleration between the controlled and uncontrolled seat suspension systems with bumpy and random disturbances. The proposed controller can reduce the RMS values of drivers' acceleration by 46.08% and 46.75% to bumpy and random disturbances, respectively, which shows the effectiveness of the proposed control method.

Table 3.2: The comparison of RMS values of drivers' acceleration

disturbance type	uncontrolled (m/s^2)	controlled (m/s^2)	reduction
bumpy	0.7706	0.4155	46.08%
random	1.3108	0.6980	46.75%

3.6.3 Experiment in the frequency domain

To better show the advantages of the proposed controller, the control performance in the frequency domain for the active singular seat suspension system is shown in this section. According to ISO 2631-1 (the international standard to evaluate human exposure to whole-body vibration), the frequency-weighted RMS (FWRMS) acceleration (a_ω) can be calculated based on time history and defined as

$$(a_\omega) = \left[\frac{1}{T}\int_0^T a(t)^2 dt\right]^{1/2}.$$

And the seat effective amplitude transmissibility (SEAT) is used here to judge the ability of vibration reduction and defined as

$$\text{SEAT} = \frac{a_{\omega,\text{driver}}}{a_{\omega,\text{excitation}}},$$

where $a_{\omega,\text{driver}}$ and $a_{\omega,\text{excitation}}$ are the RMS accelerations of the driver and the external excitation.

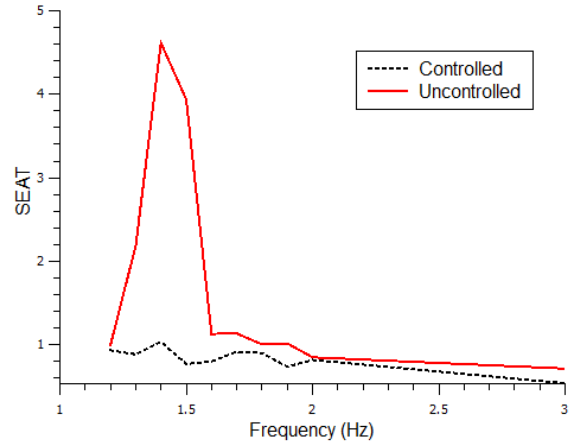

Figure 3.11: The seat effective amplitude transmissibility comparison between the controlled and uncontrolled singular seat suspension system

Figure 3.11 shows the seat effective amplitude transmissibility (SEAT) comparison between controlled and uncontrolled singular seat suspension system, where we can see that the resonant frequency of the uncontrolled seat suspension system is around 1.4 Hz and

the SEAT value is very large around the resonant frequency. The proposed controller can have very good control performance around the resonant frequency which greatly helps to reduce vibration to drivers and improve the driving comfort among 1.2 Hz to 3 Hz.

3.7 Conclusion

A singular system based approach is investigated for active vibration control of vehicle seat suspension. Compared with conventional control methods for seat suspension systems, the proposed controller only uses easily measurable variables, so it is more useful for practical application. An H_∞ controller is designed by considering friction compensation, actuator saturation and time-delay issues. The nonlinear constraints of the inequalities are solved by the cone complementary linearization algorithm. A bumpy and a random road disturbance excitation are used to test the control performance for the controlled seat suspension system compared with the uncontrolled seat suspension system in the time domain by simulation and experiment. The seat effective amplitude transmissibility is applied as the standard to judge the control performance of the proposed controller in the frequency domain. Both the simulations and experiments show that the proposed controller has good control performance to reduce vibrations and improve driving comfort. The friction estimation is not precise in practice, because the practical seat suspension system is more complicated than the model given in this chapter and the integration method is used here to calculate the estimated friction value, which is easy to amplify measuring error. The robust H_∞ control method, combined with the event-triggered scheme is introduced in the next chapter.

Chapter 4

Continuous Event-triggered H_∞ Control Strategy

4.1 Introduction

The previous chapter proposes a singular system based control strategy for active seat suspension systems. The acceleration signal is considered as one of the system states, which makes the system singular. This method makes full use of all measurable signals of the seat suspension to design the seat suspension system and H_∞ controller. In this chapter, an H_∞ controller with a continuous event-triggered scheme is proposed for active seat suspension systems.

Most of those control methods need continuous dynamic system states, but it is impossible to update controllers continuously in practice [73, 74]. Usually, some sensors and computers are used to acquire and process data for the practical control plant [75]. The resolution of the sensors and computers determines the control performance of the control system. The higher the resolution is, the closer the practical control performance will be to the theoretical one. However, the high resolution also needs fast data transmission and controller updating speed, which costs a lot of CPU. Additionally, not all of the acquired dynamic data are useful for controllers. To solve this problem, some trigger mechanisms are used to send just part of the measured data. The simplest method is a periodic trigger, but it sends measured data even when the changes of system state values are too small to change the controller signal significantly [76]. To avoid these "redundant" packets, the event trigger is adopted where the control signal only renews when an event is triggered [77, 78]. Therefore, the event-triggered control can reduce processor, transmission load, and resource utilization, which is closer to the way a human behaves like a controller [79, 80].

The event trigger scheme has been combined with many control methods used in many fields, such as event-triggered sliding mode control for stochastic systems [81], multi-area

power systems [82], linear time-invariant systems [83], event-triggered H_∞ control for network control systems [84, 85]. The distributed observer-based event-triggered bipartite tracking control problem is investigated for stochastic nonlinear multi-agent systems with input saturation in [86]. The event-triggered control problem is investigated for stochastic nonlinear systems with unmeasured states and unknown backlash-like hysteresis based on fuzzy logic systems in [87]. In [61], an event-triggered and distributed H_∞ filtering is proposed for a cloud-aided active semi-vehicle suspension system, where the controller is built in the cloud. It is noted that most of the event-triggered control scheme is applied to network control systems to reduce the network transmission burden and hence communication broadband requirement. Although the event-triggered scheme has shown many advantages, the issue about how to use an event-triggered scheme to control the seat suspension system has not been explored in literature, which motivates us to design an event-triggered controller for seat suspension systems. However, the event-triggered control certainly introduces the time-delay problem for the controller because the value of the control input only updates when the defined event trigger happens. Hence, the continuous event-triggered scheme is chosen to be combined with an H_∞ controller to control the active seat suspension system in this chapter, which can both reduce the workload of data transmission and improve the robustness of the seat suspension system.

The time delay is an important issue for the event-triggered H_∞ control of the seat suspension system because the value of the control signal remains the same between two event-triggered time instants. To reduce the conservatism of the controlled system, a Lyapunov function is presented where some matrices are introduced with relaxed conditions. An inequality in [88] is used as a lemma to prove the positive definiteness of the proposed Lyapunov function. Another inequality in [67] is applied to calculate the stability criteria for the controlled system.

The main contributions of this chapter are listed as follows:

- The event-triggered H_∞ control is first presented for active seat suspension systems. The continuous event-triggered scheme is applied here to reduce the data processor and transmission load. Both theoretical analysis and experimental tests for the seat suspension system with the event-triggered H_∞ controller are shown in this chapter.

- The event-triggered scheme makes the value of the controller only change when the defined event triggers, so it also works as a filter to remove noise caused by the measurement of sensors. Therefore, it can reduce the resolution requirement of the actuator to reduce the cost of seat suspensions. This makes a good trade-off between the control performance and other system aspects (such as processor load, communication load, and system cost price).

- Two tight inequalities are applied in this chapter to prove the positive definiteness of the proposed Lyapunov function and to obtain the stability criteria for the controlled

seat suspension system, which helps to reduce the conservatism of the controlled system to the time delay of the input force.

4.2 Seat suspension model and event-triggered scheme

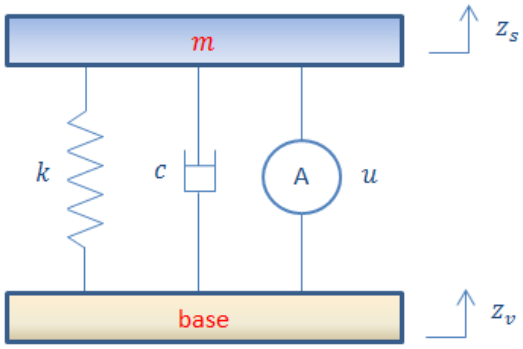

Figure 4.1: Active seat suspension model

An active vehicle seat suspension model is shown in Figure 4.1 and the dynamic equation of the seat suspension system can be written as follows:

$$m\ddot{z}_s(t) + c(\dot{z}_s(t) - \dot{z}_v(t)) + k(z_s(t) - z_v(t)) = u(t) \tag{4.1}$$

where m is the sprung mass including a driver and the seat; k and c are the stiffness and the damping coefficient of the seat suspension, respectively; z_s and z_v are the displacements of the suspension upper and base, respectively; $\dot{z}_s$ and $\dot{z}_v$ are the velocities of the suspension upper and base, respectively; u is the control input.

Define the state variables as follows:

$$x_1 = z_s - z_v, x_2 = \dot{z}_s$$

where x_1 represents the suspension deflection, x_2 is the sprung mass speed. $\ddot{z}_s$ is chosen as the performance output because the body acceleration is closely related to the ride comfort. Define the disturbance input $\omega(t) = \dot{z}_v(t)$ and $x = [\ x_1 \quad x_2\ ]^T$, so the state-space equation of the seat suspension system can be written as:

$$\begin{aligned} \dot{x}(t) &= Ax(t) + Bu(t) + E\omega(t), \\ z(t) &= Cx(t) + Du(t) + F\omega(t), \end{aligned} \tag{4.2}$$

where

$$A=\begin{bmatrix} 0 & 1 \\ -\frac{k}{m} & -\frac{c}{m} \end{bmatrix}, B=\begin{bmatrix} 0 \\ \frac{1}{m} \end{bmatrix}, E=\begin{bmatrix} -1 \\ \frac{c}{m} \end{bmatrix},$$
$$C=\begin{bmatrix} -\frac{k}{m} & -\frac{c}{m} \end{bmatrix}, D=\frac{1}{m}, F=\frac{c}{m}.$$

Assume that the seat suspension system states are sampled and transmitted at time instants $t_0, t_1, \cdots, t_k, t_{k+1}, \cdots, k \in \mathbf{N}$. The continuous event-triggered scheme is designed as

$$t_{k+1}=\min\left\{\min\left[t \geq t_k | \left(x(t)-x(t_k)\right)^T \Omega \left(x(t)-x(t_k)\right) \geq \delta x^T(t) \Omega x(t)\right], (t_k+\bar{d})\right\} \tag{4.3}$$

where $\Omega > 0$, $0 < \delta < 1$ and $\bar{d} > 0$ is set as the maximum state delay, so we have $t_{k+1} - t_k \leq \bar{d}$.

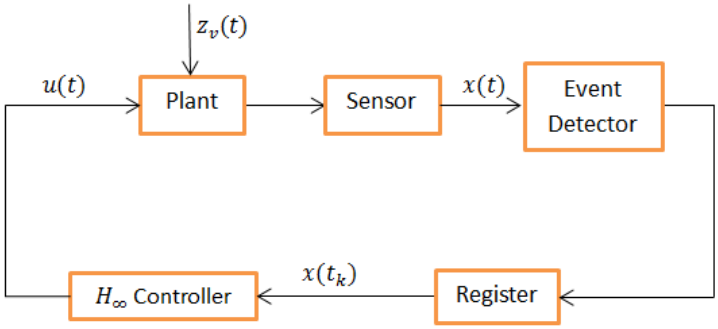

Figure 4.2: Diagram of the active seat suspension system with the event-triggered H_∞ controller

Figure 4.2 shows the working diagram of the active seat suspension system with the event-triggered H_∞ controller. Some sensors measure system state values in real-time. Then the event detector estimates whether the event should be triggered or not. A register is used to store the event-triggered state values and transfer them to the H_∞ controller.

The control main objective of the H_∞ controller is to reduce the driver's acceleration to improve driving comfort. This H_∞ controller uses the event-triggered system state values, so the H_∞ controller is in the form of

$$u(t)=Kx(t_k) \tag{4.4}$$

Substituting the controller (4.4) into system (4.2), we can get the controlled system as

$$\begin{aligned} \dot{x}(t) &= Ax(t)+BKx(t-d(t))+E\omega(t), \\ z(t) &= Cx(t)+DKx(t-d(t))+F\omega(t), \end{aligned} \tag{4.5}$$

where $d(t) = t - t_k$, $t \in [t_k, t_{k+1})$, $k \in \mathbf{N}$, $0 \leq d(t) \leq \bar{d}$, and $\bar{d}$ is the maximum time delay of the controller.

4.3 Event-triggered H_∞ controller design

In this section, the event-triggered H_∞ controller for the active seat suspension system is designed. Firstly, two lemmas are given from [88] and [67], which provide tight equalities to deal with the time-delay problem of the controller.

Lemma 4.1 *[88] Let $x \in \boldsymbol{R}^n$ be a continuous function and admit a continuous derivative differentiable function: $[\alpha, \beta] \to \boldsymbol{R}^n$. For symmetric matrices $R \in \boldsymbol{R}^{n\times n}$ and $Z_1 \in \boldsymbol{R}^{2n\times 2n}$, and any matrix $Z_2 \in \boldsymbol{R}^{2n\times n}$ satisfying*

$$\begin{bmatrix} Z_1 & Z_2 \\ * & R \end{bmatrix} \geq 0,$$

the following inequality holds:

$$-\int_\alpha^\beta x^T(t)Rx(t) \leq \varpi_1^T(\alpha,\beta)\Psi_1\varpi_1(\alpha,\beta),$$

where

$$\varpi_1(\alpha,\beta) = \begin{bmatrix} \int_\alpha^\beta x^T(s)ds & \frac{1}{\beta-\alpha}\int_\alpha^\beta\int_v^\beta x^T(s)dsdv \end{bmatrix}^T,$$
$$\Psi_1 = \frac{(\beta-\alpha)}{3}Z_1 + \mathrm{sym}\left\{Z_2\begin{bmatrix} -I & 2I \end{bmatrix}\right\}.$$

Lemma 4.2 *[67] Let x be a differentiable function: $[\alpha, \beta] \to \boldsymbol{R}^n$. For symmetric matrices $R \in \boldsymbol{R}^{n\times n}$ and Z_1, $Z_3 \in \boldsymbol{R}^{3n\times 3n}$, and any matrices $Z_2 \in \boldsymbol{R}^{3n\times 3n}$ and $N_1, N_2 \in \boldsymbol{R}^{3n\times n}$ satisfying*

$$\begin{bmatrix} Z_1 & Z_2 & N_1 \\ * & Z_3 & N_2 \\ * & * & R \end{bmatrix} \geq 0,$$

the following inequality holds:

$$-\int_\alpha^\beta \dot{x}^T(t)R\dot{x}(t) \leq \varpi_2^T(\alpha,\beta)\Psi_2\varpi_2(\alpha,\beta),$$

where

$$\varpi_2(\alpha,\beta)=\left[\begin{array}{cccc} x^T(\beta) & x^T(\alpha) & \frac{1}{\beta-\alpha}\int_\alpha^\beta x^T(s)ds \end{array}\right]^T,$$
$$\Psi_2=(\beta-\alpha)\left(Z_1+\frac{1}{3}Z_3\right)+\mathrm{sym}\left\{N_1[\begin{array}{ccc} I & -I & 0 \end{array}]+N_2[\begin{array}{ccc} -I & -I & 2I \end{array}]\right\}.$$

Theorem 4.1 *For given positive scalars $\bar{d}$, δ, and α_i $(i=1,2,3)$, the closed-loop system (4.5), under event-triggered scheme (4.3) and feedback controller (4.4), is asymptotically stable with H_∞ performance index γ, if there exist positive definite matrices $Q\in\boldsymbol{R}^{6\times6}$, $R\in\boldsymbol{R}^{2\times2}$, symmetric matrices $P\in\boldsymbol{R}^{8\times8}$, $G\in\boldsymbol{R}^{12\times12}$, $Z_i\in\boldsymbol{R}^{6\times6}$, $(i=1,2)$, $\Omega\in\boldsymbol{R}^{2\times2}$, and any matrices $Y\in\boldsymbol{R}^{6\times6}$, $N_i\in\boldsymbol{R}^{6\times2}$, $(i=1,2)$, $H\in\boldsymbol{R}^{12\times6}$, $U\in\boldsymbol{R}^{2\times2}$, satisfying the following inequalities:*

$$\Sigma\geq0, \tag{4.6}$$
$$\left[\begin{array}{cc} G & H \\ * & Q \end{array}\right]\geq0, \tag{4.7}$$
$$\left[\begin{array}{ccc} Z_1 & Y & N_1 \\ * & Z_2 & N_2 \\ * & * & R \end{array}\right]\geq0, \tag{4.8}$$
$$\Psi\leq0, \tag{4.9}$$
$$\Theta=\left[\begin{array}{cc} \Psi & \Theta_1 \\ * & \Theta_2 \end{array}\right]\leq0 \tag{4.10}$$

where

$$\Sigma=\Pi_1P\Pi_1^T-\Sigma_1,\Sigma_1=\frac{\bar{d}}{3}\Pi_2G\Pi_2^T+\mathrm{sym}\left\{\Pi_2H\Pi_3^T\right\},$$
$$\Pi_1=\left[\begin{array}{cccc} l_1 & l_2 & l_3 & \bar{d}l_4 \end{array}\right],$$
$$\Pi_2=\left[\begin{array}{ccccc} \bar{d}l_4 & l_1-l_3 & \bar{d}(l_1-l_4) & l_5 & l_1-l_4 & \frac{\bar{d}}{2}l_1-l_5 \end{array}\right],$$
$$\Pi_3=\left[\begin{array}{ccc} 2l_5-\bar{d}l_4 & l_1+l_3-2l_4 & \bar{d}l_4-2l_5 \end{array}\right],$$
$$l_i=\left[\begin{array}{ccc} 0_{2\times2(i-1)} & I_2 & 0_{2\times2(5-i)} \end{array}\right]^T,i=1,2,\cdots,5,$$
$$\Psi=\mathrm{sym}\left\{\Gamma_1P\Gamma_2^T\right\}+\Gamma_3Q\Gamma_3^T-\Gamma_4Q\Gamma_4^T+\bar{d}e_4Re_4^T+\Phi+\Xi_1+\Xi_2,$$
$$\Phi=\bar{d}\Gamma_5\left(Z_1+\frac{1}{3}Z_2\right)\Gamma_5^T+\mathrm{sym}\left\{\Gamma_5\left(N_1(e_1-e_2)^T+N_2(2e_6-e_1-e_2)^T\right)\right\},$$
$$\Xi_1=(\delta-1)e_1\Omega e_1^T+\mathrm{sym}(e_1\Omega e_2^T)-e_2\Omega e_2^T,$$
$$\Xi_2=\mathrm{sym}\left\{(e_1A^T+e_2K^TB^T-e_4)U(\alpha_1e_1^T+\alpha_2e_2^T+\alpha_3e_4^T)\right\},$$
$$\Gamma_1=\left[\begin{array}{cccc} e_1 & e_2 & e_3 & \bar{d}e_6 \end{array}\right],\Gamma_2=\left[\begin{array}{cccc} e_4 & e_0 & e_5 & e_1-e_3 \end{array}\right],$$
$$\Gamma_3=\left[\begin{array}{ccc} e_1 & e_4 & e_0 \end{array}\right],\Gamma_4=\left[\begin{array}{ccc} e_3 & e_5 & e_1-e_3 \end{array}\right],\Gamma_5=\left[\begin{array}{ccc} e_1 & e_3 & e_6 \end{array}\right],$$

$$
\begin{aligned}
e_i =& \begin{bmatrix} 0_{2\times 2(i-1)} & I_2 & 0_{2\times 2(6-i)} \end{bmatrix}^T, i = 1,2,\cdots,6, e_0 = 0_{12\times 2},\\
\Theta_1 =& e_1 \begin{bmatrix} U^T E + C^T F & C^T \end{bmatrix} + e_2 \begin{bmatrix} U^T E & 0 \end{bmatrix} + e_4 \begin{bmatrix} 0 & (DK)^T \end{bmatrix},\\
\Theta_2 =& \begin{bmatrix} -\gamma^2 I & F^T \\ * & -I \end{bmatrix}.
\end{aligned}
$$

Proof. Firstly, to prove the asymptotic stability of the closed-loop system (4.5), we can assume $\omega(t) = 0$ and define the Lyapunov functional as follows:

$$V(t) = V_P(t) + V_Q(t) + V_R(t) \tag{4.11}$$

where

$$
\begin{aligned}
V_P(t) =& \eta_1^T(t) P \eta_1(t),\\
V_Q(t) =& \int_{t-\bar{d}}^{t} \eta_2^T(v) Q \eta_2(v) dv,\\
V_R(t) =& \int_{-\bar{d}}^{0} \int_{t+v}^{t} \dot{x}^T(s) R \dot{x}(s) ds dv,\\
\eta_1(t) =& \begin{bmatrix} x^T(t) & x^T(t-d(t)) & x^T(t-\bar{d}) & \int_{t-\bar{d}}^{t} x^T(s) ds \end{bmatrix}^T,\\
\eta_2(v) =& \begin{bmatrix} x^T(v) & \dot{x}^T(v) & \int_{v}^{t} \dot{x}^T(s) ds \end{bmatrix}^T,
\end{aligned}
$$

Define a state vector as

$$\chi(t) = \begin{bmatrix} x^T(t) & x^T(t-d(t)) & x^T(t-\bar{d}) & \frac{1}{\bar{d}} \int_{t-\bar{d}}^{t} x^T(s) ds & \frac{1}{\bar{d}} \int_{t-\bar{d}}^{t} \int_{v}^{t} x^T(s) ds dv \end{bmatrix}^T$$

According to Lemma 4.1, we have

$$\int_{t-d}^{t} \eta_2^T(v) Q \eta_2(v) dv \geq -\eta_3^T(t) \Lambda \eta_3(t),$$

where

$$
\begin{aligned}
\eta_3(t) = \Big[& \int_{t-\bar{d}}^{t} x^T(s) ds \quad x^T(t) - x^T(t-\bar{d}) \quad \bar{d} x^T(t) - \int_{t-\bar{d}}^{t} x^T(s) ds \\
& \frac{1}{\bar{d}} \int_{t-\bar{d}}^{t} \int_{v}^{t} x^T(s) ds dv \quad x^T(t) - \frac{1}{\bar{d}} \int_{t-\bar{d}}^{t} x^T(s) ds \quad \frac{\bar{d}}{2} x^T(t) - \frac{1}{\bar{d}} \int_{t-\bar{d}}^{t} \int_{v}^{t} x^T(s) ds dv \Big]^T,
\end{aligned}
$$

$$\Lambda = \frac{\bar{d}}{3} G + \mathrm{sym}\left\{ H \begin{bmatrix} -I & 2I \end{bmatrix} \right\}.$$

Thus, we can get

$$V_Q(t) \geq -\chi^T(t)\Sigma_1\chi(t),$$

so

$$V_P(t)+V_Q(t) \geq \chi^T(t)\Sigma\chi(t).$$

Based on (4.6) and $R>0$, we have

$$V(t) = V_P(t)+V_Q(t)+V_R(t) \geq 0,$$

so the positive definiteness of $V(t)$ is ensured.

Then, we need to get the derivative of $V(t)$. Firstly, define another state vector as

$$\xi(t) = \left[\begin{array}{ccccccc} x^T(t) & x^T(t-d(t)) & x^T(t-\bar{d}) & \dot{x}^T(t) & \dot{x}^T(t-\bar{d}) & \frac{1}{\bar{d}}\int_{t-\bar{d}}^{t} x^T(s)ds \end{array} \right]^T.$$

When $t \in [t_k, t_{k+1})$, $t-d(t) = t_k$ is a constant, so $\dot{x}(t-d(t)) = 0$. Then, we can get

$$\begin{aligned} \dot{V}_P(t) =& 2\eta_1^T(t)P\dot{\eta}_1(t) = \xi^T(t)\left\{\mathrm{sym}(\Gamma_1 P\Gamma_2^T)\right\}\xi(t), && (4.12)\\ \dot{V}_Q(t) =& \eta_2^T(t)Q\eta_2(t) - \eta_2^T(t-\bar{d})Q\eta_2(t-\bar{d}) \\ =& \xi^T(t)(\Gamma_3 Q\Gamma_3^T - \Gamma_4 Q\Gamma_4^T)\xi(t), && (4.13)\\ \dot{V}_R(t) =& \bar{d}\dot{x}^T(t)R\dot{x}(t) - \int_{-\bar{d}}^{0}\dot{x}^T(t+s)R\dot{x}(t+s)ds && (4.14) \end{aligned}$$

According to Lemma 4.2, we have

$$-\int_{-\bar{d}}^{0}\dot{x}^T(t+s)R\dot{x}(t+s)ds \leq \xi^T(t)\Phi\xi(t) \tag{4.15}$$

Based on the event-triggered scheme (4.3), the following inequality holds:

$$\delta x^T(t)\Omega x(t) - e^T(t)\Omega e(t) \geq 0 \tag{4.16}$$

where $e(t) = x(t) - x(t_k)$ for $t \in [t_k, t_{k+1})$.

Define an invertible matrix U with proper dimensions, and the following equality always holds:

$$\begin{aligned} &2\left(Ax(t) - \dot{x}(t) + BKx(t-d(t))\right)^T U\left(\alpha_1 x(t) + \alpha_2 x(t-d(t)) + \alpha_3\dot{x}(t)\right)) \\ =&\xi(t)^T \mathrm{sym}\left\{(e_1A^T + e_2K^TB^T - e_4)U(\alpha_1 e_1^T + \alpha_2 e_2^T + \alpha_3 e_4^T)\right\}\xi(t) = 0 \end{aligned} \tag{4.17}$$

where α_i $(i = 1,2,3)$ are given scalars, which are used to modify the controller and event-triggered matrix.

In accordance with inequalities (4.12)-(4.17), we have the following inequality:

$$\dot{V}(t) \leq \xi(t)^T \Psi \xi(t) < 0 \tag{4.18}$$

Therefore, when $\omega(t) \equiv 0$, we have $\dot{V}(t) < 0$, which implies the closed-loop system (4.5) with $\omega(t) \equiv 0$ is asymptotically stable.

When $\omega(t) \neq 0$, we can define

$$J = ||z(t)||_2^2 - \gamma^2 ||\omega(t)||_2^2. \tag{4.19}$$

By inequality (4.18), under zero initial conditions, we have the following inequality:

$$\begin{aligned} J \leq & ||z(t)||_2^2 - \gamma^2 ||\omega(t)||_2^2 + V(\infty) - V(0) \\ = & \int_0^\infty \left(z^T(t) z(t) - \gamma^2 \omega^T(t) \omega(t) + \dot{V}(t, x(t)) \right) dt \\ \leq & \int_0^\infty \zeta^T(t) \Theta' \zeta(t) dt \end{aligned} \tag{4.20}$$

where

$$\begin{aligned} \zeta(t) = & \Big[\; x^T(t) \quad x^T(t - d(t)) \quad x^T(t - \bar{d}) \quad \dot{x}^T(t) \\ & \dot{x}^T(t - \bar{d}) \quad \tfrac{1}{\bar{d}} \textstyle\int_{t-\bar{d}}^t x^T(s) ds \quad \omega^T(t) \; \Big]^T, \\ \Theta' = & \begin{bmatrix} \Theta'_{11} & \Theta'_{12} \\ * & \Theta'_{22} \end{bmatrix}, \\ \Theta'_{11} = & \Psi + e_1 C^T C e_1^T + \mathrm{sym}(e_1 C^T D K e_2^T) + e_2 (DK)^T D K e_2^T, \\ \Theta'_{12} = & e_1 (U^T E + C^T F) + e_2 (DK)^T F + e_4 U^T E, \\ \Theta'_{22} = & -\gamma^2 I + F^T F. \end{aligned}$$

According to Schur complement, $\Theta' < 0$ is equivalent to the inequality (4.10), which indicates $J < 0$, so the closed-loop seat suspension system (4.5) is stable with H_∞ performance γ under the zero initial condition. The proof of this theorem is completed. ■

The controller K cannot be solved through Theorem 4.1 by the LMI toolbox directly, because it is coupled with another matrix invariable U in inequalities (4.9) and (4.10). Therefore, the following theorem is introduced to solve this issue.

Theorem 4.2 *For given positive scalars $\bar{d}$, δ, and α_i $(i = 1,2,3)$, the closed-loop system (4.5), under event-triggered scheme (4.3) and feedback controller (4.4), is asymptotically stable with H_∞ performance index γ, if there exist positive definite matrices $\tilde{Q} \in \boldsymbol{R}^{6\times6}$, $\tilde{R} \in \boldsymbol{R}^{2\times2}$, symmetric matrices $\tilde{P} \in \boldsymbol{R}^{8\times8}$, $\tilde{G} \in \boldsymbol{R}^{12\times12}$, $\tilde{Z}_i \in \boldsymbol{R}^{6\times6}$, $(i = 1,2)$, $\tilde{\Omega} \in \boldsymbol{R}^{2\times2}$, and any matrices $\tilde{Y} \in \boldsymbol{R}^{6\times6}$, $\tilde{N}_i \in \boldsymbol{R}^{6\times2}$, $(i = 1,2)$, $\tilde{H} \in \boldsymbol{R}^{12\times6}$, $\tilde{U} \in \boldsymbol{R}^{2\times2}$, and $\tilde{K} \in \boldsymbol{R}^{1\times2}$,*

satisfying the following inequalities:

$$\tilde{\Sigma} \geq 0, \tag{4.21}$$

$$\begin{bmatrix} \tilde{G} & \tilde{H} \\ * & \tilde{Q} \end{bmatrix} \geq 0, \tag{4.22}$$

$$\begin{bmatrix} \tilde{Z}_1 & \tilde{Y} & \tilde{N}_1 \\ * & \tilde{Z}_2 & \tilde{N}_2 \\ * & * & \tilde{R} \end{bmatrix} \geq 0, \tag{4.23}$$

$$\tilde{\Psi} \leq 0, \tag{4.24}$$

$$\tilde{\Theta} = \begin{bmatrix} \tilde{\Psi} & \tilde{\Theta}_1 \\ * & \Theta_2 \end{bmatrix} \leq 0 \tag{4.25}$$

where Π_i $(i = 1,2,3)$, l_i $(i = 1,2,...,5)$, Γ_i $(i = 1,2,...,5)$, e_i $(i = 1,2,...,6)$, *and* Θ_2 *are consistent with Theorem 4.1 and*

$$\begin{aligned}
\tilde{\Sigma} =& \Pi_1 \tilde{P} \Pi_1^T - \tilde{\Sigma}_1, \\
\tilde{\Sigma}_1 =& \frac{\bar{d}}{3} \Pi_2 \tilde{G} \Pi_2^T + \mathrm{sym}\left\{\Pi_2 \tilde{H} \Pi_3^T\right\}, \\
\tilde{\Psi} =& \mathrm{sym}\left\{\Gamma_1 \tilde{P} \Gamma_2^T\right\} + \Gamma_3 \tilde{Q} \Gamma_3^T - \Gamma_4 \tilde{Q} \Gamma_4^T + \bar{d} e_4 \tilde{R} e_4^T + \tilde{\Phi} + \tilde{\Xi}_1 + \tilde{\Xi}_2, \\
\tilde{\Phi} =& \bar{d} \Gamma_5 \left(\tilde{Z}_1 + \frac{1}{3}\tilde{Z}_2\right) \Gamma_5^T + \mathrm{sym}\left\{\Gamma_5 \left(\tilde{N}_1 (e_1 - e_2)^T + \tilde{N}_2 (2e_6 - e_1 - e_2)^T\right)\right\}, \\
\tilde{\Xi}_1 =& (\delta - 1) e_1 \tilde{\Omega} e_1^T + \mathrm{sym}(e_1 \tilde{\Omega} e_2^T) - e_2 \tilde{\Omega} e_2^T, \\
\tilde{\Xi}_2 =& \mathrm{sym}\left\{(e_1 \tilde{U}^T A^T + e_2 \tilde{K}^T B^T - e_4 \tilde{U}^T)(\alpha_1 e_1^T + \alpha_2 e_2^T + \alpha_3 e_4^T)\right\}, \\
\tilde{\Theta}_1 =& e_1 \begin{bmatrix} E + \tilde{U}^T C^T F & \tilde{U}^T C^T \end{bmatrix} + e_2 \begin{bmatrix} E & 0 \end{bmatrix} + e_4 \begin{bmatrix} 0 & (D\tilde{K})^T \end{bmatrix}.
\end{aligned}$$

Then, the controller and event-triggered matrix can be obtained as $K = \tilde{K}\tilde{U}^{-1}$ *and* $\Omega = \tilde{U}^{-T}\tilde{\Omega}\tilde{U}^{-1}$.

Proof. Define $\tilde{U} = U^{-1}$, $\tilde{P} = \mathrm{diag}\left\{\tilde{U}^T, \tilde{U}^T, \tilde{U}^T, \tilde{U}^T\right\} P \mathrm{diag}\left\{\tilde{U}, \tilde{U}, \tilde{U}, \tilde{U}\right\}$, $\tilde{Q} = \mathrm{diag}\left\{\tilde{U}^T, \tilde{U}^T, \tilde{U}^T\right\} Q \mathrm{diag}\left\{\tilde{U}, \tilde{U}, \tilde{U}\right\}$, $\tilde{R} = \tilde{U}^T R \tilde{U}$, $\tilde{\Omega} = \tilde{U}^T \Omega \tilde{U}$, $\tilde{G} = \mathrm{diag}\left\{\tilde{U}^T, \tilde{U}^T, \tilde{U}^T, \tilde{U}^T, \tilde{U}^T, \tilde{U}^T\right\} G \mathrm{diag}\left\{\tilde{U}, \tilde{U}, \tilde{U}, \ \tilde{U}, \tilde{U}, \tilde{U}\right\}$, $\tilde{H} = \mathrm{diag}\left\{\tilde{U}^T, \tilde{U}^T, \tilde{U}^T, \tilde{U}^T, \tilde{U}^T, \tilde{U}^T\right\} H \mathrm{diag}\left\{\tilde{U}, \tilde{U}, \tilde{U}\right\}$, $\tilde{Z}_i = \mathrm{diag}\left\{\tilde{U}^T, \tilde{U}^T, \tilde{U}^T\right\} Z_i \mathrm{diag}\left\{\tilde{U}, \tilde{U}, \tilde{U}\right\}$ $(i = 1,2)$, $\tilde{Y} = \mathrm{diag}\left\{\tilde{U}^T, \tilde{U}^T, \tilde{U}^T\right\} Y \mathrm{diag}\left\{\tilde{U}, \tilde{U}, \tilde{U}\right\}$, $\tilde{N}_i = \mathrm{diag}\left\{\tilde{U}^T, \tilde{U}^T, \tilde{U}^T\right\} N_i$ $(i = 1,2)$, $\tilde{K} = K\tilde{U}$. Pre- and post-multiplying (4.6), (4.7), (4.8), (4.9), (4.10) by $\mathrm{diag}\left\{\tilde{U}^T, \tilde{U}^T, \tilde{U}^T, \tilde{U}^T, \tilde{U}^T\right\}$, $\mathrm{diag}\left\{\tilde{U}^T, \tilde{U}^T, \tilde{U}^T, \tilde{U}^T, \tilde{U}^T, \tilde{U}^T, \tilde{U}^T, \tilde{U}^T, \tilde{U}^T\right\}$, $\mathrm{diag}\left\{\tilde{U}^T, \tilde{U}^T, \tilde{U}^T, \tilde{U}^T, \tilde{U}^T, \tilde{U}^T, \tilde{U}^T\right\}$, $\mathrm{diag}\left\{\tilde{U}^T, \tilde{U}^T, \tilde{U}^T, \tilde{U}^T, \tilde{U}^T, \tilde{U}^T\right\}$, $\mathrm{diag}\{\tilde{U}^T, \tilde{U}^T, \tilde{U}^T, \tilde{U}^T, \tilde{U}^T, \tilde{U}^T, I, I\}$, and their transpose matrices, respectively, we can get inequalities (4.21), (4.22), (4.23), (4.24), (4.25). Then, we complete the proof of this theorem. ■

4.4 Simulation results

Some simulation results of the event-triggered controller for the active seat suspension system are shown in this section. The bump, sinusoidal and random vibration responses are considered. The parameters of the active seat suspension system and the controller are shown in Table 4.1. α_i $(i = 1,2,3)$ are the weights of the system states, which influence the results of the controller and the event-triggered matrix. The values of α_i selected by both considering the stability and control performance of the system (4.5) through simulation. Based on the LMI toolbox of MATLAB, we can get the H_∞ controller K and the event-triggered matrix Ω by solving the inequalities in Theorem 4.2 as $K = [2066 \ -24.5]$ and $\Omega = \begin{bmatrix} 2550 & 50 \\ 50 & 70 \end{bmatrix}$.

Table 4.1: The active seat suspension system parameters and some given scalars

m(kg)	k(N/m)	c(Ns/m)	$\bar{d}$	δ	α_1	α_2	α_3
80	4600	300	0.5	0.2	0.1	1	30

4.4.1 Bump vibration response

A bump vibration is one common road excitation, which is often chosen to evaluate the vibration control performance for the seat suspension system in the time domain. The same bumpy road surface of (3.36) in Chapter 3 is chosen here to do the test.

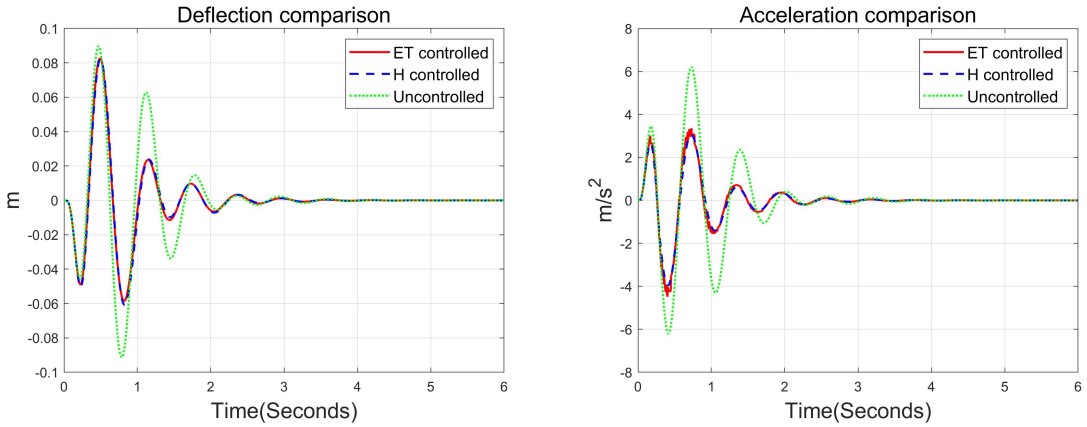

Figure 4.3: The deflection and acceleration comparison for the seat suspension system with a bump road disturbance

This bump road vibration will transfer to the vehicle suspension first and then to the seat suspension. The parameters of one quarter-truck suspension model in [89] are used here to reduce the bump disturbance at first and the output will be considered as the input disturbance of the seat suspension. To show the advantages of the event-triggered H_∞ controller, we add a conventional H_∞ controller with the same controller matrix K

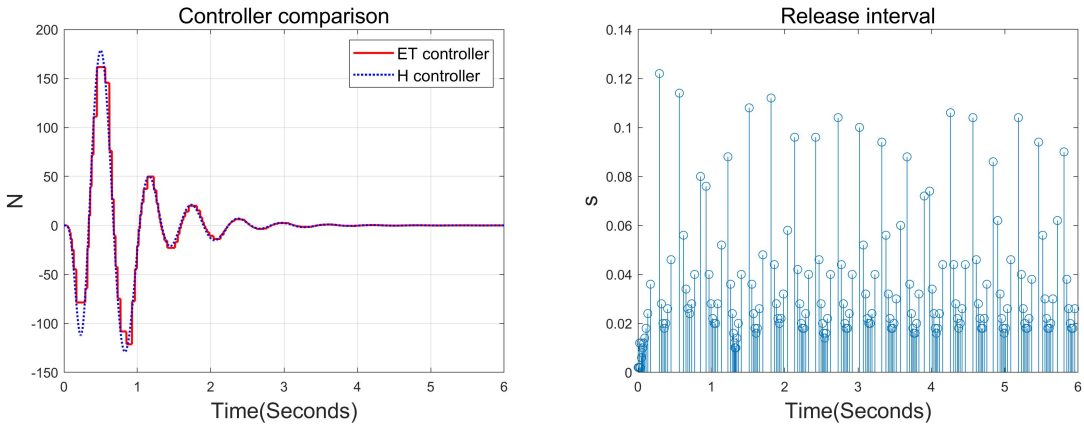

Figure 4.4: The output of the controllers, the release instants and release intervals of the seat suspension system with a bump road disturbance

without time delay to compare with the proposed controller. Figure 4.3 shows the deflection and acceleration responses comparison of the seat suspension among the controlled seat suspension systems with the event-triggered H_∞ controller (red solid curve) and the conventional H_∞ controller (blue dashed curve) and the uncontrolled seat suspension system (green dotted curve) with a bump road disturbance. These two figures imply that the deflections and accelerations are greatly reduced by both two controllers with just a small difference. Figure 4.4 shows the output of these two controllers, the release instants and release intervals with a bump road disturbance, where we can see that only some part of the system state signals is transferred to the controller by the event-trigger scheme. Compared with the output values of the two controllers, the output force signal of the event-triggered H_∞ controller does not change continuously, but only changes at the event-triggered time constants. The maximum release interval in Figure 4.4 is around 0.12 seconds, and most release intervals are much larger than the default simulation resolution, 0.002 seconds, which can largely reduce the workload of data transmission.

4.4.2 Sinusoidal vibration response

Define $z_v = 0.02\sin(1.4 \times 2\pi t)$. The sinusoidal vibration control performance of the event-triggered H_∞ controller and the conventional H_∞ controller for the seat suspension system are shown in Figures 4.5-4.6. Figure 4.5 shows the deflection and acceleration comparison of the seat suspension system, which shows that the event-triggered H_∞ controller and the conventional H_∞ controller can both reduce the amplitudes of the deflection and acceleration of the driver with just small differences with sinusoidal vibration disturbance. Figure 4.6 shows the output of the controllers, the release instants, and release intervals of the seat suspension with sinusoidal vibration disturbance. Here we can see that only a small part of the state values are transferred to the controller by the event-triggered scheme, so the output value of the event-triggered H_∞ controller only changes at

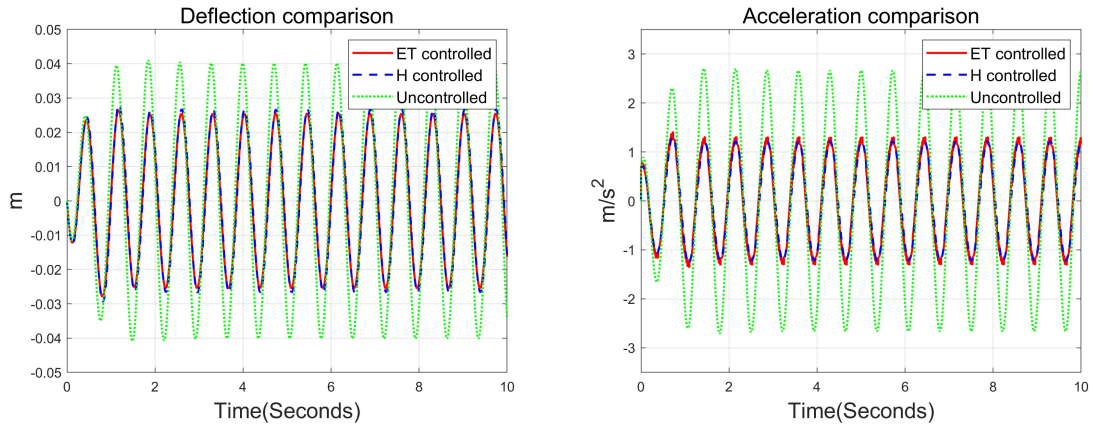

Figure 4.5: The deflection and acceleration comparison for the seat suspension system with a sinusoidal disturbance

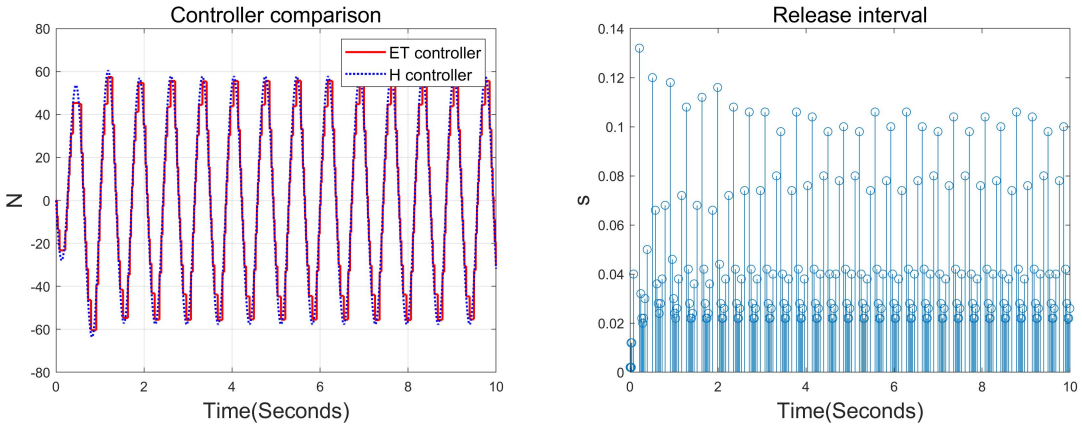

Figure 4.6: The output of the controllers, the release instants and release intervals of the seat suspension system with a sinusoidal disturbance

the event-triggered time constants. Most release intervals are much larger than the simulation resolution, so the event-triggered scheme can greatly reduce the data transmission.

4.4.3 Random vibration response

To better simulate the real road surface, a random road profile is used to test the control performance of the seat suspension system with the event-triggered H_∞ controller and the conventional H_∞ controller. Similar to the bump vibration response, the random road disturbance is firstly dealt with the quarter-truck suspension in [89] and then transferred to the active vehicle seat suspension system. Figure 4.7 shows that both the event-triggered H_∞ controller and the conventional H_∞ controller can reduce the deflection and acceleration values of the driver. Figure 4.8 shows the output of the two controllers, the release instants, and release intervals of the seat suspension system with a random road disturbance. The output force signal of both controllers is similar. Compared with the conventional H_∞ controller, the output value of the event-triggered H_∞ controller does not change continuously, but only changes at the event-triggered time constants. Similar to the responses of

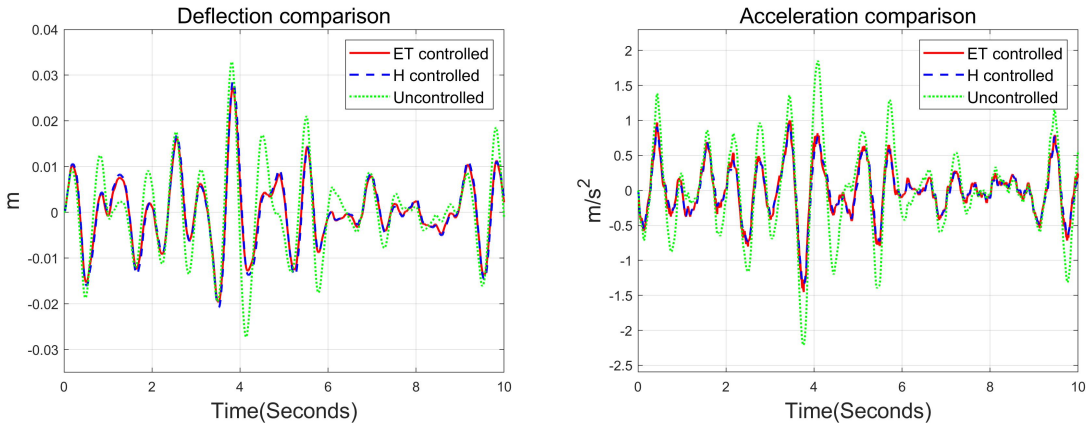

Figure 4.7: The deflection and acceleration comparison for the seat suspension system with a random road disturbance

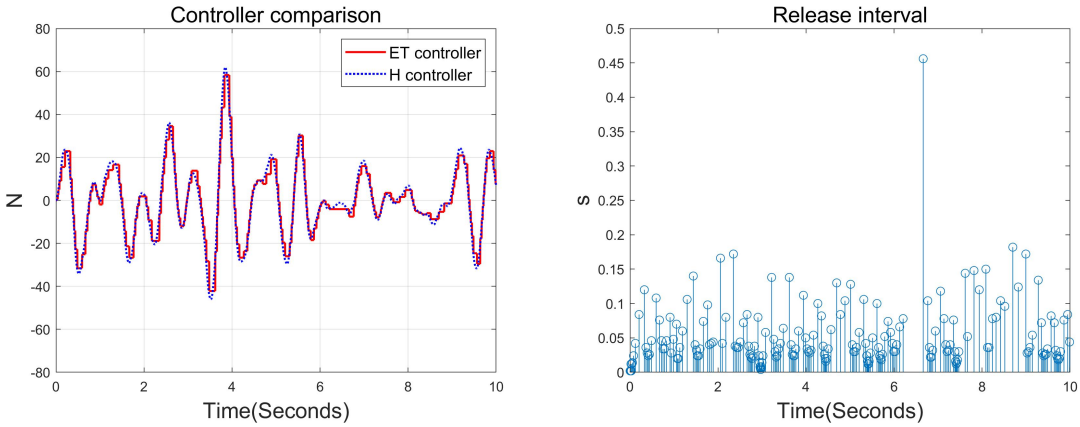

Figure 4.8: The output of the controllers, the release instants and release intervals of the seat suspension system with a random road disturbance

the bumpy road and sinusoidal disturbances, the release intervals are much larger than the simulation resolution, so the event-triggered scheme works very efficiently to reduce the workload of data transmission.

4.5 Experimental Evaluation

In this section, experimental results about the proposed control method for the active seat suspension system are shown, which include the experimental setup, the comparison of the performance of the seat suspension system with the proposed control method, the conventional H_∞ controller and uncontrolled system with several different vibration disturbances.

The experimental setup of the active seat suspension is similar to Chapter 3. The event-triggered scheme estimates whether the real-time measured data should be transferred to the controller or not. Different from the event-triggered control of other papers, which often use zero-order-holder (ZOH) to keep the measured system state values between

two triggered time instants, we use shift registers on the while loop structure here to temporarily store the event-triggered value. A case structure is used here to transfer the event-triggered data to the controller. The shift registers and case structure of the LabView instruments make it easier to operate experimental tests. When the event-trigger scheme is triggered, the condition of the case structure is true and the real-time measured data will be transferred to the controller. When the event-triggered scheme is not triggered, the condition of the case structure is false and the shift register stored data will be transferred to the controller. Therefore, it can be ensured that when $t \in [t_k, t_{k+1})$, $k \in \mathbf{N}$, the event-triggered signal keeps at $x(t_k)$, so the controller can remain constant as $u(t_k)$. The same controller K and the event-triggered matrix Ω are used here as the above section. The operating principle of the event-trigger scheme is shown in Figure 4.9.

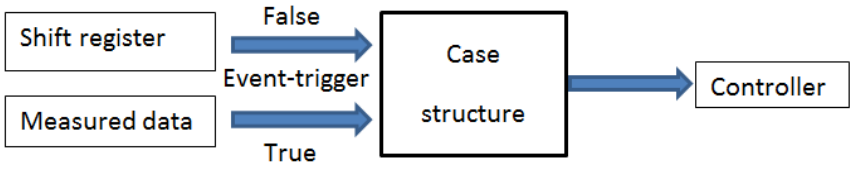

Figure 4.9: Schematic diagram of the event-trigger scheme in LabView

Several different types of vibrations (bump, sinusoidal, random vibrations) are applied to test the performance of seat suspensions. To evaluate the ride comfort of seat suspension, the seat acceleration is considered as the main factor of the experimental output signal.

4.5.1 Sinusoidal vibration

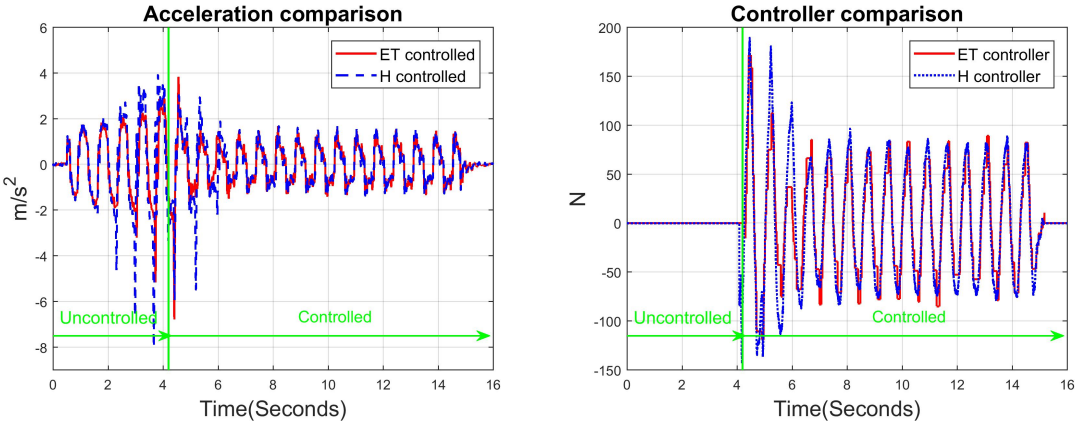

Figure 4.10: Experimental acceleration results of the seat suspension with a sinusoidal vibration and the output of the controllers

The resonant frequency of the active seat suspension is around 1.4 Hz. To show

good control performance of the proposed controller, a sinusoidal excitation is chosen as $z_v(t) = 0.02\sin(1.4 \times 2\pi t)$. The acceleration performance of the active seat suspension with two controllers and the uncontrolled seat suspension is shown in Figure 4.10. In the acceleration response figure, the left side is the performance of the uncontrolled seat suspension system. The acceleration of the seat becomes divergent because of the resonant frequency. However, when the event-triggered H_∞ controller or the conventional H_∞ controller is applied on the right side, the acceleration of the seat reduces quickly and remains in a small limited area. The control performance of these two controllers is quite similar. The output of the two controllers figure shows that the output value of the event-triggered H_∞ controller only changes at event-triggered time constants while the output value of the conventional H_∞ controller changes continuously. The average change frequency of the controller value is only 37.43 Hz (much smaller than the NI CompactRio frequency 500 Hz), so the event-trigger scheme can help to reduce the data transmission and block the effect of noise.

4.5.2 Bump and random vibration

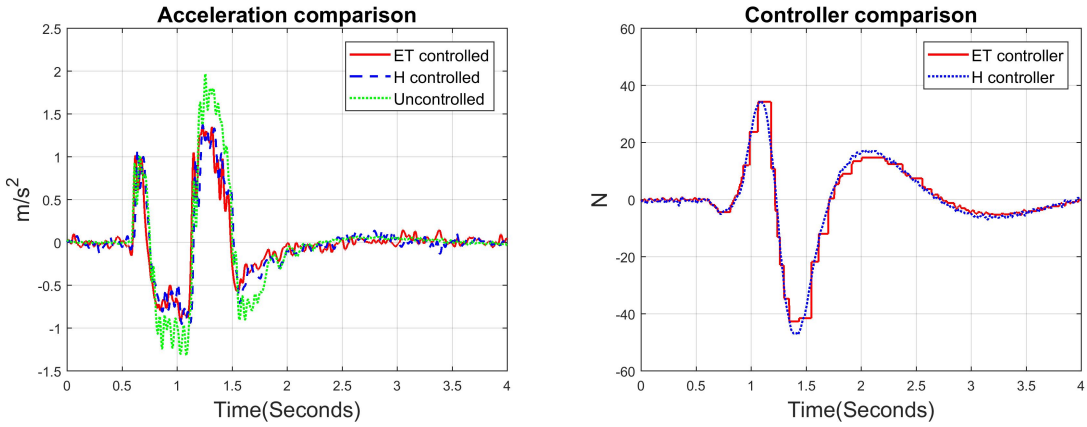

Figure 4.11: Experimental acceleration results of the seat suspension system with a bump vibration and the output of the controllers

Bump and random vibrations are similar to the real-road profiles, so these two types of road excitation are chosen to evaluate the seat suspension performance in the time domain. Similarly, as the simulation section, a bump and random vibrations are first introduced into a quarter-car vehicle suspension model with the parameter values in [90] and sprung mass displacement is used as the cab floor vibration. The 6-DOF vibration platform can generate this excitation vibration for the seat suspension system.

The same bumpy road surface (3.36) and the same random road surface (3.37) in Chapter 3 are used here to do the test.

Figure 4.11 shows the acceleration performance of the seat suspension system with a bump excitation and the output of the two controllers. It is clear to see that both the

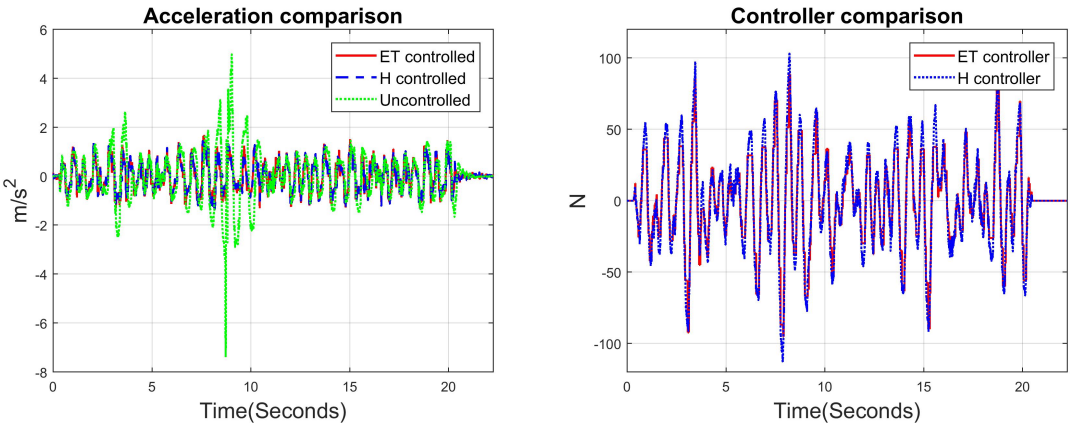

Figure 4.12: Experimental acceleration results of the seat suspension system with a random vibration and the output of the controllers

two controllers can well reduce the seat acceleration to improve the driving comfort with small differences. The output value of the proposed controller only changes at the event-triggered time instants and the average change frequency is 75 Hz during this bump excitation control which is far smaller than the NI CompactRio working frequency. Therefore, the event-triggered scheme can reduce data transmission and works as a filter to remove the influence of signal noise.

Figure 4.12 shows the acceleration performance of the seat suspension system with a random excitation and the output of the two controllers. From this figure, we can see that both the two controllers have good control performance to reduce the seat acceleration, especially for the excitation around the resonant frequency with small differences but the event-triggered H_∞ controller value only changes at event-triggered time instants. The average change frequency is only 52.19 Hz during this random excitation control, which shows the filter effect of the event-trigger scheme. Therefore, the resolution of the actuator does not need to have high-precision, which can help to reduce the cost of actuators of seat suspensions.

4.6 Conclusion

This chapter presents an event-triggered H_∞ controller for active seat suspension systems. Delay-dependent stability criteria are provided in LMI form to ensure the control system asymptotically stable and H_∞ control performance. Two tight inequalities are used to reduce the conservatism of the system to time delay. The proposed controller can reduce the workload of data transmission and remove the effect of noise as a filter. Both simulation and experimental results show the good performance of the proposed controller to balance the control performance and other system aspects (data communication load, processor load, and system cost). The H_∞ control method with a discrete event-triggered scheme is proposed in the next chapter.

Chapter 5

Discrete Event-triggered H_∞ Control Strategy

5.1 Introduction

The event-triggered H_∞ controller with a continuous event-triggered scheme is designed in the previous chapter. The event-triggered scheme can reduce the data processor and transmission load without a big influence on the control performance. However, the continuous event-triggered scheme is only theoretically possible, while data acquisition and analysis happens in discrete time in practice. To make this event-triggered control more practical, a discrete-time event-triggered H_∞ controller is designed in this chapter.

During recent years, network cloud control becomes more and more popular in different areas because of the fast development of data transmission and communication [91–94]. However, it is still a problem for the big data transmission in real-time limited by the influence of the bandwidth and the transmission rate, which brings in the state time delay or data-packet dropouts [84]. To solve this problem, event-triggered control is presented by some researchers [82], which can select valid data to transmit and discard invalid data. Therefore, in comparison with the conventional control with sampled data, it can reduce the workload of data transmission and the number of the execution of control tasks [76]. Some event-triggered control problems for vehicle suspension systems have been investigated in [95] and [72]. However, a few works of the event-triggered control for seat suspension systems have been done, which greatly motivates the authors' interest.

A discrete-time event-triggered H_∞ controller is designed for an active seat suspension system in this chapter, which considers the discrete-time state signal collection, control input, and event-triggered scheme by computer control in practice. A less conservative inequality [67] is applied here to reduce the conservation of the considered system to time delay. The results of both the simulation and experiment illustrate that the event-triggered H_∞ controller can improve the driving comfort and reduce the workload of data

transmission simultaneously.

The main contribution of this chapter is that the event-triggered H_∞ control problem is investigated for active seat suspension systems. The discrete-time event-triggered scheme is applied here to reduce the workload of data transmission, which is more suitable for practical application in comparison with the continuous-time event-triggered scheme. Both simulation and experimental tests for the seat suspension system with the event-triggered H_∞ controller are shown compared with the conventional H_∞ controlled and uncontrolled seat suspension systems in this chapter.

5.2 Seat suspension model and event-triggered scheme

The active vehicle seat suspension model system and the dynamic equation are the same as Figure 4.1 in Chapter 4.

The state-space equation of the seat suspension system is written as:

$$\begin{aligned} \dot{x}(t) &= Ax(t) + Bu(t) + E\omega(t), \\ z(t) &= Cx(t) + Du(t) + F\omega(t), \end{aligned} \tag{5.1}$$

where the state variables, disturbance, and state matrices are defined as the same as Chapter 4.

Assuming that the seat suspension system is under an event-triggered scheme, the system data are sampled and transmitted at time instants t_0, t_1,$\cdots$, t_k, t_{k+1},$\cdots$, $k \in \mathbf{N}$. The discrete-time event-triggered scheme is defined as

$$\begin{aligned} t_{k+1} =& t_k + \min_{i\in\mathbf{N}} \Big\{ ih \big| \left(x(t_k+ih) - x(t_k)\right)^T \Omega \\ & \times \left(x(t_k+ih) - x(t_k)\right) \geq \delta x^T(t_k+ih)\Omega x(t_k+ih) \Big\} \end{aligned} \tag{5.2}$$

where $\Omega > 0$, $0 < \delta < 1$.

Figure 5.1 shows the event-triggered control diagram for the considered system. Some sensors collect the real-time data of the considered system in discrete time. The event detector evaluates whether the system data should be transmitted or not through a network to the cloud by the discrete-time event-triggered scheme (5.2). If it is not triggered, the system data collected at this time instant will be discarded directly. If it is triggered, the system data will be transferred to the cloud and then to a zero-order holder (ZOH) through a network which will hold the data until the next event trigger happens. The time delay of data transmission is omitted here. Therefore, the H_∞ controller holds its value during the time intervals $[t_k, t_{k+1})$, $k \in \mathbf{N}$, which can reduce the workload of data transmission.

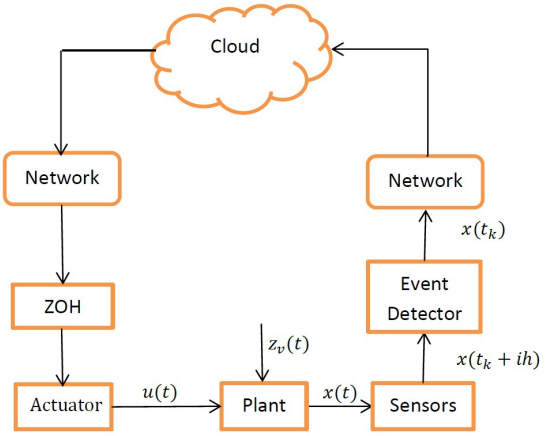

Figure 5.1: Event-triggered control diagram

The H_∞ controller is designed as

$$u(t) = Kx(t_k). \tag{5.3}$$

Then, substitute the controller (5.3) into the system (5.1), so we can get the controlled system as follows for $\forall t \in [t_k, t_{k+1})$

$$\begin{aligned} \dot{x}(t) &= Ax(t) + BKx(t_k) + E\omega(t), \\ z(t) &= Cx(t) + DKx(t_k) + F\omega(t), \end{aligned} \tag{5.4}$$

or for $\forall t \in I_i^k$

$$\begin{aligned} \dot{x}(t) &= Ax(t) + BKx(t-\tau(t)) - BKe(t-\tau(t)) + E\omega(t), \\ z(t) &= Cx(t) + DKx(t-\tau(t)) - DKe(t-\tau(t)) + F\omega(t), \end{aligned} \tag{5.5}$$

where

$$I_i^k = [t_k + ih, t_k + (i+1)h), k \in \mathbf{N}, [t_k, t_{k+1}) = \bigcup_{i=0}^{N_k} I_i^k, N_k = \frac{t_{k+1} - t_k}{h} - 1,$$
$$\tau(t) = t - t_k - ih, \dot{\tau}(t) = 1, \forall t \in I_i^k, 0 \leqslant \tau(t) \leqslant h, e(t-\tau(t)) = x(t-\tau(t)) - x(t_k), \forall t \in I_i^k.$$

5.3 The event-triggered H_∞ controller design

In this section, the event-triggered H_∞ controller is designed for the system (5.5). A less conservative inequality [67] is introduced at firstly, which is used for the following theorem to reduce the conservation of the considered system to time delay. The stability criteria of the system (5.5) are verified in the form of linear matrix inequalities (LMIs)

and the event-triggered scheme and the H_∞ controller are solved by the LMI toolbox.

Lemma 5.1 *[67] Define x as a differentiable function: $[\alpha,\beta]\to \boldsymbol{R}^n$. If there exist symmetric matrices Z_1, $Z_3\in \boldsymbol{R}^{3n\times 3n}$ and $R\in \boldsymbol{R}^{n\times n}$, any matrices $Z_2\in \boldsymbol{R}^{3n\times 3n}$ and $N_1,N_2\in \boldsymbol{R}^{3n\times n}$ which satisfy*

$$\begin{bmatrix} Z_1 & Z_2 & N_1 \\ * & Z_3 & N_2 \\ * & * & R \end{bmatrix} > 0,$$

the following inequality holds:

$$-\int_\alpha^\beta \dot{x}^T(t)R\dot{x}(t) < \varpi^T(\alpha,\beta)\Psi\varpi(\alpha,\beta),$$

where

$$\begin{aligned}\varpi(\alpha,\beta) &= \begin{bmatrix} x^T(\beta) & x^T(\alpha) & \frac{1}{\beta-\alpha}\int_\alpha^\beta x^T(s)ds \end{bmatrix}^T,\\ \Psi &= (\beta-\alpha)\left(Z_1+\frac{1}{3}Z_3\right)+\mathrm{sym}\left\{N_1\begin{bmatrix} I & -I & 0 \end{bmatrix}+N_2\begin{bmatrix} -I & -I & 2I \end{bmatrix}\right\}.\end{aligned}$$

Theorem 5.1 *For given positive scalalrs h, δ, and α_i $(i=1,2,3)$, the system (5.5) is stable with H_∞ control performance γ, if there exist symmetric positive definite matrices $P\in \boldsymbol{R}^{2\times 2}$, $R\in \boldsymbol{R}^{2\times 2}$, $Q\in \boldsymbol{R}^{2\times 2}$, $S\in \boldsymbol{R}^{2\times 2}$, $U\in \boldsymbol{R}^{2\times 2}$ symmetric matrices $Z_i\in \boldsymbol{R}^{6\times 6}$, $(i=1,2,3,4)$, $\Omega\in \boldsymbol{R}^{2\times 2}$, and any matrices $Y_i\in \boldsymbol{R}^{6\times 6}$, $(i=1,2)$, $N_i\in \boldsymbol{R}^{6\times 2}$, $(i=1,2,3,4)$ and the controller $K\in \boldsymbol{R}^{2\times 1}$ satisfying the following inequalities:*

$$\begin{bmatrix} Z_1 & Y_1 & N_1 \\ * & Z_2 & N_2 \\ * & * & R \end{bmatrix} > 0, \begin{bmatrix} Z_3 & Y_2 & N_3 \\ * & Z_4 & N_4 \\ * & * & R+Q \end{bmatrix} > 0, \tag{5.6}$$

$$\Theta_1 = \begin{bmatrix} \Xi_0+h\Xi_1+\Sigma & \Gamma_1^T \\ * & -I \end{bmatrix} < 0, \tag{5.7}$$

$$\Theta_2 = \begin{bmatrix} \Xi_0+h\Xi_2+\Sigma & \Gamma_1^T \\ * & -I \end{bmatrix} < 0, \tag{5.8}$$

where

$$\begin{aligned}
\Xi_0 =& \mathrm{sym}(e_1^T P e_5) + h e_5^T R e_5 + \eta_1^T \Lambda_1 \eta_1 + \eta_2^T \Lambda_2 \eta_2 - (e_1 - e_2)^T S (e_1 - e_2) - e_4^T \Omega e_4 \\
&+ \delta e_2^T \Omega e_2 + \mathrm{sym}(\Gamma_0^T U(\alpha_1 e_1 + \alpha_2 e_4 + \alpha_3 e_5)), \\
\Xi_1 =& e_5^T Q e_5 + \mathrm{sym}((e_1 - e_2)^T S e_5) + \eta_1^T \left(Z_1 + \frac{1}{3} Z_2 \right) \eta_1, \Xi_2 = \eta_2^T \left(Z_3 + \frac{1}{3} Z_4 \right) \eta_2, \\
\eta_1 =& \begin{bmatrix} e_2^T & e_3^T & e_6^T \end{bmatrix}^T, \eta_2 = \begin{bmatrix} e_1^T & e_2^T & e_7^T \end{bmatrix}^T, \\
e_i =& \begin{bmatrix} 0_{2\times 2(i-1)} & I_2 & 0_{2\times 2(8-i)} \end{bmatrix}, i = 1, 2, \cdots, 8, \\
\Lambda_1 =& \mathrm{sym}\left\{ N_1 [\, I \quad -I \quad 0 \,] + N_2 [\, -I \quad -I \quad 2I \,] \right\}, \\
\Lambda_2 =& \mathrm{sym}\left\{ N_3 [\, I \quad -I \quad 0 \,] + N_4 [\, -I \quad -I \quad 2I \,] \right\}, \\
\Gamma_0 =& -e_5 + A e_1 + BK e_2 - BK e_4 + E e_8, \Gamma_1 = C e_1 + DK e_2 - DK e_4 + F e_8, \Sigma = -\gamma^2 e_8^T e_8.
\end{aligned}$$

Proof. Firstly, to prove the system (5.5) is stable, we define the Lyapunov functional as follows:

$$V(t) = V_1(t) + V_2(t) + V_3(t) + V_4(t) \tag{5.9}$$

where

$$\begin{aligned}
V_1(t) =& x^T(t) P x(t), V_2(t) = \int_{-h}^{0} \int_{t+s}^{t} \dot{x}^T(v) R \dot{x}(v) dv ds, \\
V_3(t) =& (h - \tau(t)) \int_{t_k + ih}^{t} \dot{x}^T(s) Q \dot{x}(s) ds, \\
V_4(t) =& (h - \tau(t)) [x(t) - x(t_k + ih)]^T S [x(t) - x(t_k + ih)].
\end{aligned}$$

By noticing that

$$V_3((t_k + ih)^+) = V_3((t_k + (i+1)h)^-) = 0, V_4((t_k + ih)^+) = V_4((t_k + (i+1)h)^-) = 0,$$

we can find $V_3(t)$ and $V_4(t)$ are continuous at time instants $t_k + ih$, but not necessarily derivable. Therefore, we only need to prove $\dot{V}(t) < 0$ at time intervals $(t_k + ih, t_k + (i+1)h)$ to verify the system (5.5) is stable.

Define a state vector as

$$\begin{aligned}
\xi(t) = \Big[& x^T(t) \quad x^T(t - \tau(t)) \quad x^T(t - h) \quad e^T(t - \tau(t)) \quad \dot{x}^T(t) \\
& \tfrac{1}{h - \tau(t)} \textstyle\int_{t-h}^{t-\tau(t)} x^T(s) ds \quad \tfrac{1}{\tau(t)} \textstyle\int_{t-\tau(t)}^{t} x^T(s) ds \quad \omega^T(t) \Big]^T.
\end{aligned}$$

Then, the derivative of $V(t)$ can be calculated as follows.

$$\dot{V}_1(t) = \text{sym}\{x^T(t)P\dot{x}^T(t)\} = \xi^T(t)\left\{\text{sym}(e_1^T P e_5)\right\}\xi(t), \tag{5.10}$$

$$\begin{aligned}\dot{V}_2(t) =& h\dot{x}^T(t)R\dot{x}(t) - \int_{t-h}^{t}\dot{x}^T(s)R\dot{x}(s)ds \\ =& \xi^T(t)(he_5^T R e_5)\xi(t) - \int_{t-h}^{t}\dot{x}^T(s)R\dot{x}(s)ds,\end{aligned} \tag{5.11}$$

$$\begin{aligned}\dot{V}_3(t) =& -\int_{t_k+ih}^{t}\dot{x}^T(s)Q\dot{x}(s)ds + (h-\tau(t))\dot{x}^T(t)Q\dot{x}(t) \\ \leq& -\int_{t_k+ih}^{t}\dot{x}^T(s)Q\dot{x}(s)ds + \xi^T(t)(h-\tau(t))e_5^T Q e_5\xi(t),\end{aligned} \tag{5.12}$$

$$\begin{aligned}\dot{V}_4(t) =& -[x(t)-x(t_k+ih)]^T S[x(t)-x(t_k+ih)] + \text{sym}\{(h-\tau(t))[x(t)-x(t_k+ih)]^T S\dot{x}(t)\} \\ =& \xi^T(t)\left\{-(e_1-e_2)^T S(e_1-e_2) + \text{sym}\left[(h-\tau(t))(e_1-e_2)^T S e_5\right]\right\}\xi(t).\end{aligned} \tag{5.13}$$

Based on Lemma 5.1, we can get

$$\begin{aligned}&-\int_{t-h}^{t}\dot{x}^T(s)R\dot{x}(s)ds - \int_{t_k+ih}^{t}\dot{x}^T(s)Q\dot{x}(s)ds \\ =& -\int_{t-h}^{t-\tau(t)}\dot{x}^T(s)R\dot{x}(s)ds - \int_{t-\tau(t)}^{t}\dot{x}^T(s)(R+Q)\dot{x}(s)ds \\ \leq& \varpi_1^T(t-h,t-\tau(t))\Psi_1\varpi_1(t-h,t-\tau(t)) + \varpi_2^T(t-\tau(t),t)\Psi_2\varpi_2(t-\tau(t),t) \\ =& \xi^T(t)\left[\eta_1^T\Psi_1\eta_1 + \eta_2^T\Psi_2\eta_2\right]\xi(t),\end{aligned} \tag{5.14}$$

where

$$\begin{aligned}\Psi_1 =& (h-\tau(t))\left(Z_1 + \frac{1}{3}Z_2\right) + \text{sym}\left\{N_1[\ I\quad -I\quad 0\ ] + N_2[\ -I\quad -I\quad 2I\ ]\right\}, \\ \Psi_2 =& \tau(t)\left(Z_3 + \frac{1}{3}Z_4\right) + \text{sym}\left\{N_3[\ I\quad -I\quad 0\ ] + N_4[\ -I\quad -I\quad 2I\ ]\right\}.\end{aligned}$$

According to the event-triggered scheme (5.2), we have

$$[x(t_k+ih)-x(t_k)]^T\,\Omega\,[x(t_k+ih)-x(t_k)] < \delta x^T(t_k+ih)\Omega x(t_k+ih). \tag{5.15}$$

Take notice of that for a positive symmetric matrix $U \in \mathbf{R}^{2\times 2}$, according to the system (5.5) the following condition always holds:

$$\begin{aligned}0 =& \text{sym}\left\{[-\dot{x}(t) + Ax(t) + BKx(t-\tau(t)) - BKe(t-\tau(t)) \right. \\ & \left. + E\omega(t)]^T U\left[\alpha_1 x(t) + \alpha_2 e(t-\tau(t)) + \alpha_3\dot{x}(t)\right]\right\} \\ =& \text{sym}\left\{\xi^T(t)(-e_5 + Ae_1 + BKe_2 - BKe_4 + Ee_8)^T \right. \\ & \left. \times U(\alpha_1 e_1 + \alpha_2 e_4 + \alpha_3 e_5)\xi(t)\right\},\end{aligned} \tag{5.16}$$

where α_i $(i=1,2,3)$ are given scalars, which are used to modify the controller and event-triggered scheme.

Notice $t-\tau(t)=t_k+ih$, $e(t-\tau(t))=x(t_k+ih)-x(t_k)$, and then by combining inequalities from (5.10) to (5.16) we can get

$$\dot{V}(t)\leq \xi^T(\Xi_0+(h-\tau(t))\Xi_1+\tau(t)\Xi_2)\xi(t) \tag{5.17}$$

Then, we define

$$J=\|z(t)\|_2^2-\gamma^2\|\omega(t)\|_2^2. \tag{5.18}$$

By combining inequalities (5.17) and (5.18), we have

$$\begin{aligned} J\leq&\|z(t)\|_2^2-\gamma^2\|\omega(t)\|_2^2+V(\infty)-V(0)\\ =&\int_0^\infty \left(z^T(t)z(t)-\gamma^2\omega^T(t)\omega(t)+\dot{V}(t)\right)dt\leq\int_0^\infty \xi^T(t)\Phi\xi(t)dt \end{aligned} \tag{5.19}$$

where

$$\Phi=\Xi_0+(h-\tau(t))\Xi_1+\tau(t)\Xi_2+\Sigma+\Gamma_1^T\Gamma_1. \tag{5.20}$$

According to Schur Complement, $\Phi<0$ is equivalent to $\Theta<0$, where

$$\Theta=\begin{bmatrix} \Xi_0+(h-\tau(t))\Xi_1+\tau(t)\Xi_2+\Sigma & \Gamma_1^T\\ * & -I \end{bmatrix}. \tag{5.21}$$

Here by noticing that $\Theta<0$ is equal to $\Theta_1<0$ and $\Theta_2<0$, we have $J<0$, so the seat suspension system (5.5), under the zero initial condition, is stable with H_∞ performance γ. Then, the proof of this theorem has been completed. ■

In Theorem 5.1, the controller K is coupled with a matrix variable U, so it cannot be solved directly through the LMI toolbox. To solve this problem, the following theorem is introduced.

Theorem 5.2 *For given positive scalalrs h, δ, and α_i $(i=1,2,3)$, the system (5.5) is stable with H_∞ control performance γ, if there exist symmetric positive definite matrices $\bar{P}\in\boldsymbol{R}^{2\times2}$, $\bar{R}\in\boldsymbol{R}^{2\times2}$, $\bar{Q}\in\boldsymbol{R}^{2\times2}$, $\bar{S}\in\boldsymbol{R}^{2\times2}$, $\bar{U}\in\boldsymbol{R}^{2\times2}$ symmetric matrices $\bar{Z}_i\in\boldsymbol{R}^{6\times6}$, $(i=1,2,3,4)$, $\bar{\Omega}\in\boldsymbol{R}^{2\times2}$, and any matrices $\bar{Y}_i\in\boldsymbol{R}^{6\times6}$, $(i=1,2)$, $\bar{N}_i\in\boldsymbol{R}^{6\times2}$, $(i=1,2,3,4)$ and the controller $\bar{K}\in\boldsymbol{R}^{2\times1}$ satisfying the following inequalities:*

$$\begin{bmatrix} \bar{Z}_1 & \bar{Y}_1 & \bar{N}_1\\ * & \bar{Z}_2 & \bar{N}_2\\ * & * & \bar{R} \end{bmatrix}>0,\begin{bmatrix} \bar{Z}_3 & \bar{Y}_2 & \bar{N}_3\\ * & \bar{Z}_4 & \bar{N}_4\\ * & * & \bar{R}+\bar{Q} \end{bmatrix}>0, \tag{5.22}$$

$$\bar{\Theta}_1=\begin{bmatrix} \bar{\Xi}_0+h\bar{\Xi}_1+\bar{\Sigma} & \bar{\Gamma}_1^T\\ * & -I \end{bmatrix}<0, \tag{5.23}$$

$$\bar{\Theta}_2 = \begin{bmatrix} \bar{\Xi}_0 + h\bar{\Xi}_2 + \bar{\Sigma} & \bar{\Gamma}_1^T \\ * & -I \end{bmatrix} < 0, \tag{5.24}$$

where

$$\begin{aligned}
\bar{\Xi}_0 =& \text{sym}(e_1^T \bar{P} e_5) + h e_5^T \bar{R} e_5 + \eta_1^T \bar{\Lambda}_1 \eta_1 + \eta_2^T \bar{\Lambda}_2 \eta_2 - (e_1 - e_2)^T \bar{S}(e_1 - e_2) - e_4^T \bar{\Omega} e_4 \\
&+ \delta e_2^T \bar{\Omega} e_2 + \text{sym}(\bar{\Gamma}_0^T(\alpha_1 e_1 + \alpha_2 e_4 + \alpha_3 e_5)), \\
\bar{\Xi}_1 =& e_5^T \bar{Q} e_5 + \text{sym}((e_1 - e_2)^T \bar{S} e_5) + \eta_1^T \left(\bar{Z}_1 + \frac{1}{3}\bar{Z}_2 \right) \eta_1, \bar{\Xi}_2 = \eta_2^T \left(\bar{Z}_3 + \frac{1}{3}\bar{Z}_4 \right) \eta_2, \\
\eta_1 =& \begin{bmatrix} e_2^T & e_3^T & e_6^T \end{bmatrix}^T, \eta_2 = \begin{bmatrix} e_1^T & e_2^T & e_7^T \end{bmatrix}^T, \\
e_i =& \begin{bmatrix} 0_{2\times 2(i-1)} & I_2 & 0_{2\times 2(8-i)} \end{bmatrix}, i = 1, 2, \cdots, 8, \\
\bar{\Lambda}_1 =& \text{sym}\left\{ \bar{N}_1 [\, I \quad -I \quad 0 \,] + \bar{N}_2 [\, -I \quad -I \quad 2I \,] \right\}, \\
\bar{\Lambda}_2 =& \text{sym}\left\{ \bar{N}_3 [\, I \quad -I \quad 0 \,] + \bar{N}_4 [\, -I \quad -I \quad 2I \,] \right\}, \\
\bar{\Gamma}_0 =& -\bar{U} e_5 + A\bar{U} e_1 + B\bar{K} e_2 - B\bar{K} e_4 + E e_8, \\
\bar{\Gamma}_1 =& C\bar{U} e_1 + D\bar{K} e_2 - D\bar{K} e_4 + F e_8, \bar{\Sigma} = -\gamma^2 e_8^T e_8.
\end{aligned}$$

and then the event-triggered controller can be obtained as $K = \bar{K}\bar{U}^{-1}$, *and* $\Omega = \bar{U}^{-T}\Omega\bar{U}^{-1}$.

Proof. Define $\bar{U} = U^{-1}$, $\bar{P} = \bar{U}^T P \bar{U}$, $\bar{R} = \bar{U}^T R \bar{U}$, $\bar{Q} = \bar{U}^T Q \bar{U}$, $\bar{S} = \bar{U}^T S \bar{U}$, $\bar{\Omega} = \bar{U}^T \Omega \bar{U}$, $\bar{Z}_i = \text{diag}\left\{\bar{U}^T, \bar{U}^T, \bar{U}^T\right\} Z_i \text{diag}\{\bar{U}, \bar{U}, \bar{U}\}$, $(i = 1, 2, 3, 4)$, $\bar{Y}_i = \text{diag}\left\{\bar{U}^T, \bar{U}^T, \bar{U}^T\right\} Y_i \text{diag}\{\bar{U}, \bar{U}, \bar{U}\}$, $(i = 1, 2)$, $\bar{N}_i = \text{diag}\left\{\bar{U}^T, \bar{U}^T, \bar{U}^T\right\} N_i$, $(i = 1, 2, 3, 4)$. Pre- and post-multiplying (5.6) by $\text{diag}\left\{\bar{U}^T, \bar{U}^T, \bar{U}^T, \bar{U}^T, \bar{U}^T, \bar{U}^T, \bar{U}^T\right\}$ and $\text{diag}\{\bar{U}, \bar{U}, \bar{U}, \bar{U}, \bar{U}, \bar{U}, \bar{U}\}$, we can get inequation (5.22). Similarly, pre- and post-multiplying (5.7) and (5.8) by $\text{diag}\left\{\bar{U}^T, \bar{U}^T, \bar{U}^T, \bar{U}^T, \bar{U}^T, \bar{U}^T, \bar{U}^T, I, I\right\}$ and $\text{diag}\{\bar{U}, \bar{U}, \bar{U}, \bar{U}, \bar{U}, \bar{U}, \bar{U}, I, I\}$, we can get inequations (5.23) and (5.24). Hence, the proof of this theorem is completed. ■

5.4 Simulation results

Some simulation results are shown in this section to illustrate the effectiveness of the event-triggered H_∞ controller for the considered system. The parameters of the seat suspension system and some given scalars are shown in Table 5.1. Based on LMI toolbox of MATLAB and Theorem 5.2, the H_∞ controller and event-triggered scheme are solved as $K = [\, 1658 \quad -489 \,]$ and $\Omega = \begin{bmatrix} 7974 & 679 \\ 679 & 375 \end{bmatrix}$.

Table 5.1: The parameters of the active seat suspension system and some given scalars

m(kg)	k(N/m)	c(Ns/m)	$h(s)$	δ	α_1	α_2	α_3
80	4600	300	0.002	0.2	1	1	0.1

5.4.1 Bumpy road response

A bumpy road disturbance is a very common road disturbance for vehicles, so it is chosen here to test the control performance for the seat suspension system (5.5). The same bumpy road surface (3.36) in Chapter 3 is used here to do the test.

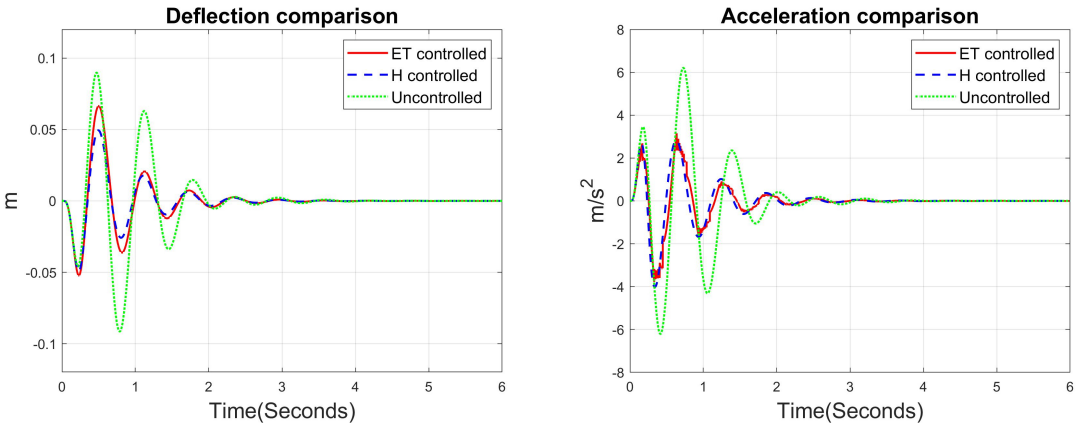

Figure 5.2: The deflection and acceleration comparison for the considered system with a bumpy road disturbance

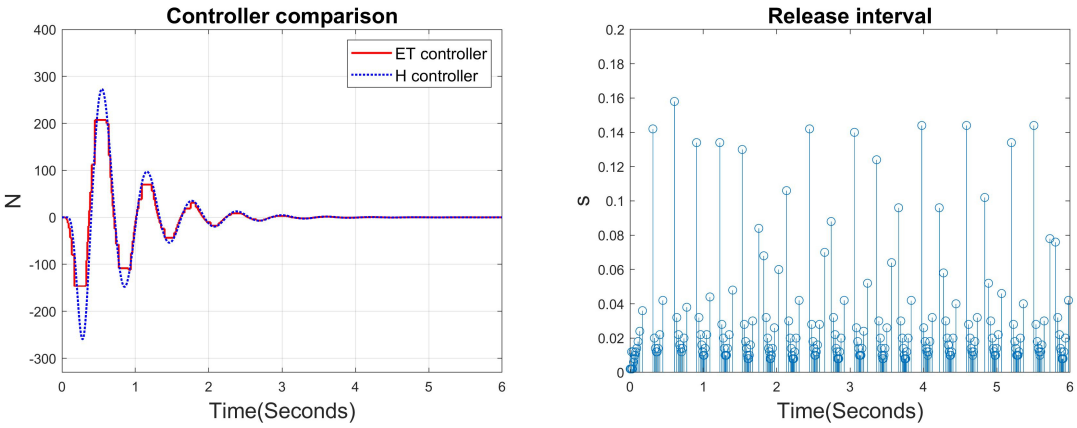

Figure 5.3: The control output comparison between the event-triggered H_∞ controller and the conventional H_∞ controller and the release intervals of the event-triggered scheme with a bumpy road disturbance

The bumpy road disturbance firstly transfers to one quarter-truck suspension model in [89] and the output is considered as the input disturbance of the considered system. Here we introduce a conventional H_∞ controller $K = \begin{bmatrix} 3391 & -302 \end{bmatrix}$, which is calculated according to the basic H_∞ controller design method. To compare with the event-triggered H_∞ controller reasonably, we introduce a small time delay 0.05 s for the conventional H_∞ controller. Figure 5.2 shows the deflection and acceleration comparison among the event-triggered H_∞ controlled (red solid curve), the conventional H_∞ controlled (blue dashed curve), and the uncontrolled (green dotted curve) seat suspension systems with a bumpy

road disturbance. Here we can see that compared with the uncontrolled seat suspension system, both the event-triggered H_∞ controller and the conventional H_∞ controller can both reduce the seat suspension deflection and the drivers' acceleration. Figure 5.3 shows the control output comparison between the event-triggered H_∞ controller and the conventional H_∞ controller and the release intervals of the event-triggered scheme. Here we can see that compared with the conventional H_∞ controller, the output value of the event-triggered H_∞ controller only changes when the event-triggered scheme is triggered, which greatly reduces the workload of the data transmission and the requirement of the actuator precision.

5.4.2 Sinusoidal disturbance response

The sinusoidal disturbance response is tested here for the active seat suspension system. Define $z_v(t) = 0.02\sin(1.6 \times 2\pi t)$. The control performance is shown in Figures 5.4 and 5.5. From Figure 5.4, we can see that both the event-triggered H_∞ controller and the conventional H_∞ controller can decrease both the seat suspension deflection and the drivers' acceleration, compared with the uncontrolled seat suspension system. From Figure 5.5, we can see that compared with the conventional H_∞ controller, the value of output of the event-triggered H_∞ controller only changes at event-triggered time points. Similarly, with the bumpy road disturbance, the event-triggered H_∞ controller can reduce the workload of the data transmission and the requirement of the actuator precision for the active seat suspension system with the sinusoidal disturbance.

Table 5.2: The average data transmission times per second

disturbance type	event-triggered H_∞ controller	conventional H_∞ controller	reduction percentage
bumpy road	35.5	500	92.9%
sinusoidal	46.9	500	90.6%

The working frequency of the simulation test is chosen as 500 Hz. Table 5.2 shows the average data transmission times per second of the event-triggered H_∞ controller and the conventional H_∞ controller for two different kinds of disturbances. The event-triggered scheme can reduce 92.9% (for bumpy road disturbance) and 90.6% (for sinusoidal disturbance) of the workload of data transmission without big influence on the control performance to improve the driving comfort, which shows the great effectiveness and efficiency of the event-triggered H_∞ control method for the considered system.

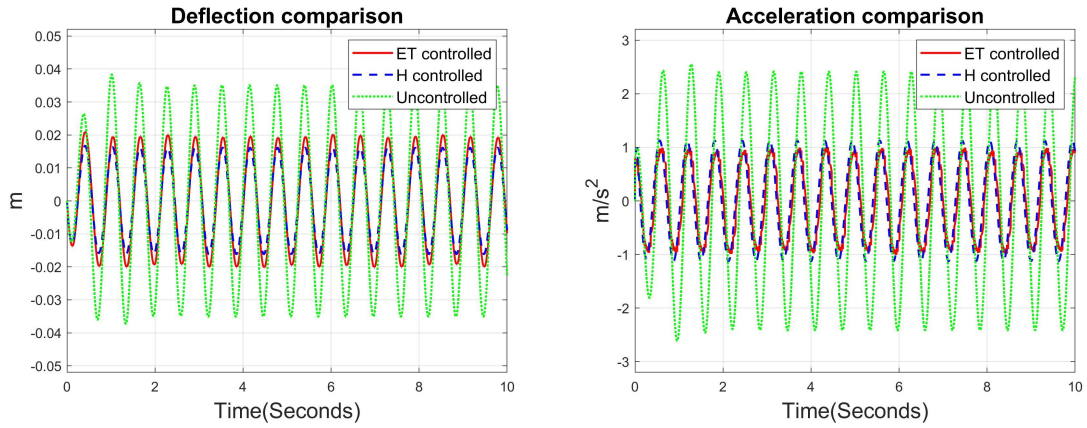

Figure 5.4: The deflection and acceleration comparison for the considered system with a sinusoidal disturbance

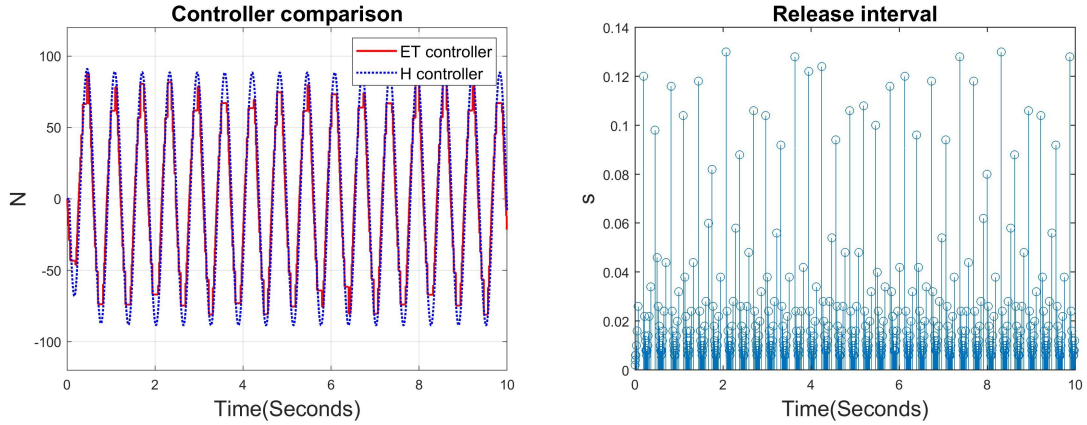

Figure 5.5: The control output comparison between the event-triggered H_∞ controller and the conventional H_∞ controller and the release intervals of the event-triggered scheme with a sinusoidal disturbance

5.5 Experimental results

In this section, the experimental results for the active seat suspension system are given, which contain the experimental setup, the comparison of the control performance of the considered system with the event-triggered H_∞ controller and the conventional H_∞ controller, and the response of the uncontrolled system with a random road disturbance. The experimental setup is similar to Chapter 3.

Random road disturbances are another common disturbance for vehicles. To test the control performance of the proposed method under experimental conditions, the same random road surface (3.37) in Chapter 3 is used here to do the test.

Figure 5.6 shows some experimental results of the proposed controller. The first figure shows the acceleration comparison for the active seat suspension system with the event-triggered H_∞ controller and the conventional H_∞ controller and the uncontrolled system,

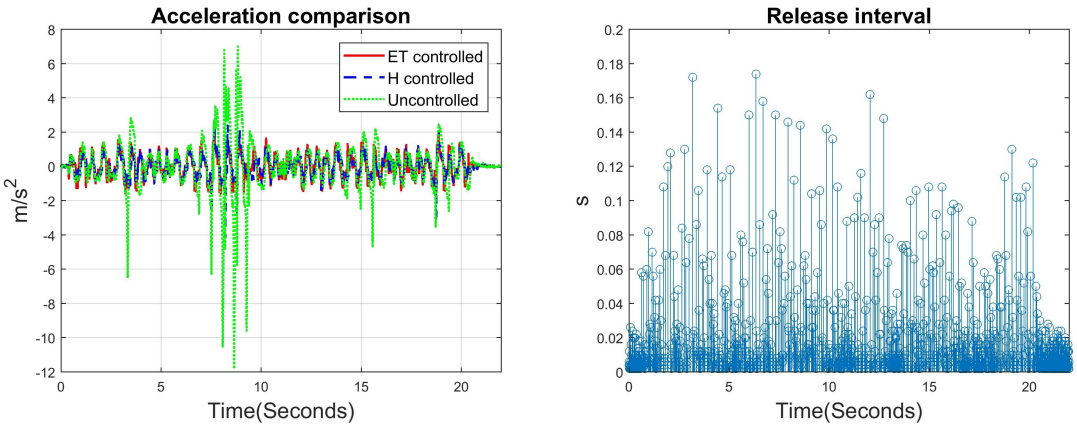

Figure 5.6: The acceleration comparison for the considered system and the release intervals of the event-triggered scheme with a random disturbance

where we can see that compared with the uncontrolled system, both of the two controllers can reduce the drivers' acceleration with little difference, especially around the resonant frequency of the seat suspension system. The second figure shows the release intervals generated by the event-triggered scheme. Here we can see that data transmission only happens when the event-triggered scheme is triggered. The working frequency of the computers and NI CompactRio is 500 Hz. Compared with the conventional H_∞ controlled system (500 Hz), the average frequency of the data transmission of the event-triggered H_∞ controlled seat suspension system is 66.77 Hz with a random road disturbance, which can reduce 86.65% of the workload of data transmission without a big influence on the control performance. Therefore, the event-triggered H_∞ controller also has a good control performance in the experimental situation to reduce the workload of the data transmission.

5.6 Conclusion

The event-triggered H_∞ control method is established for active seat suspension systems in this chapter, which considers the discrete-time data collection and control input with time delay. Some Lyapunov functions are chosen to verify that the considered system is stable and a less conservative inequality is applied to reduce the system conservation to time delay. Some simulation results show that for a bumpy road and a sinusoidal disturbance, the event-triggered H_∞ controller has a similar control performance to reduce the vibration with the conventional H_∞ controller with a big workload reduction of the data transmission. The experimental results also illustrate the efficiency and effectiveness of the proposed event-triggered H_∞ controller to improve the driving comfort and reduce data transmission for the considered system with a random disturbance under experimental conditions. The next chapter considers the event-triggered control for more complicated seat suspension systems, such as the human-in-loop seat suspension system.

Chapter 6

Output-feedback H_∞ Control Strategy

6.1 Introduction

The previous chapter introduces the discrete-time event-triggered H_∞ control method for active seat suspension systems. The discrete-time scheme considers the actual work conditions of data acquisition and analysis and can reduce data transmission, which is useful for network cloud control for seat suspension systems. This chapter considers a more complicated seat suspension system, which also considers a human body in the loop to design the system and the controller.

Some previous works of some researchers simplify the seat suspension into a second-order system and use the absolute or relative displacement and velocity of the seat suspension as the system states [96]. Other works consider the human body in the loop and define a more complicated seat suspension system with different human body models such as [97]. The seat suspension system with a human body in the loop is closer to the real practical situation, while it is more difficult to deal with the control problem of such complicated systems.

The system states are measured through discrete sampling by different types of sensors. Generally, the higher the sampling accuracy is, the more easily the system can be controlled because it can minimize the impact of time delay on the system [98]. However, the smaller the sampling time is, the more data it produces per unit time, but not all of the data are necessary for the controller, which increases the burden of data transmission and leads to time-delay problem [99]. Event-triggered control is one approach to deal with this problem which can evaluate if it is necessary to transmit the current data [100].

In most previous suspension related works, the absolute or relative displacement and velocity signals are considered as system states while the acceleration signals are not considered even though they can be easily measured in real-time by acceleration sensors [101]. Moreover, absolute displacement or velocity signals usually cannot be measured in real-time in practice. In this chapter, the human body is simply separated into two parts

(head and body torso), which is considered as part of the seat suspension system together with the seat frame. The relative displacements, velocities, and accelerations of each part are defined as system states, which makes the seat suspension system a singular system [102]. The outputs of this system are chosen as the deflection and relative velocity of the seat frame, the accelerations of the upper seat suspension, body torso, and head, so these signals are easily measured in real-time. The output feedback controller design is only based on the measurable states, which makes the control method more practical. Then the discrete output event-triggered scheme is designed for the seat suspension system, which can avoid the 'redundant' data packets and reduce the workload of data transmission.

The main contributions of this chapter are listed as follows.

- A singular seat suspension system with a human body in the loop is established. Compared with traditional seat suspension systems, the singular seat suspension system also defines the acceleration signals as system states, which makes full use of all measurable signals in real-time.
- The output feedback controller of the active singular seat suspension system is designed by only using easily measurable state variables, which makes the control method more practical.
- The discrete-time event-triggered scheme is designed for the singular active seat suspension system, which can make the value of the controller only changes when the defined event triggers. Therefore, it can reduce the processor load and data transmission load.
- The output-feedback H_∞ controller is designed at first and then the event-triggered scheme is designed based on the obtained controller. Compared with the traditional output-feedback controller, this two-step design method can minimize the complication of the control system, especially for this complicated seat suspension system, which makes the control process simpler.

6.2 Model of singular active seat suspension system with a human body

Figure 6.1 shows the simplified active seat suspension with human body model. m_h, m_b, and m_s are the masses of human's head, body torso, and seat frame, respectively; k_h, k_b, k_s are their spring stiffness, respectively; c_h, c_b, c_s are their damping coefficients, respectively; u is the active control input; z_h, z_b, z_s and z_v are the displacements of human head, body torso, seat frame and the base platform, respectively. The dynamic equations

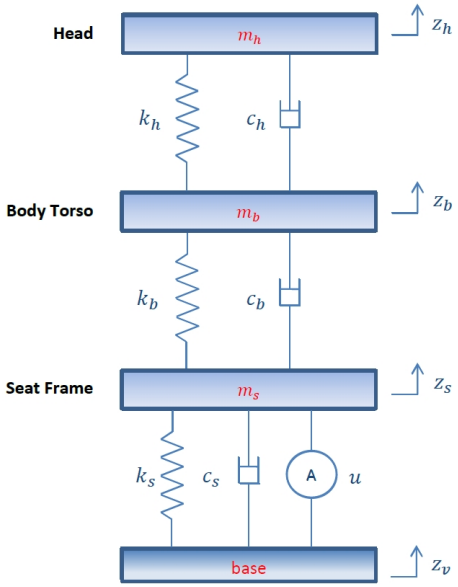

Figure 6.1: Active seat suspension with a human body model

of this model for each part can be derived as follows. Seat frame:

$$m_s\ddot{z}_s = -k_s(z_s - z_v) - c_s(\dot{z}_s - \dot{z}_v) + k_b(z_b - z_s) + c_b(\dot{z}_b - \dot{z}_s) + u \tag{6.1}$$

Body torso:

$$m_b\ddot{z}_b = -k_b(z_b - z_s) - c_b(\dot{z}_b - \dot{z}_s) + k_h(z_h - z_b) + c_h(\dot{z}_h - \dot{z}_b) \tag{6.2}$$

Head:

$$m_h\ddot{z}_h = -k_h(z_h - z_b) - c_h(\dot{z}_h - \dot{z}_b) \tag{6.3}$$

Here we define some state variables as

$$\begin{aligned} x_1 =& z_s - z_v, x_2 = \dot{z}_s - \dot{z}_v, x_3 = \ddot{z}_s, x_4 = z_b - z_s, x_5 = \dot{z}_b - \dot{z}_s, \\ x_6 =& \ddot{z}_b, x_7 = z_h - z_b, x_8 = \dot{z}_h - \dot{z}_b, x_9 = \ddot{z}_h, \end{aligned}$$

and the state vector as $x = \begin{bmatrix} x_1 & x_2 & x_3 & x_4 & x_5 & x_6 & x_7 & x_8 & x_9 \end{bmatrix}^T$. The deflection variable between seat frame and the base platform x_1 can be measured by a laser displacement sensor in real-time and its relative velocity x_2 can be derived by differentiating x_1. The acceleration variables of the seat frame x_3, body torso x_6, and human's head x_9 can be measured by accelerometers in real-time. These five measurable system state variables are chosen as the system state output y, which are used to design the output-feedback controller. The human head's acceleration is closely related to the driving comfort, so x_9 is chosen as the system performance output z. Define the disturbance of the seat suspen-

sion system as $\omega = \ddot{z}_v$. Then, the state space equation of the seat active suspension system with a human body can be written as follows:

$$\begin{aligned} E\dot{x}(t) &= Ax(t) + Bu(t) + F\omega(t), \\ y(t) &= Cx(t), \\ z(t) &= Dx(t), \end{aligned} \tag{6.4}$$

where

$$E = \begin{bmatrix} 1 & 0 & 0 & 0 & 0 & 0 & 0 & 0 & 0 \\ 0 & 1 & 0 & 0 & 0 & 0 & 0 & 0 & 0 \\ 0 & 0 & 0 & 0 & 0 & 0 & 0 & 0 & 0 \\ 0 & 0 & 0 & 1 & 0 & 0 & 0 & 0 & 0 \\ 0 & 0 & 0 & 0 & 1 & 0 & 0 & 0 & 0 \\ 0 & 0 & 0 & 0 & 0 & 0 & 0 & 0 & 0 \\ 0 & 0 & 0 & 0 & 0 & 0 & 1 & 0 & 0 \\ 0 & 0 & 0 & 0 & 0 & 0 & 0 & 1 & 0 \\ 0 & 0 & 0 & 0 & 0 & 0 & 0 & 0 & 0 \end{bmatrix}, A = \begin{bmatrix} 0 & 1 & 0 & 0 & 0 & 0 & 0 & 0 & 0 \\ 0 & 0 & 1 & 0 & 0 & 0 & 0 & 0 & 0 \\ k_s & c_s & m_s & -k_b & -c_b & 0 & 0 & 0 & 0 \\ 0 & 0 & 0 & 0 & 1 & 0 & 0 & 0 & 0 \\ 0 & 0 & -1 & 0 & 0 & 1 & 0 & 0 & 0 \\ 0 & 0 & 0 & k_b & c_b & m_b & -k_h & -c_h & 0 \\ 0 & 0 & 0 & 0 & 0 & 0 & 0 & 1 & 0 \\ 0 & 0 & 0 & 0 & 0 & -1 & 0 & 0 & 1 \\ 0 & 0 & 0 & 0 & 0 & 0 & k_h & c_h & m_h \end{bmatrix},$$

$$B = \begin{bmatrix} 0 & 0 & -1 & 0 & 0 & 0 & 0 & 0 & 0 \end{bmatrix}^T, F = \begin{bmatrix} 0 & -1 & 0 & 0 & 0 & 0 & 0 & 0 & 0 \end{bmatrix}^T,$$

$$C = \begin{bmatrix} 1 & 0 & 0 & 0 & 0 & 0 & 0 & 0 & 0 \\ 0 & 1 & 0 & 0 & 0 & 0 & 0 & 0 & 0 \\ 0 & 0 & 1 & 0 & 0 & 0 & 0 & 0 & 0 \\ 0 & 0 & 0 & 0 & 0 & 1 & 0 & 0 & 0 \\ 0 & 0 & 0 & 0 & 0 & 0 & 0 & 0 & 1 \end{bmatrix}, D = \begin{bmatrix} 0 & 0 & 0 & 0 & 0 & 0 & 0 & 0 & 1 \end{bmatrix}.$$

6.3 The output-feedback H_∞ controller design

Define the output-feedback controller as $u(t) = Ky(t)$. Subsituting it into (6.4), we have

$$\begin{aligned} E\dot{x}(t) &= (A + BKC)x(t) + F\omega(t), \\ y(t) &= Cx(t), \\ z(t) &= Dx(t). \end{aligned} \tag{6.5}$$

To design the controller K, we consider the following equivalent system

$$\begin{aligned} \bar{E}\dot{\bar{x}}(t) &= \bar{A}\bar{x}(t) + \bar{F}\omega(t), \\ y(t) &= \bar{C}\bar{x}(t), \\ z(t) &= \bar{D}\bar{x}(t), \end{aligned} \tag{6.6}$$

where $\bar{x}(t) = \begin{bmatrix} x^T(t) & u^T(t) \end{bmatrix}^T$ and

$$\bar{E} = \begin{bmatrix} E & 0 \\ 0 & 0 \end{bmatrix}, \bar{A} = \begin{bmatrix} A & B \\ KC & -I \end{bmatrix}, \bar{F} = \begin{bmatrix} F \\ 0 \end{bmatrix}, \bar{C} = \begin{bmatrix} C & 0 \end{bmatrix}, \bar{D} = \begin{bmatrix} D & 0 \end{bmatrix}.$$

Theorem 6.1 *The continuous-time singular system (6.6) is admissible with H_∞ performance index γ if there exist matrices $P > 0$ and Q with appropriate dimensions and Z with $\bar{E}^T Z = 0$ satisfying the following conditions*

$$\Theta = \begin{bmatrix} \bar{A}^T(P\bar{E} + ZQ) + (P\bar{E} + ZQ)^T\bar{A} + \bar{D}^T\bar{D} & (P\bar{E} + ZQ)^T\bar{F} \\ * & -\gamma^2 I \end{bmatrix} < 0. \tag{6.7}$$

Proof. Firstly, we need to prove the system (6.6) is regular and impulse-free. Since the system (6.6) is equivalent to the system (6.5), the regularity and impulse free are the same for these two systems. When the control input u and disturbance ω are not considered, according to the system (6.5), we have

$$sE - A = \begin{bmatrix} s & -1 & 0 & 0 & 0 & 0 & 0 & 0 & 0 \\ 0 & s & -1 & 0 & 0 & 0 & 0 & 0 & 0 \\ -k_s & -c_s & -m_s & k_b & c_b & 0 & 0 & 0 & 0 \\ 0 & 0 & 0 & s & -1 & 0 & 0 & 0 & 0 \\ 0 & 0 & 1 & 0 & s & -1 & 0 & 0 & 0 \\ 0 & 0 & 0 & -k_b & -c_b & -m_b & k_h & c_h & 0 \\ 0 & 0 & 0 & 0 & 0 & 0 & s & -1 & 0 \\ 0 & 0 & 0 & 0 & 0 & 1 & 0 & s & -1 \\ 0 & 0 & 0 & 0 & 0 & 0 & -k_h & -c_h & -m_h \end{bmatrix}. \tag{6.8}$$

Then we can get $\det(sE - A) = a_6 s^6 + a_5 s^5 + +a_4 s^4 + +a_3 s^3 + +a_2 s^2 + +a_1 s + a_0$, where $a_6 = -m_b m_h m_s$. Due to $a_6 \neq 0$, $\det(sE - A)$ is not identically zero and deg($\det(sE - A)$)=rank(E)=6, so the system (6.5) and (6.6) are regular and impulse free.

Then, we need to prove the stability of the system (6.6). Define $\mathscr{P} = P\bar{E} + ZQ$ and $\bar{E}^T Z = 0$. Due to $P > 0$, we have

$$\bar{E}^T\mathscr{P} = \mathscr{P}^T\bar{E} \geq 0. \tag{6.9}$$

If the disturbance ω is not considered, define a Lyapunov function as $V(t) = \bar{x}^T(t)\bar{E}^T\mathscr{P}\bar{x}(t) \geq 0$, so the derivative of $V(t)$ can be derived as

$$\dot{V}(t) = \bar{x}^T(t)\left(\bar{A}^T\mathscr{P} + \mathscr{P}^T\bar{A}\right)\bar{x}(t). \tag{6.10}$$

From the inequality (6.7), we have $\bar{A}^T\mathscr{P} + \mathscr{P}^T\bar{A} < 0$, which ensures $\dot{V}(t) < 0$, so the

system (6.6) is stable. Therefore, when $\omega(t) \equiv 0$, the system (6.6) is admissible.

Then, considering the condition $\omega(t) \neq 0$, we define

$$J = \| z(t) \|_2^2 - \gamma^2 \| \omega(t) \|_2^2, \tag{6.11}$$

and a state vector as

$$\xi(t) = \begin{bmatrix} \bar{x}^T(t) & \omega(t) \end{bmatrix}^T. \tag{6.12}$$

Based on the inequality (6.10), under zero initial conditions, we can get

$$\begin{aligned} J &\leq \| z(t) \|_2^2 - \gamma^2 \| \omega(t) \|_2^2 + V(\infty) - V(0) \\ &= \int_0^\infty \left(z^T(t) z(t) - \gamma^2 \omega^T(t) \omega(t) + \dot{V}(t) \right) dt \\ &\leq \int_0^\infty \xi^T(t) \Theta \xi(t) dt. \end{aligned} \tag{6.13}$$

The inequality (6.7) ensures $J < 0$, so the system (6.6), under zero initial conditions, is admissible with H_∞ performance γ. Then, the proof has been completed. ■

The controller K cannot be solved by Theorem 6.1 through LMI toolbox, because it is coupled with other matrices. To solve this issue, we introduce the following theorem.

Theorem 6.2 *The continuous-time singular system (6.6) is admissible with H_∞ performance index γ if there exist matrices G_{11}, G_{12}, G_{13}, M and L with appropriate dimensions satifying the following condition*

$$\begin{bmatrix} \Theta_{11} + D^T D & \Theta_{12} & G_{11} F \\ * & \Theta_{22} & G_{13} F \\ * & * & -\gamma^2 I \end{bmatrix} < 0, \tag{6.14}$$

where

$$\begin{aligned} \Theta_{11} &= (G_{11} A + LMC) + (G_{11} A + LMC)^T, \\ \Theta_{12} &= G_{11} B - L G_{12} + A^T G_{13}^T + C^T M^T, \\ \Theta_{22} &= (G_{13} B - G_{12}) + (G_{13} B - G_{12})^T, \end{aligned}$$

then the controller gain can be obtained as $K = G_{12}^{-1} M$.

Proof. Define $G = \begin{bmatrix} G_{11} & LG_{12} \\ G_{13} & G_{12} \end{bmatrix}$, where L is a given matrix to set weights for different state variables. Define $P = \begin{bmatrix} P_1 & P_2 \\ P_2^T & P_3 \end{bmatrix} > 0$, $Z = \begin{bmatrix} Z_1 \\ Z_2 \end{bmatrix}$ and $Q = \begin{bmatrix} Q_1 & Q_2 \end{bmatrix}$. Then we have $(P\bar{E} + ZQ)^T = \begin{bmatrix} (P_1 E + Z_1 Q_1)^T & E^T P_2 + Q_1^T Z_2^T \\ Q_2^T Z_1^T & Q_2^T Z_2^T \end{bmatrix}$. If $E^T P_2 = 0$ and $Q_1^T = L Q_2^T$,

we can define $G_{11} = (P_1E + Z_1Q_1)^T$, $G_{12} = Q_2^T Z_2^T$, and $G_{13} = Q_2^T Z_1^T$. Then we can set $G = (P\bar{E} + ZQ)^T$ and $M = G_{12}K$. Substituting them to the inequality (6.7), we can get the inequality (6.14). Basd on the proof of Theorem 6.1, Theorem 6.2 is conformed. ■

6.4 Event-triggered scheme design

The output feedback controller is designed in the above section. To reduce the data transmission load of the system, a discrete event-triggered scheme is designed here. Firstly, define the sampling interval of the seat suspension system as h. The output of the system $y(t)$ is firstly sampled by the sensors at time instants ih $(i \in \mathbf{N})$ as $y(t_k + ih)$. Then the event-triggered scheme checks whether the output signal should be transmitted or not by the following condition

$$\begin{aligned} t_{k+1} =& t_k + \min\left\{ \min_{i\in\mathbf{N}} \left[ih | \left(y(t_k+ih) - y(t_k)\right)^T \Omega \left(y(t_k+ih) - y(t_k)\right) \right.\right. \\ & \left.\left. \geq \delta y^T(t_k+ih)\Omega y(t_k+ih) \right], \tau_M \right\}, \end{aligned} \tag{6.15}$$

where t_0, t_1,$\cdots$, t_k, t_{k+1},$\cdots$, $k \in \mathbf{N}$ are event-triggered time instants, τ_M is the maximum time delay, and $\Omega > 0$, $0 < \delta < 1$.

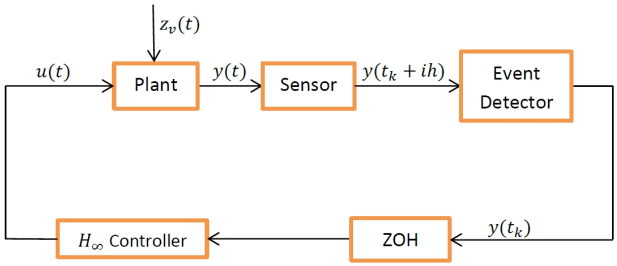

Figure 6.2: Event-triggered control diagram

The event-triggered control diagram for the system (6.4) is shown in Figure 6.2. The external disturbance $z_v(t)$ influences the plant of the seat suspension system with a human body directly. Some sensors collect the measurable system state signals $y(ih)$ at the sampling time interval h in real-time. Then, the event-detector estimates whether the data should be transferred or not according to the condition (6.15). If triggered, the event detector allows the output $y(t_k)$ to transmit to the zero-order holder (ZOH), which holds the data value until the next event is triggered. The event-triggered output data $y(t_k)$ come to H_∞ controller, so $u(t)$ holds its value during the time intervals $[t_k, t_{k+1})$, $k \in \mathbf{N}$. Therefore, the event-triggered scheme cannot only decrease the workload of data transmission.

Considering the event-triggered output $y(t_k)$ for $\forall t \in [t_k, t_{k+1})$, for convenience, we define

$$\tau(t) = t - t_k - ih \tag{6.16}$$

where $t \in [t_k, t_{k+1})$ and we have

$$0 < \tau_m \leq \tau(t) \leq \tau_M, \tag{6.17}$$

where τ_m and τ_M are the minimum and maximum value of $\tau(t)$, respectively.

Based on the event-triggered scheme, the system (6.4) can be rewritten as

$$\begin{aligned} E\dot{x}(t) &= Ax(t) + BKCx(t-\tau(t)) + BKe(t-\tau(t)) + F\omega(t), \\ y(t) &= Cx(t), \\ z(t) &= Dx(t), \end{aligned} \tag{6.18}$$

where K is obtained in the above section and $e(t-\tau(t)) = y(t_k+ih) - y(t_k)$.

Lemma 6.1 *[103] Let f_1, f_1,...,f_N: $\mathbf{R}^m \mapsto \mathbf{R}$ have positive values in an open subset $\mathbf{D}$. Then, the reciprocally convex combination of f_i over $\mathbf{D}$ satisfies*

$$\min_{\left\{\alpha_i | \alpha_i > 0, \sum\limits_i \alpha_i = 1\right\}} \sum_i \frac{1}{\alpha_i} f_i(t) = \sum_i f_i(t) + \max_{g_{i,j}(t)} \sum_{i \neq j} g_{i,j}(t)$$

subject to

$$\left\{ g_{i,j}(t) : \mathbf{R}^m \mapsto \mathbf{R}, g_{j,i}(t) = g_{i,j}(t), \begin{bmatrix} f_i(t) & g_{i,j}(t) \\ g_{j,i}(t) & f_i(t) \end{bmatrix} \geq 0 \right\}.$$

Theorem 6.3 *For given scalars $0 < \delta < 1$, τ_m, τ_M, and $\alpha_i > 0$ $(i = 1,2,3)$, under the event-triggered scheme (6.15), the closed-loop system (6.18) is admissible with H_∞ performance index γ, if there exist positive-definite matries Q_j, R_j, $(j = 1,2)$, and Ω, non-singular matrix P, X, and U, with appropriate dimensions, satisfying the following inequaties:*

$$E^T P = P^T E \geq 0, \tag{6.19}$$

$$\Psi = \begin{bmatrix} \Phi + e_1 D^T D e_1 & \Gamma \\ * & -\gamma^2 I \end{bmatrix} < 0, \tag{6.20}$$

where

$$\Phi = \begin{bmatrix} \Phi_{11} & \Phi_{12} & \Phi_{13} & 0 & \Phi_{15} & \Phi_{16} \\ * & \Phi_{22} & \Phi_{23} & \Phi_{24} & \Phi_{25} & \Phi_{26} \\ * & * & \Phi_{33} & \Phi_{34} & 0 & 0 \\ * & * & * & \Phi_{44} & 0 & 0 \\ * & * & * & * & \Phi_{55} & \Phi_{56} \\ * & * & * & * & * & \Phi_{66} \end{bmatrix},$$

$$\begin{aligned}
\Phi_{11} =& Q_1 + Q_2 - E^T R_1 E + \alpha_1 A^T U + \alpha_1 U^T A, \\
\Phi_{12} =& \alpha_1 U^T BKC + \alpha_2 A^T U, \Phi_{13} = E^T R_1 E, \\
\Phi_{15} =& \alpha_1 U^T BK, \Phi_{16} = P^T - \alpha_1 U^T + \alpha_3 A^T U, \\
\Phi_{22} =& \delta C^T \Omega C - 2E^T R_2 E + X + X^T + \alpha_2 (BKC)^T U + \alpha_2 U^T BKC, \\
\Phi_{23} =& E^T R_2 E - X^T, \Phi_{24} = -X + E^T R_2 E, \Phi_{25} = \alpha_2 U^T BK, \\
\Phi_{26} =& -\alpha_2 U^T + \alpha_3 (BKC)^T U, \Phi_{33} = -Q_1 - E^T R_1 E - E^T R_2 E, \\
\Phi_{34} =& X, \Phi_{44} = -Q_2 - E^T R_2 E, \Phi_{55} = -\Omega, \Phi_{56} = \alpha_3 (BK)^T U, \\
\Phi_{66} =& \tau_m^2 R_1 + (\tau_M - \tau_m)^2 R_2 - \alpha_3 (U + U^T), \\
\Gamma =& (\alpha_1 e_1^T + \alpha_2 e_2^T + \alpha_3 e_6^T) UF, \\
e_i =& \begin{bmatrix} 0_{n \times n(i-1)} & I & 0_{n \times n(6-i)} \end{bmatrix}, (i = 1, 2, ..., 6).
\end{aligned}$$

Proof. At first, we need to prove the system (6.18) to be regular and impulse free. Since rank $E = r < n$, there must exist two invertible matrices M and N such that

$$\tilde{E} = MEN = \begin{bmatrix} I_r & 0 \\ 0 & 0 \end{bmatrix}.$$

Define

$$\begin{aligned}
\tilde{A} =& NAN = \begin{bmatrix} A_{11} & A_{12} \\ A_{21} & A_{22} \end{bmatrix}, \tilde{U} = M^{-T} UN = \begin{bmatrix} U_{11} & U_{12} \\ U_{21} & U_{22} \end{bmatrix}, \\
\tilde{R}_1 =& M^{-T} R_1 M^{-1} = \begin{bmatrix} R_{1,11} & R_{1,12} \\ R_{1,21} & R_{1,22} \end{bmatrix}.
\end{aligned}$$

According to (6.20), we have $\Phi_{11} < 0$. Due to $Q_1 > 0$ and $Q_2 > 0$, so we have

$$\alpha_1 U^T \bar{A} + \alpha_1 \bar{A}^T U - \bar{E}^T R_1 \bar{E} < 0. \tag{6.21}$$

Pre- and post-multiplying (6.21) by N^T and N respectively, we have

$$\alpha_1 \tilde{U}^T \tilde{A} + \alpha_1 \tilde{A}^T \tilde{U} - \tilde{E}^T \tilde{R}_1 \tilde{E} = \begin{bmatrix} \bullet & \bullet \\ \bullet & \alpha_1 A_{22}^T U_{22} + \alpha_1 U_{22}^T A_{22} \end{bmatrix} < 0, \tag{6.22}$$

where • represents matrix elements which do not need to be considered. Hence, we can see that $\alpha_1 A_{22}^T U_{22} + \alpha_1 U_{22}^T A_{22} < 0$, so A_{22} is nonsingular. Therefore, the singular seat suspension system (6.6) is regular and impulse free.

To verify the stability of the system (6.18), assuming $\omega(t) = 0$, we design a Lyapunov function as

$$V(t) = V_1(t) + V_2(t) + V_3(t), \tag{6.23}$$

where

$$\begin{aligned}
V_1(t) =& x^T(t) E^T P x(t), \\
V_2(t) =& \int_{t-\tau_m}^{t} x^T(\alpha) Q_1 x(\alpha) d\alpha + \int_{t-\tau_M}^{t} x^T(\alpha) Q_2 x(\alpha) d\alpha, \\
V_3(t) =& \tau_m \int_{-\tau_m}^{0} \int_{t+\beta}^{t} \dot{x}^T(\alpha) E^T R_1 E \dot{x}(\alpha) d\alpha d\beta + (\tau_M - \tau_m) \int_{-\tau_M}^{-\tau_m} \int_{t+\beta}^{t} \dot{x}^T(\alpha) E^T R_2 E \dot{x}(\alpha) d\alpha d\beta.
\end{aligned}$$

Now we define a state vector as follows

$$\xi(t) = \begin{bmatrix} x^T(t) & x^T(t-\tau(t)) & x^T(t-\tau_m) & x^T(t-\tau_M) & e^T(t-\tau(t)) & (E\dot{x}(t))^T \end{bmatrix}^T$$

Calculating the derivative of $V(t)$ for $t \in [t_k, t_{k+1})$, we have

$$\dot{V}(t) = \dot{V}_1(t) + \dot{V}_2(t) + \dot{V}_3(t), \tag{6.24}$$

where

$$\dot{V}_1(t) = \text{sym}\left(x^T(t) P^T E \dot{x}(t)\right) = \xi^T(t) \left(e_1^T P^T e_6 + e_6^T P e_1\right) \xi(t), \tag{6.25}$$

$$\begin{aligned}
\dot{V}_2(t) =& x^T(t)(Q_1 + Q_2) x(t) - x^T(t-\tau_m) Q_1 x(t-\tau_m) - x^T(t-\tau_M) Q_2 x(t-\tau_M) \\
=& \xi^T(t) \left[e_1^T (Q_1 + Q_2) e_1 - e_3^T Q_1 e_3 - e_4^T Q_2 e_4\right] \xi(t),
\end{aligned} \tag{6.26}$$

$$\begin{aligned}
\dot{V}_3(t) =& \tau_m^2 \dot{x}^T(t) E^T R_1 E \dot{x}(t) - \tau_m \int_{t-\tau_m}^{t} \dot{x}^T(\alpha) E^T R_1 E \dot{x}(\alpha) d\alpha \\
&+ (\tau_M - \tau_m)^2 \dot{x}^T(t) E^T R_2 E \dot{x}(t) - (\tau_M - \tau_m) \int_{t-\tau_M}^{t-\tau_m} \dot{x}^T(\alpha) E^T R_2 E \dot{x}(\alpha) d\alpha \\
\le& \xi^T(t) \left[e_6^T \left(\tau_m^2 R_1 + (\tau_M - \tau_m)^2 R_2\right) e_6 - (e_1 - e_3)^T E^T R_1 E (e_1 - e_3)\right] \xi(t) \\
&- (\tau_M - \tau_m) \int_{t-\tau_M}^{t-\tau_m} \dot{x}^T(\alpha) E^T R_2 E \dot{x}(\alpha) d\alpha.
\end{aligned} \tag{6.27}$$

According to Lemma 6.1, when $\tau_m < \tau(t) < \tau_M$, we have

$$\begin{aligned}
&- (\tau_M - \tau_m) \int_{t-\tau_M}^{t-\tau_m} \dot{x}^T(\alpha) E^T R_2 E \dot{x}(\alpha) d\alpha \\
=& - (\tau_M - \tau_m) \int_{t-\tau(t)}^{t-\tau_m} \dot{x}^T(\alpha) E^T R_2 E \dot{x}(\alpha) d\alpha - (\tau_M - \tau_m) \int_{t-\tau_M}^{t-\tau(t)} \dot{x}^T(\alpha) E^T R_2 E \dot{x}(\alpha) d\alpha
\end{aligned}$$

$$\leq -\xi^T(t)\left[\frac{\tau_M-\tau_m}{\tau(t)-\tau_m}(e_3-e_2)^T E^T R_2 E(e_3-e_2)+\frac{\tau_M-\tau_m}{\tau(t)-\tau_m}(e_2-e_4)^T E^T R_2 E(e_2-e_4)\right]\xi(t)$$

$$\leq -\xi^T(t)\begin{bmatrix} e_3-e_2 \\ e_2-e_4 \end{bmatrix}^T \begin{bmatrix} E^T R_2 E & X \\ X^T & E^T R_2 E \end{bmatrix}\begin{bmatrix} e_3-e_2 \\ e_2-e_4 \end{bmatrix}\xi(t). \tag{6.28}$$

When $\tau(t)=\tau_m$ or $\tau(t)=\tau_M$, we have $(e_2-e_3)\xi(t)=0$ or $(e_2-e_4)\xi(t)=0$, respectively, so then inequality (6.28) still holds.

Based on the system (6.18), there exist a nonsingular matrix U satisfying the following free weighting equation as

$$\begin{aligned} &2\left[Ax(t)+BKCx(t-\tau(t))+BKe(t-\tau(t))-E\dot{x}(t)\right]^T \\ &\times U\left[\alpha_1 x(t)+\alpha_2 x(t-\tau(t))+\alpha_3 E\dot{x}(t)\right]=0. \end{aligned} \tag{6.29}$$

Based on the event-triggered condition (6.15), we can get

$$e^T(t-\tau(t))\Omega e(t-\tau(t)) < \delta x^T(t-\tau(t))C^T\Omega C x(t-\tau(t)). \tag{6.30}$$

Combing equations (6.25) to (6.30) and according to Lemma 6.1, we have

$$\dot{V}(t)\leq \xi^T(t)\Phi\xi(t). \tag{6.31}$$

Based on (6.20), we can get $\Phi<0$, so we have $\dot{V}(t)<0$. Then the system (6.18) is stable.

Then, when the condition $\omega(t)\neq 0$, we define

$$J=\| z(t)\|_2^2-\gamma^2\| \omega(t)\|_2^2, \tag{6.32}$$

and a new state vector as

$$\zeta(t)=\begin{bmatrix} x^T(t) & x^T(t-\tau(t)) & x^T(t-\tau_m) & x^T(t-\tau_M) & e^T(t-\tau(t)) & (E\dot{x}(t))^T & \omega(t) \end{bmatrix}^T.$$

Based on the inequality (6.31), under zero initial conditions, we can get

$$\begin{aligned} J &\leq \| z(t)\|_2^2-\gamma^2\| \omega(t)\|_2^2+V(\infty)-V(0) \\ &=\int_0^\infty \left(z^T(t)z(t)-\gamma^2\omega^T(t)\omega(t)+\dot{V}(t)\right)dt \\ &\leq \int_0^\infty \zeta^T(t)\Psi\zeta(t)dt. \end{aligned} \tag{6.33}$$

The inequality (6.20) ensures $J<0$, so the system (6.18), under zero initial conditions, is admissible with H_∞ performance γ. Then, we complete the proof. ■

6.5 Simulation results

In this section, some simulation results of the output-feedback event-triggered H_∞ controller are given for the singular active seat suspension system with a human body in the loop. The system parameters are shown in Table 6.1. Define the sampling time $h = 0.002$ s, so $\tau_m = 0.002$. A too-large value of time delay of the output-feedback controller may easily lead the seat suspension system unstable, so here we set $\tau_M = 0.05$.

Table 6.1: The seat suspension system parameters

m_h(kg)	m_b(kg)	m_s(kg)	k_h(N/m)	k_b(N/m)	k_s(N/m)
4.58	46	13	2857	15000	4600
c_h(Ns/m)	c_b(Ns/m)	c_s(Ns/m)	τ_m	τ_M	δ
0.8	2000	500	0.002	0.05	0.4

Based on Theorem 6.2, the output-feedback controller can be obtained as

$$K = \begin{bmatrix} 169.2 & -990 & 6 & 4.95 & 3.66 \end{bmatrix}.$$

According to Theorem 6.3 and the controller K, the event-triggered matrix Ω can be obtained as

$$\Omega = \begin{bmatrix} 2280618 & -282359 & 459 & 1207 & -1235 \\ -282359 & 672884 & -3469 & -2513 & -2550 \\ 459 & -3469 & 113 & -79 & 123 \\ 1207 & -2513 & -79 & 431 & -745 \\ -1235 & -2550 & 123 & -745 & 6007 \end{bmatrix}.$$

6.5.1 Bump road response

A bump disturbance is a common road excitation, so it is chosen here to evaluate the performance of the proposed control method for the seat suspension system. A bump road surface is defined as

$$z_v(t) = \begin{cases} 0.02\sin(2\pi t), & 0 \le t \le 1 \\ 0, & t > 1 \end{cases} \tag{6.34}$$

This bump road excitation firstly transfers to a vehicle suspension [89] and then the output is considered as the input disturbance of the seat suspension. To show the effectiveness of the proposed control method, the performance of the output-feedback controller K with and without the event-triggered scheme for the seat suspension system is compared with the uncontrolled seat suspension system. Figure 6.3 shows the seat deflection and the head's acceleration comparison under the bump road disturbance among

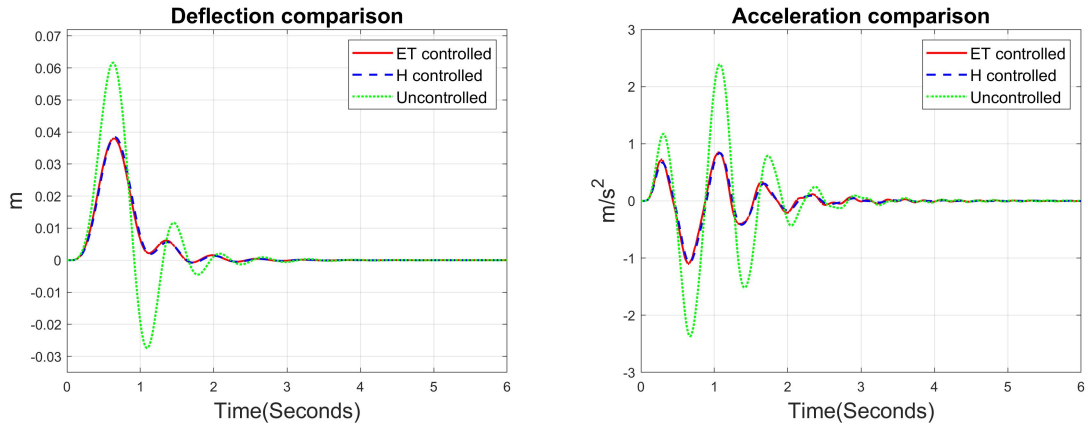

Figure 6.3: The seat suspension deflection and the head's acceleration comparison for the seat suspension system with a bump road disturbance

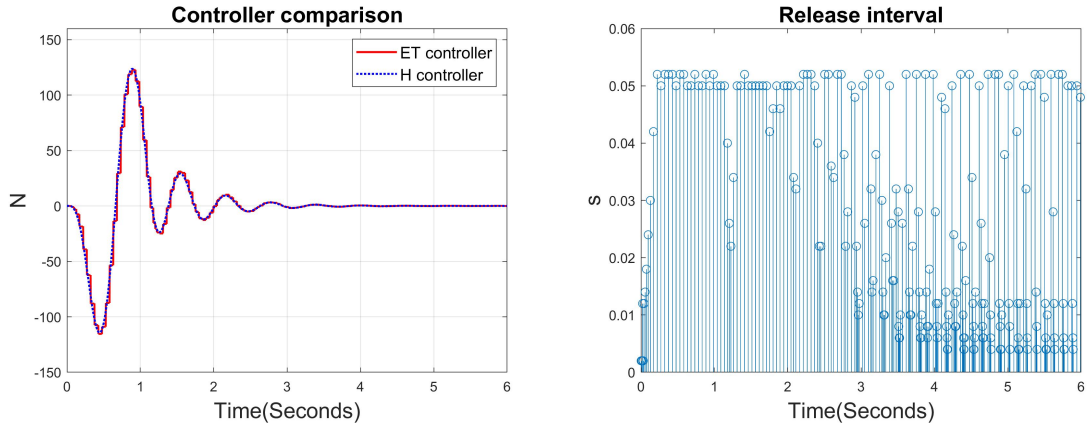

Figure 6.4: The output of the controllers, the release instants and release intervals of the seat suspension system with a bump road disturbance

the output-feedback controlled seat suspension system with the event-triggered scheme (red solid curve), without event-triggered scheme (blue dashed curve), and the uncontrolled seat suspension system (green dotted curve). Compared with the response of the uncontrolled seat suspension system, here we can see both two controllers can reduce the seat deflection and the head's acceleration effectively without big differences, so the controllers can both improve driving comfort for drivers. Figure 6.4 shows the controller comparison between the output-feedback controller with the event-triggered scheme (red solid curve) and without the event-triggered scheme (blue dotted curve) and the release intervals of the event-triggered scheme. Here we can see that the values of the event-triggered output-feedback controller only change when the event trigger happens, so it can reduce the workload of data transmission of this seat suspension system.

6.5.2 Sinusoidal vibration response

Set $z_v = 0.02\sin(1.4 \times 2\pi t)$ as the sinusoidal disturbance. Figure 6.5 shows the seat suspension deflection and the head's acceleration comparison among the output-feedback

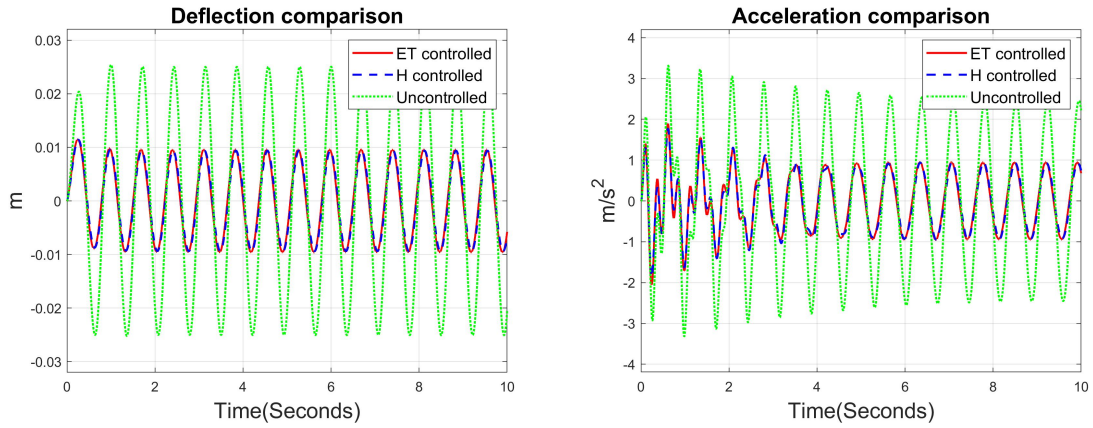

Figure 6.5: The seat suspension deflection and the head's acceleration comparison for the seat suspension system with a sinusoidal disturbance

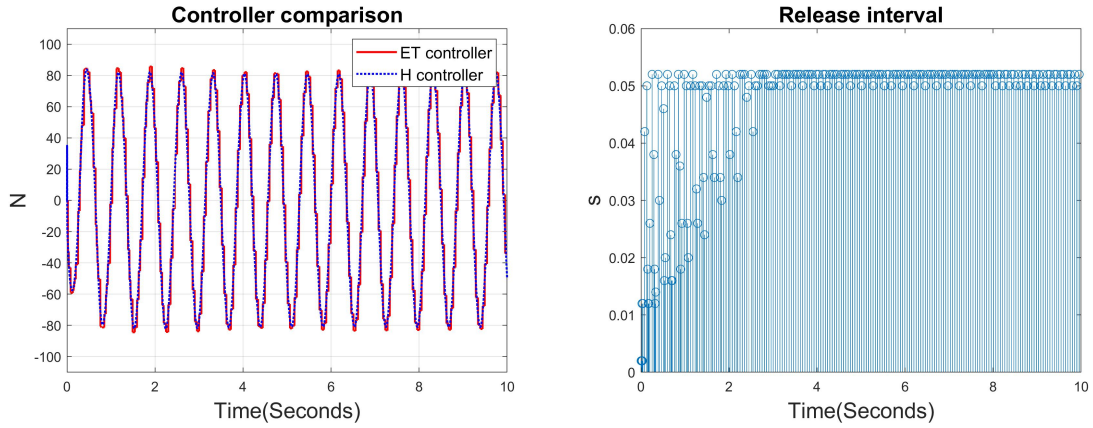

Figure 6.6: The output of the controllers, the release instants and release intervals of the seat suspension system with a sinusoidal disturbance

controlled system with and without the event-triggered scheme and the uncontrolled seat suspension system with a sinusoidal disturbance. From this figure, it is clear to see that both two controllers can greatly reduce both the seat suspension deflection and the head's acceleration with little differences compared with the response of the uncontrolled seat suspension system. Therefore, the proposed control method can largely improve driving comfort for vehicle drivers. Figure 6.6 shows the output of the two controllers comparison, the release instants, and release intervals of the seat suspension system with a sinusoidal disturbance. From this figure, we can see the values of the output-feedback controller with the event-triggered scheme only change when the event trigger happens, which can greatly reduce the workload of data transmission.

Table 6.2 shows the average data transmission times per second of the output-feedback controller with and without event-triggered scheme under bump road and sinusoidal disturbance. We set the sampling time as $h = 0.002$ s, so the controller without the event-triggered scheme needs 500 times of data transmission per second. However, the controller with the event-triggered scheme only needs 36.8 and 21.2 times average of data

transmission for bump road disturbance and sinusoidal disturbance, respectively, which can reduce 92.64% and 95.76% of data transmission without big influence on the control performance to reduce vibration and improve driving comfort.

Table 6.2: The average data transmission times per second

disturbance type	output-feedback controller with event-triggered scheme	output-feedback controller without event-triggered scheme	reduction percentage
bump road	36.8	500	92.64%
sinusoidal	21.2	500	95.76%

6.6 Conclusion

An output-feedback event-triggered H_∞ controller is designed for the singular active seat suspension system with a human body in the loop in this chapter. The acceleration signals of the upper seat suspension frame, body torso, and head of the human body are considered as parts of the system states, which makes the seat suspension system a singular system. The output-feedback controller is designed by using all easily measurable signals and the event-triggered scheme is designed to reduce the workload of data transmission. The LMIs criteria are given to obtain the controller and event-triggered scheme. Some simulation results show the effectiveness of the proposed control method to improve driving comfort and reduce data transmission. Experimental tests will be considered as our future work. In the next chapter, a two-degrees-of-freedom (2-DOF) seat suspension system is built and a robust H_∞ control method is designed to deal with the whole body vibrations.

Chapter 7

H_∞ Control Strategy for 2-DOF Seat Suspension

7.1 Introduction

The previous chapter introduces a seat suspension system with a human body model in the loop. A dynamic output-feedback H_∞ controller is designed at first to reduce drivers' vibration and an event-triggered scheme is designed to reduce the workload of data transmission. In this chapter, a 2-DOF seat suspension system is applied to reduce whole body vibration (WBV).

The impact of WBV on drivers has been investigated by many researchers during the past decades [104–106]. Long-time exposure to WBV may cause physical and mental fatigue, or back pain, which harms professional drivers' health or even causes accidents [107]. It is an much severer problem for heavy vehicle drivers, like drivers of trucks [108], buses [109], agricultural vehicles [110], mining vehicles [111], and industrial vehicles [112, 113] because of their big masses, harsh working conditions, or special operations. Therefore, to protect the health of these heavy vehicle drivers and improve their driving comfort, seat suspensions are widely used to reduce WBV.

During the past years, many research works have been done for WBV of heavy vehicles [114, 115]. WBV of mobile machines in the steelmaking industry is quantified in [116]. The effect of drivers' different postures on seat transmissibility during exposure to vertical WBV is studied in [117]. The impact of different and WBV exposures on truck driver vigilance and discomfort is studied in [118]. The impact for drivers exposed to WBV in agricultural tractors is investigated in [119]. However, most previous research about WBV was only about ergonomic analysis [120] or harm evaluation to drivers' health [121], while relatively little research has been done about the design of the multiple-DOF seat suspensions and control strategies for them to reduce WBV. The design of an innovative two-layer multiple-DOF seat suspension is proposed in [9] to reduce WBV for heavy

vehicles and a control strategy is proposed in [10] to reduce roll and vertical vibration simultaneously for this novel multiple-DOF seat suspension. The control strategy in [10] is very complex and many parameters need to be adjusted based on the control performance, which motivates us to develop a simple control method for this multiple-DOF seat suspension system.

In this chapter, an H_∞ control approach is investigated for the multiple-DOF seat suspension in [9, 10]. Firstly, based on the dynamic equations of the multiple-DOF seat suspension system, a nonlinear system with multiple inputs and multiple outputs of this seat suspension is designed. To simplify the control problem for this complicated system, it is separated into two subsystems (vertical vibration subsystem and rotational vibration subsystem). Under some reasonable assumptions, these two subsystems become two linear systems. Then, two H_∞ controllers are designed for these subsystems, respectively, and the stability of these subsystems are also proved. At last, some simulation results are shown to illustrate the effectiveness of the proposed control method to reduce both vertical and rotational vibrations to improve driving comfort for heavy vehicle drivers.

7.2 2-DOF Seat suspension model

Most conventional seat suspensions for road vehicles only have a single degree of freedom (S-DOF) and only provide vertical vibration isolation for drivers and passengers. However, for some heavy vehicles (like agricultural vehicles and construction vehicles), some uneven road surfaces also cause some severe roll vibrations, which also greatly affects the driving comfort of drivers. The conventional seat suspensions cannot isolate those vibrations. A 2-DOF seat suspension model is shown in Figure 7.1 (the same model in [10]), which can provide the vibration reduction of 2 degrees of freedom (vertical and roll). In Figure 7.1, m_1 is the mass of the driver body and upper seat frame; m_2 is the mass of the block between top and bottom layer of the seat suspension; h_b is the distance between frame 2 and frame 4; h_s is the distance from frame 2 to the the center of m_2; h_0 is the initial distance between frame 1 and frame 2; $h(t)$ is the dynamic displacement variable of frame 2 referred to frame 1. For the bottom layer, the spring stiffness is k_s, the friction force is f_{rt}, and the active control force is u_t. For the top layer, the rotational stiffness is k_r, the rotational friction torque is f_{rr}, and the active torque is u_r. The 2-DOF seat suspension model decomposition is shown in Figure 7.2. Five coordinate frames and the transformation matrices among each frame are the same as paper [10].

Based on the equations (27) and (37) in [10], the dynamic equations of the multiply

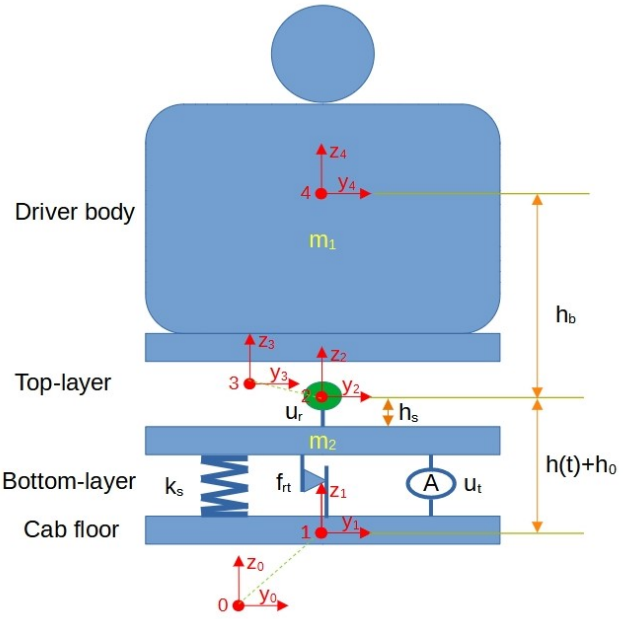

Figure 7.1: The Y-Z plane model of 2-DOF seat suspension model.

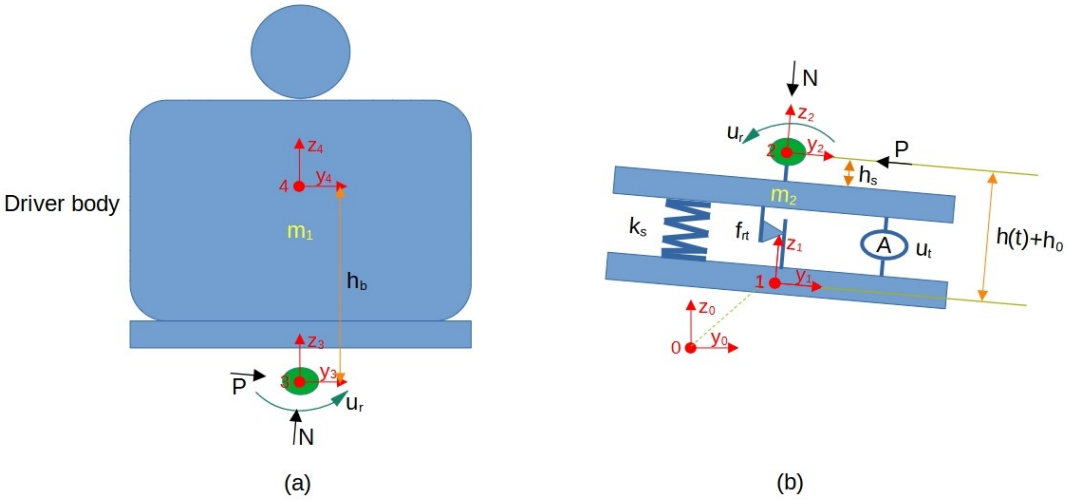

Figure 7.2: The 2-DOF seat suspension model decomposition (a) Top-layer, (b) Bottom-layer.

DOF seat suspension system are:

$$
\begin{aligned}
(I_{m1}+m_1h_b^2)\ddot{\alpha} = &-k_r\beta - f_{rr} + u_r - m_1\left\{\mathrm{s}\beta\left[\dot{\theta}^2(h+h_0)-\ddot{h}\right]\right. \\
&\left.+\mathrm{c}\beta\left[\ddot{\theta}(h+h_0)+2\dot{\theta}\dot{h}\right]-\mathrm{s}\alpha\ddot{z}_s-\mathrm{s}\alpha g\right\}h_b, \qquad (7.1)\\
(m_1+m_2)\ddot{h} = &-k_sh - f_{rt} + u_t - m_1\left[-\dot{\theta}^2(h+h_0)-\dot{\alpha}^2h_b\mathrm{c}\beta-\ddot{\alpha}h_b\mathrm{s}\beta\right. \\
&\left.+\mathrm{c}\theta\ddot{z}_s+\mathrm{c}\theta g-g\right]-m_2\left[-\dot{\theta}^2(h+h_0-h_s)+\mathrm{c}\theta\ddot{z}_s-g+\mathrm{c}\theta g\right], \qquad (7.2)
\end{aligned}
$$

where θ represents the roll angle vibration around axis x_1 from the cab floor; β represents the relative rotary angle of frames 2 and 3; α represents the roll angle of the driver's body around axis x_4 where $\alpha = \theta + \beta$; z_s represents the external vertical displacement along axis z_0 of the cab floor; $f_{rr} = F_{rr}\mathrm{sgn}(\dot{\beta})$ where F_{rr} is the Coulomb friction torque coefficient; $f_{rt} = F_{rt}\mathrm{sgn}(\dot{h})$ where F_{rt} is the Coulomb friction force coefficient; s and c represent trigonometric functions sin and cos, respectively.

According to the equations (23) and (24) in [10], we can calculate the interactioin force P as

$$P = m_1\left\{-\ddot{\theta}(h+h_0) - 2\dot{\theta}\dot{h} - \mathrm{c}\beta\ddot{\alpha}h_b + \mathrm{s}\beta\dot{\alpha}^2 h_b + \mathrm{s}\theta\ddot{z}_s + \mathrm{s}\theta g\right\}$$

Define the rotational inertial of m_2 around x_1 axis as I_{m2}. Because the seat frame is a prismatic joint and a rigid body and fixed on the vehicle cab floor, so we assume its rotary parameters are all zero. The rotational dynamic equation of m_2 around x_1 axis can be written as

$$\begin{aligned} I_{m2}\ddot{\theta} =& u_v + P(h+h_0) - u_r \\ =& u_v + m_1\left\{-\ddot{\theta}(h+h_0) - 2\dot{\theta}\dot{h} - \mathrm{c}\beta\ddot{\alpha}h_b \right. \\ & \left. + \mathrm{s}\beta\dot{\alpha}^2 h_b + \mathrm{s}\theta\ddot{z}_s + \mathrm{s}\theta g\right\}(h+h_0) - u_r. \end{aligned} \tag{7.3}$$

7.3 2-DOF seat suspension system design

Define the system states as

$$x_1 = \alpha, x_2 = \dot{\alpha}, x_3 = h, x_4 = \dot{h}, x_5 = \theta, x_6 = \dot{\theta}.$$

According to the equations (7.1) to (7.3), we can get the following equations:

$$\begin{aligned} \dot{x}_1 =& x_2, \\ \dot{x}_2 =& \frac{1}{I_{m1} + m_1 h_b^2}\left\{-k_r(x_1 - x_5) - F_{rr}\mathrm{sgn}(x_2 - x_6) + u_r - m_1 h_b\left[\mathrm{s}(x_1 - x_5)\times\right.\right. \\ & \left.\left.\left(x_2^2(x_3 + h_0) - \dot{x}_4\right) + \mathrm{c}(x_1 - x_5)\left(\dot{x}_6(x_3 + h_0) + 2x_6x_4\right) - \mathrm{s}x_1\ddot{z}_s - \mathrm{s}x_1 g\right]\right\} \\ \dot{x}_3 =& x_4, \\ \dot{x}_4 =& \frac{1}{m_1 + m_2}\left\{-k_s x_3 - F_{rt}\mathrm{sgn}(x_4) + u_t - m_1\left[-x_6^2(x_3 + h_0) - x_2^2 h_b \mathrm{c}(x_1 - x_5)\right.\right. \\ & \left.\left. - \dot{x}_2 h_b \mathrm{s}(x_1 - x_5) + \mathrm{c}x_5\ddot{z}_s + \mathrm{c}x_5 g - g\right] - m_2\left[-x_6^2(x_3 + h_0 - h_s) + \mathrm{c}x_5\ddot{z}_s - g + \mathrm{c}x_5 g\right]\right\}, \\ \dot{x}_5 =& x_6, \\ \dot{x}_6 =& \frac{1}{I_{m2}}\left\{u_v + m_1(x_3 + h_0)\left[-\dot{x}_6(x_3 + h_0) - 2x_6x_4 - \mathrm{c}(x_1 - x_5)\dot{x}_2 h_b\right.\right. \\ & \left.\left. + \mathrm{s}(x_1 - x_5)x_2^2 h_b + \mathrm{s}x_5\ddot{z}_s + \mathrm{s}x_5 g\right] - u_r\right\}. \end{aligned} \tag{7.4}$$

The above system is a very complicated nonlinear system with multiple inputs and multiple outputs, which makes it very difficult to design a controller for the system. To simplify the control issue for this 2-DOF seat suspension system, we can separate it into two subsystems and each subsystem only considers a S-DOF vibration control problem.

For the vertical vibration, we assume that there is no rotional vibration, which means $x_1 = x_2 = \dot{x}_2 = x_5 = x_6 = u_v = 0$, so the system (7.4) can be reduced as

$$\begin{aligned}\dot{x}_3 =& x_4,\\ \dot{x}_4 =& \frac{1}{m_1+m_2}\left\{-k_s x_3 - F_{rt}\mathrm{sgn}(x_4) + u_t - (m_1+m_2)\ddot{z}_s\right\}.\end{aligned} \tag{7.5}$$

Define $\bar{x} = \begin{bmatrix} x_3 & x_4 \end{bmatrix}^T$, $u_1 = u_t - F_{rt}\mathrm{sgn}(x_4)$, $\omega_1 = \ddot{z}_s$. Then the system (7.5) becomes a linear system as

$$\begin{aligned}\dot{\bar{x}}(t) =& A_1\bar{x}(t) + B_1 u_1(t) + B_{d1}\omega_1(t)\\ \bar{y}(t) =& C_1\bar{x}(t)\end{aligned} \tag{7.6}$$

where

$$A_1 = \begin{bmatrix} 0 & 1 \\ -\dfrac{k_s}{m_1+m_2} & 0 \end{bmatrix}, B_1 = \begin{bmatrix} 0 \\ \dfrac{1}{m_1+m_2} \end{bmatrix}, B_{d1} = \begin{bmatrix} 0 \\ -1 \end{bmatrix}, C_1 = \begin{bmatrix} 1 \\ 0 \end{bmatrix}^T.$$

For the rotational vibration, we assume that there is no vertical translation, which means $x_3 = x_4 = \dot{x}_4 = \ddot{z}_s = 0$, so the system (7.4) can be reduced as

$$\begin{aligned}\dot{x}_1 =& x_2,\\ \dot{x}_2 =& \frac{1}{I_{m1}+m_1h_b^2}\left\{-k_r(x_1-x_5) - F_{rr}\mathrm{sgn}(x_2-x_6) + u_r\right.\\ & \left. -m_1h_b\left[\mathrm{s}(x_1-x_5)x_2^2h_0 + \mathrm{c}(x_1-x_5)\dot{x}_6h_0 - \mathrm{s}x_1 g\right]\right\}\\ \dot{x}_5 =& x_6,\\ \dot{x}_6 =& \frac{1}{I_{m2}+m_1h_0^2}\left\{u_v + m_1h_0\left[-\mathrm{c}(x_1-x_5)\dot{x}_2h_b + \mathrm{s}(x_1-x_5)x_2^2h_b + \mathrm{s}x_5 g\right] - u_r\right\}.\end{aligned} \tag{7.7}$$

Normally, the rotational angles α and θ are limited in a small bound for the seat suspension system, so $\mathrm{s}x_1 \approx x_1$, $\mathrm{s}x_5 \approx x_5$, $\mathrm{s}(x_1-x_5) \approx x_1 - x_5 \approx 0$, and $\mathrm{c}(x_1-x_5) \approx 1$. Define the system states, input, and disturbance for the system (7.7) as

$$\begin{aligned}\tilde{x} =& \begin{bmatrix} x_1 & x_2 & x_5 & x_6 \end{bmatrix}^T,\\ u_2 =& u_r - F_{rr}\mathrm{sgn}(x_2-x_6),\end{aligned}$$

$$
\begin{aligned}
\upsilon_1 =& \mathrm{s}(x_1-x_5)x_2^2h_0+\mathrm{c}(x_1-x_5)\dot{x}_6h_0-\dot{x}_6h_0-\mathrm{s}x_1g+x_1g,\\
\upsilon_2 =& u_v+m_1h_0\left\{-\mathrm{c}(x_1-x_5)\dot{x}_2h_b+\dot{x}_2h_b+\mathrm{s}(x_1-x_5)x_2^2h_b+\mathrm{s}x_5g-x_5g\right\}-F_{rr}\mathrm{sgn}(x_2-x_6),\\
\omega_2 =& \begin{bmatrix} \upsilon_1 & \upsilon_2 \end{bmatrix}^T,
\end{aligned}
$$

where υ_1 and υ_2 are bounded.

Therefore, the system (7.7) can be rewritten as

$$
\begin{aligned}
\dot{x}_1 =& x_2,\\
\dot{x}_2 =& \frac{1}{I_{m1}+m_1h_b^2}\left\{-k_r(x_1-x_5)+u_2-m_1h_b(\dot{x}_6h_0-x_1g+\upsilon_1)\right\}\\
\dot{x}_5 =& x_6,\\
\dot{x}_6 =& \frac{1}{I_{m2}+m_1h_0^2}\left\{m_1h_0\left(-\dot{x}_2h_b+x_5g\right)+\upsilon_2-u_2\right\}.
\end{aligned}
\tag{7.8}
$$

Rearrange the system (7.8) and remove $\dot{x}_2$ and $\dot{x}_6$ at the right side of the equations, so we can get

$$
\begin{aligned}
\dot{x}_1 =& x_2,\\
\left[(I_{m1}+m_1h_b^2)-\frac{(m_1h_bh_0)^2}{I_{m2}+m_1h_0^2}\right]\dot{x}_2 =& (m_1h_bg-k_r)x_1+\left[k_r-\frac{(m_1h_0)^2h_bg}{I_{m2}+m_1h_0^2}\right]x_5\\
&+\left[\frac{m_1h_bh_0}{I_{m2}+m_1h_0^2}+1\right]u_2-m_1h_b\upsilon_1-\frac{m_1h_bh_0}{I_{m2}+m_1h_0^2}\upsilon_2,\\
\dot{x}_5 =& x_6,\\
\left[(I_{m2}+m_1h_0^2)-\frac{(m_1h_bh_0)^2}{I_{m1}+m_1h_b^2}\right]\dot{x}_6 =& \frac{m_1h_bh_0}{I_{m1}+m_1h_b^2}(k_r-m_1h_bg)x_1+\left(m_1h_0g-\frac{m_1h_bh_0k_r}{I_{m1}+m_1h_b^2}\right)x_5\\
&-\left(\frac{m_1h_bh_0}{I_{m1}+m_1h_b^2}+1\right)u_2+\frac{(m_1h_b)^2h_0}{I_{m1}+m_1h_b^2}\upsilon_1+\upsilon_2.
\end{aligned}
\tag{7.9}
$$

Then the system (7.9) becomes a linear system as

$$
\begin{aligned}
\dot{\tilde{x}}(t) =& A_2\tilde{x}(t)+B_2u_2(t)+B_{d2}\omega_2(t),\\
\tilde{y}(t) =& C_2\tilde{x}(t),
\end{aligned}
\tag{7.10}
$$

where

$$
A_2=\begin{bmatrix} 0 & 1 & 0 & 0\\ A_{21} & 0 & A_{23} & 0\\ 0 & 0 & 0 & 1\\ A_{41} & 0 & A_{43} & 0 \end{bmatrix},
B_2=\begin{bmatrix} 0\\ B_{22}\\ 0\\ B_{24} \end{bmatrix},
B_{d2}=\begin{bmatrix} 0 & 0\\ B_{d21} & B_{d22}\\ 0 & 0\\ B_{d41} & B_{d42} \end{bmatrix},
C_2=\begin{bmatrix} 1\\ 0\\ 0\\ 0 \end{bmatrix}^T,
$$

$$A_{21} = \frac{m_1 h_b g - k_r}{\Omega_1}, A_{23} = \frac{k_r - \frac{(m_1 h_0)^2 h_b g}{I_{m2} + m_1 h_0^2}}{\Omega_1}, A_{41} = \frac{m_1 h_b h_0 (k_r - m_1 h_b g)}{(I_{m1} + m_1 h_b^2)\Omega_2},$$

$$A_{43} = \frac{m_1 h_0 g - \frac{m_1 h_b h_0 k_r}{I_{m1} + m_1 h_b^2}}{\Omega_2}, B_{22} = \frac{\frac{m_1 h_b h_0}{I_{m2} + m_1 h_0^2} + 1}{\Omega_1}, B_{24} = -\frac{\frac{m_1 h_b h_0}{(I_{m1} + m_1 h_b^2)} + 1}{\Omega_2},$$

$$B_{d21} = -\frac{m_1 h_b}{\Omega_1}, B_{d22} = -\frac{m_1 h_b h_0}{(I_{m2} + m_1 h_0^2)\Omega_1}, B_{d41} = \frac{(m_1 h_b)^2 h_0}{(I_{m1} + m_1 h_b^2)\Omega_2}, B_{d42} = \frac{1}{\Omega_2},$$

$$\Omega_1 = (I_{m1} + m_1 h_b^2) - \frac{(m_1 h_b h_0)^2}{I_{m2} + m_1 h_0^2}, \Omega_2 = (I_{m2} + m_1 h_0^2) - \frac{(m_1 h_b h_0)^2}{I_{m1} + m_1 h_b^2}.$$

7.4 Controller design

For systems (7.6) and (7.10) are both linear systems, compared with system (7.4), it is much easier to design controllers for them. Here the H_∞ controller design mothod is applied.

Theorem 7.1 *The seat suspension subsystems (7.6) and (7.10) are stable with H_∞ control performance γ_i $(i = 1, 2)$, if there exist symmetric positive matrices $P_i > 0$ and matrices K_i with appropriate dimensions satisfying*

$$\Phi_i = \begin{bmatrix} \mathrm{sym}(P_i A_i + P_i B_i K_i) & P_i B_{di} & C_i^T \\ * & -\gamma_i^2 I & 0 \\ * & * & -I \end{bmatrix} < 0. \tag{7.11}$$

Proof. To prove the stability of the seat suspension subsystems (7.6) and (7.10), a Lyapunov function is designed as

$$V_i(t) = x^T(t) P_i x(t), \tag{7.12}$$

where $x(t)$ represents $\bar{x}(t)$ for the system (7.6) and $\tilde{x}(t)$ for the system (7.10).

Then, based on the equations (7.6) and (7.10), we can get the derivative of $V_i(t)$ as

$$\dot{V}_i(t) = \mathrm{sym}\left\{ x^T(t) P_i \left[(A_i + B_i K_i) x(t) + B_{di} \omega_i(t) \right] \right\}. \tag{7.13}$$

Define a state vector as

$$\xi_i^T(t) = \begin{bmatrix} x^T(t) & \omega_i^T(t) \end{bmatrix}.$$

Adding $y^T y - \gamma_i^2 \omega_i^T \omega_i$ into both sides of the equation (7.13), where $y(t)$ represents $\bar{y}(t)$

for the system (7.6) and $\tilde{y}(t)$ for the system (7.10) we have

$$\begin{aligned}\dot{V}_i(t)+y^T y-\gamma_i^2\omega_i^T\omega_i =& x^T(t)(\mathrm{sym}(P_iA_i+P_iB_iK_i)+C_i^TC_i)x(t)\\ &+\mathrm{sym}(x^T(t)P_iB_{di}\omega_i(t))-\gamma_i^2\omega_i^T\omega_i\\ =&\xi_i^T(t)\Xi_i\xi_i(t),\end{aligned}\tag{7.14}$$

where $\Xi_i=\begin{bmatrix}\mathrm{sym}(P_iA_i+P_iB_iK_i)+C_i^TC_i & P_iB_{di}\\ * & -\gamma_i^2I\end{bmatrix}$.

According to Schur complement, $\Phi_i<0$ $(i=1,2)$ are equivalent to $\Xi_i<0$. Based on inequation (7.11), we have $\dot{V}_i(t)+y^Ty-\gamma_i^2\omega_i^T\omega_i<0$, so the seat suspension subsystems (7.6) and (7.10) are stable with H_∞ control performance γ_i. The proof of the Theorem 7.1 is completed. ■

In inequality (7.11), we can not solve the controller K_i directly by the LMI toolbox of MATLAB, because there exist two-variable matrices in one term $P_iB_iK_i$. To solve this problem, the following theorem is introduced.

Theorem 7.2 *The seat suspension subsystem (7.6) and (7.10) are stable with H_∞ control performance γ_i $(i=1,2)$, if there exist symmetric positive matrice Q_i and matrice $\bar{K}_i$ with appropriate dimensions satisfying*

$$\bar{\Phi}_i=\begin{bmatrix}\mathrm{sym}(A_iQ_i+B_i\bar{K}_i) & B_{di} & Q_iC_i^T\\ * & -\gamma_i^2I & 0\\ * & * & -I\end{bmatrix}<0.\tag{7.15}$$

Furthermore, if inequalition (7.15) is feasible, the state feedback H_∞ controllers can be given by $K_i=\bar{K}_iQ_i^{-1}$.

Proof. Define $Q_i=P_i^{-1}$. Pre- and post-multiplying (7.11) by $\mathrm{diag}(Q_i,I,I)$, we can get inequation (7.15). Then, the H_∞ controllers can be solved by $K_i=\bar{K}_iQ_i^{-1}$. The proof of Theorem 7.2 is completed. ■

7.5 Simulation results

In this section, some simulation results are illustrated to show the advantages of the proposed control method. The parameters of this 2-DOF seat suspension system are shown in Table 7.1.

Table 7.1: The 2-DOF seat suspension system parameters

m_1(kg)	m_2(kg)	k_s(N/m)	h_0(m)	h_s(m)	h_b(m)
80	8	5000	0.2	0.05	0.3
F_{rr}(Nm)	F_{rt}(Nm)	k_r(Nm/rad)	I_{m1}(kgm^2)	I_{m2}(kgm^2)	g(m/s^2)
8	80	700	2	0.1	9.8

Based on Theorem 7.2, we can get the two controllers as $K_1 = \begin{bmatrix} 4634.5 & -135.4 \end{bmatrix}$ and $K_2 = \begin{bmatrix} 360.4 & 110.6 & 792.3 & 79.3 \end{bmatrix}$. Then, the vertical controller is obtained as $u_t = K_1\bar{x} + F_{rt}\text{sgn}(x_4)$ and the rotational controller as $u_r = K_2\tilde{x} + F_{rr}\text{sgn}(x_2 - x_6)$.

7.5.1 S-DOF disturbance test

To test the response of this 2-DOF seat suspension system, we choose a white noise signal of the rough road surface as the external disturbance. This disturbance is firstly transferred to a half car model system and then the response of the vehicle chassis provides a vertical displacement input z_s and a rotational angle input θ for the 2-DOF seat suspension system.

Firstly, some S-DOF disturbances are used to test the seat suspension system to show the system responses. The vertical and rotational disturbances are separately tested for the 2-DOF seat suspension to show the control performance of the vertical controller and rotational controller, respectively.

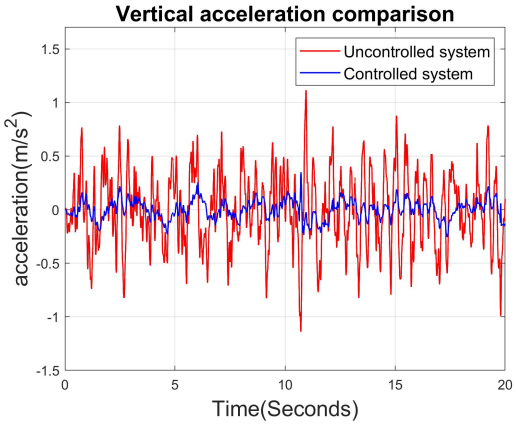

Figure 7.3: The vertical (along axis z_0) acceleration comparison of the center of the gravity of m_1 between the uncontrolled and controlled seat suspension systems.

We set the rotational angle input $\theta = 0$ and only use the vertical displacement input z_s as an external disturbance. Figure 7.3 shows the vertical acceleration comparison of the center of the gravity of m_1 under a random disturbance along axis z_0, where we can see that compared with the uncontrolled system, the vertical controller can effectively reduce the vertical acceleration of the driver.

Then we set the vertical displacement input $z_s = 0$ and only use the rotational angle input θ as an external disturbance. Figure 7.4 shows the seat suspension system performance under a random rotational disturbance around axis y_0. Here we can see that the rotational controller can effectively reduce both the rotational angle position and acceleration of the driver compared with the uncontrolled system. Therefore, both the vertical and rotational controllers can effectively reduce the vertical and rotational vibrations, respectively.

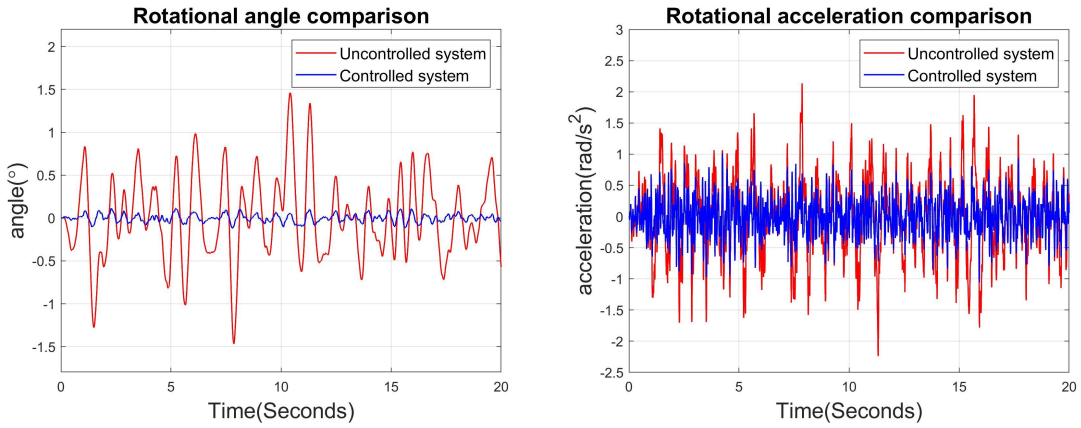

Figure 7.4: The rotational angle position and acceleration comparison of the center of the gravity of m_1 (around axis y_0) between the uncontrolled and controlled seat suspension systems.

7.5.2 Multiple-DOF disturbance test

After the test of S-DOF disturbance for the seat suspension system, the combination of the vertical and rotational disturbance is tested in this part. Here we use the same random disturbance as the S-DOF disturbance test, but both vertical and rotational disturbances are input to the 2-DOF seat suspension system together.

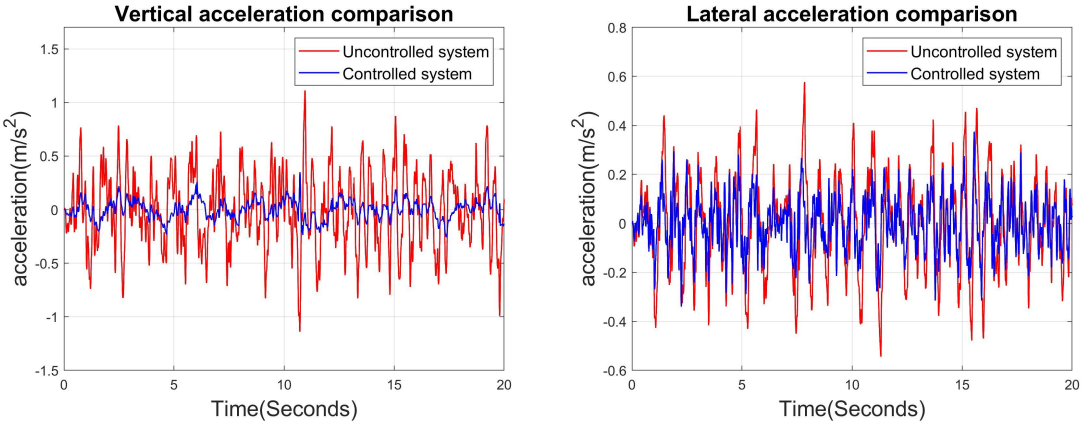

Figure 7.5: The vertical (along axis z_0) and lateral (along axis y_0) acceleration comparison of the center of the gravity of m_1 between the uncontrolled and controlled seat suspension systems.

Figure 7.5 shows the responses of the vertical and lateral acceleration comparison of the driver's body between the uncontrolled and controlled seat suspension systems. Here it is clear to see that the proposed controllers can both reduce the driver's acceleration along axes z_0 and y_0. Figure 7.6 shows the responses of the rotational angle position and acceleration comparison of the driver's body between the uncontrolled and controlled seat suspension systems. We can see that the proposed control method can reduce rotational

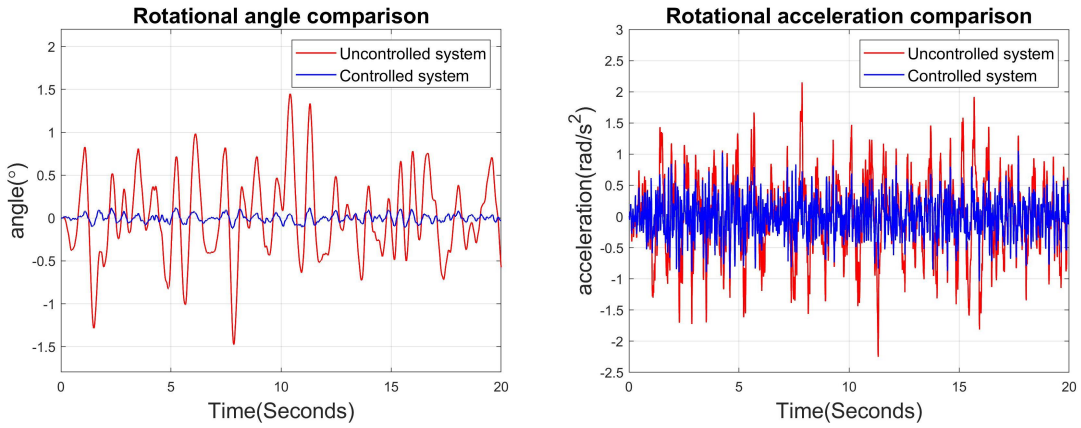

Figure 7.6: The rotational angle position and acceleration comparison of the center of the gravity of m_1 (around axis y_0) between the uncontrolled and controlled seat suspension systems.

vibration effectively. Figure 7.7 shows the outputs of the vertical control force u_t along axis z_1 and the rotational control torque u_r around axis x_2/x_3.

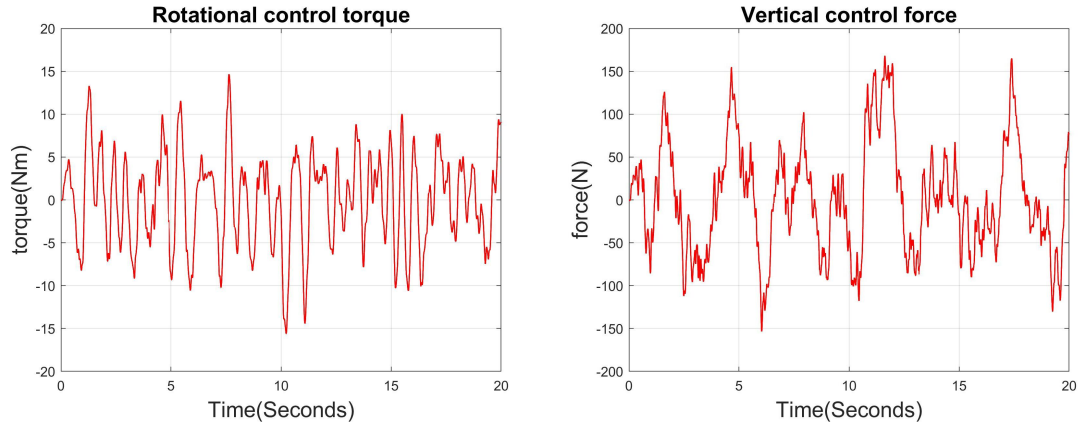

Figure 7.7: The outputs of the vertical control force u_t and the rotational control torque u_r.

Table 7.2 shows the simulation results comparison of the root mean square (RMS) values between the uncontrolled and controlled 2-DOF seat suspension system. Here we can see that the proposed control method can reduce the RMS value of the vertical acceleration for 72.32%, the lateral acceleration for 42.29%, and the rotational acceleration for 50.48% simultaneously, which indicates that the proposed control method can effectively improve the driving comfort in both vertical and rotational degrees of freedom. Therefore, the proposed control method can deal with not only S-DOF disturbances but also multiple-DOF disturbances for the 2-DOF seat suspension system, which is able to better improve driving comfort compared with S-DOF seat suspensions.

Table 7.2: The simulation results comparison

RMS value	Uncontrolled	Controlled	Reduction (%)
Vertical acceleration	0.3475 m/s^2	0.0892 m/s^2	72.32
Lateral acceleration	0.1900 m/s^2	0.1096 m/s^2	42.29
Rotational acceleration	0.6211 rad/s^2	0.3076 rad/s^2	50.48

7.6 Conclusion

A control system and a robust H_∞ control strategy are designed for a 2-DOF seat suspension in this chapter. A nonlinear complicated system with multiple inputs and multiple outputs are established for the 2-DOF seat suspension, where the vertical and rotational vibrations can be controlled. This nonlinear system is separated into two linear subsystems (vertical vibration subsystem and rotational vibration subsystem). The robust H_∞ controllers are designed for each subsystem and the stability of these two subsystems are verified. Some simulation results show that the proposed control strategy can reduce both vertical and rotational vibrations separately and simultaneously for drivers under the rough road surface of a white noise signal to improve the driving comfort effectively. The future work will consider the experimental tests of the proposed control strategy for this 2-DOF seat suspension. The next chapter gives the conclusion of this thesis and some future research work.

Chapter 8

Conclusion and future work

8.1 Introduction

The previous chapter introduces the impact of WBV on vehicle drivers. A 2-DOF seat suspension model system is built and H_∞ controllers are designed for the vertical and rotational vibration subsystems, where the simulation results show that the proposed control method can reduce both vertical and rotational vibrations simultaneously. In this chapter, some discussions and conclusions of this thesis are given; the contributions and implications of this research are stated; finally, some possible future work is discussed.

8.2 Discussion and conclusion

This thesis focuses on the control system and control strategies for vehicle active seat suspensions, where some novel seat suspension systems are established and some control methods are proposed to reduce drivers' vibrations and improve driving comfort. Some discussions and conclusion of each part of this work are listed as follows.

Firstly, some novel seat suspension systems are considered because conventional seat suspension systems do not consider acceleration signals as system states even though this signal can be easily measured in real time and has a very close relationship with driving comfort. Besides, some conventional seat suspension systems need to use absolute displacement or velocity signals of seat suspensions to decide controllers, while those signals are not available in practice, which makes it not practical for industry. To make full use of all easily measurable signals, the acceleration signal of the seat suspension is firstly considered as a state variable, together with the deflection and relative velocity signals in the research. This novel seat suspension system is a singular system because it is described by differential and algebraic equations. The singular seat suspension systems are applied in Chapter 3 and Chapter 6.

Seat suspensions are mostly simplified as linear systems with spring stiffness and damp-

ing coefficients by some researchers in the past, while the real seat suspension systems are nonlinear. However, it is still difficult to get the real system parameters for seat suspensions. In Chapter 3, a friction observer is applied to compensate the controller for the internal seat friction disturbance, which is helpful to get better control performance to reduce vibrations.

Data processing and transmission are inevitable in almost all control engineering fields. For the active seat suspension control, we need sensors to collect data, data transmission devices to transmit data, computers to cope with data and make control instruction. However, limited by the transmission speed, data dropout and time delay always happens, which influences the control performance of the active seat suspension systems. To deal with those issues, the event-triggered schemes are proposed for active seat suspension systems in Chapter 4, Chapter 5, and Chapter 6. Both the continuous-time event-triggered scheme (Chapter 4) and the discrete-time event-triggered scheme (Chapter 5 and Chapter 6) are considered. Some simulation and experimental results show that the event-triggered schemes can greatly reduce the workload of data transmission without big influences on the control performance to reduce vibrations.

Time delay is also a common issue for many control fields. In this research, to deal with the time-delay problems, H_∞ control method is applied in all the research programs for the control of active seat suspension systems. To reduce the conservation of the seat suspension systems to time delay, several different less conservative inequalities are used in different chapters.

Apart from the simple seat suspension mode, some complicated seat suspension modes are also considered in this research. In Chapter 6, an active singular seat suspension system with a human body in the loop is established and the output-feedback event-triggered H_∞ controller is designed for this system. Simulation results show the effectiveness of the proposed control method. However, the human body is simply separated into two parts (body torso and head) with linear parameters, while the real human body is nonlinear and much more complicated than this model. If a more complicated human body model is considered, it may be very difficult to get some results from this method. Besides, the parameters of every human body may also vary a lot, so it is very difficult to get specific and accurate parameters. Therefore, the trade-off between the more accurate human body model and the feasible control method needs to be balanced.

Besides, a 2-DOF seat suspension system is established in Chapter 7, where the vertical and rotational vibrations can be controlled together. A nonlinear complicated seat suspension system with multiple inputs and multiple outputs is built first and then it is separated into two linear subsystems (vertical vibration subsystem and rotational vibration subsystem). Two H_∞ controllers are designed for each subsystem respectively and the controlled subsystems are proved to be stable. The simulation results are shown to illustrate the effectiveness and efficiency of the proposed control method to reduce both vertical and

rotational vibrations simultaneously. However, because of the insufficient time, the experimental tests of this proposed method has not been done, which will become part of future work.

To sum up, this research studies some advanced control strategies for active seat suspension systems. The proposed control strategies can deal with different kinds of issues for active seat suspension systems to reduce vibration and improve driving comfort for vehicle drivers. All of the control methods are proved to be effective from simulation results and some are also tested by experiments.

8.3 Implications

The focus of this thesis is on active seat suspension systems to design control systems and control strategies to improve the driving comfort for heavy vehicle drivers. The proposed novel seat suspension systems and control methods have brought some new ideas in the research area of seat suspensions. Acceleration signals are firstly applied as part of system state variables and used for the controller design. Both continuous and discrete event-triggered schemes are considered for the H_∞ controller design of the seat suspension systems, which makes some contributions for the network cloud control in the seat suspension area. Some more complicated control conditions are also considered in this thesis, as the seat suspension control with a human body in loop and a 2-DOF seat suspension control system. All the proposed control methods can probably be used in the field of seat suspension production, and contribute to a more comfortable and safer driving experience for heavy vehicle drivers in the future.

8.4 Some future work

Several control strategies have been proposed in this thesis, but there still exist many interesting research topics worthy of keeping study in the field of seat suspensions. Some possible future research work is listed as follows.

- Some more efficient control methods will be considered to control seat suspensions to get better control performance to improve driving comfort.
- Some more accurate and complicated seat suspension systems will be investigated to more accurately describe seat suspension systems.
- Multiple-DOF seat suspensions will be established and the corresponding control methods will be designed to reduce whole-body vibrations more efficiently.

- Active seat suspensions normally consume much more energy, which limits their development, so more energy-saving seat suspensions will be considered for heavy vehicles.
- The cooperative research of seat suspension and other related cutting-edge fields (like cloud control or artificial intelligence) will also be an important research direction in the future.

Bibliography

[1] Hyun Duck Choi, Choon Ki Ahn, Peng Shi, Ligang Wu, and Myo Taeg Lim. Dynamic output-feedback dissipative control for T-S fuzzy systems with time-varying input delay and output constraints. *IEEE Transactions on Fuzzy Systems*, 25(3): 511–526, 2016.

[2] Mirko Čorić, Joško Deur, Josip Kasać, H Eric Tseng, and Davor Hrovat. Optimisation of active suspension control inputs for improved vehicle handling performance. *Vehicle System Dynamics*, 54(11):1574–1600, 2016.

[3] Vaijayanti S Deshpande, Pramod D Shendge, and Shrivijay B Phadke. Nonlinear control for dual objective active suspension systems. *IEEE Transactions on Intelligent Transportation Systems*, 18(3):656–665, 2016.

[4] Shiyuan Han, Gongyou Tang, Yuehui Chen, Xixin Yang, and Xue Yang. Optimal vibration control for vehicle active suspension discrete-time systems with actuator time delay. *Asian Journal of Control*, 15(6):1579–1588, 2013.

[5] Shiyuan Han, Chenghui Zhang, Yuehui Chen, and Xiaofang Zhong. Discrete optimal actuator-fault-tolerant control for vehicle active suspension. *Journal of Vibroengineering*, 19(1):314–327, 2017.

[6] Rabih Alkhatib, Geza Nakhaie Jazar, and M. Farid Golnaraghi. Optimal design of passive linear suspension using genetic algorithm. *Journal of Sound and vibration*, 275(3-5):665–691, 2004.

[7] Dean Karnopp, Michael J Crosby, and RA Harwood. Vibration control using semi-active force generators. 1974.

[8] Hongyi Li, Honghai Liu, Huijun Gao, and Peng Shi. Reliable fuzzy control for active suspension systems with actuator delay and fault. *IEEE Transactions on Fuzzy Systems*, 20(2):342–357, 2011.

[9] Donghong Ning, Haiping Du, Shuaishuai Sun, Weihua Li, and Bangji Zhang. An innovative two-layer multiple-DOF seat suspension for vehicle whole body vibration control. *IEEE/ASME Transactions on Mechatronics*, 23(4):1787–1799, 2018.

[10] Donghong Ning, Shuaishuai Sun, Haiping Du, Weihua Li, and Wenxing Li. Control of a multiple-DOF vehicle seat suspension with roll and vertical vibration. *Journal of Sound and Vibration*, 435:170–191, 2018.

[11] Shian Chen, Juncheng Wang, Ming Yao, and Young Bae Kim. Improved optimal sliding mode control for a non-linear vehicle active suspension system. *Journal of Sound and Vibration*, 395:1–25, 2017.

[12] Wael Abbas, Ashraf Emam, Saeed Badran, Mohamed Shebl, and Ossama Abouelatta. Optimal seat and suspension design for a half-car with driver model using genetic algorithm. 2013.

[13] Thanh Danh Le and Kyoung Kwan Ahn. A vibration isolation system in low frequency excitation region using negative stiffness structure for vehicle seat. *Journal of Sound and Vibration*, 330(26):6311–6335, 2011.

[14] Thanh Danh Le and Kyoung Kwan Ahn. Experimental investigation of a vibration isolation system using negative stiffness structure. *International Journal of Mechanical Sciences*, 70:99–112, 2013.

[15] Shida Nie, Ye Zhuang, Weiping Liu, and Fan Chen. A semi-active suspension control algorithm for vehicle comprehensive vertical dynamics performance. *Vehicle System Dynamics*, 55(8):1099–1122, 2017.

[16] Hwan Choong Kim, Yu Jeong Shin, Wonhee You, Kyu Chul Jung, Jong Seok Oh, and Seung Bok Choi. A ride quality evaluation of a semi-active railway vehicle suspension system with MR damper: railway field tests. *Proceedings of the Institution of Mechanical Engineers, Part F: Journal of Rail and Rapid Transit*, 231(3): 306–316, 2017.

[17] Wan Ho Kim, Jhin Ha Park, Suresh Kaluvan, Yang Sup Lee, and Seung Bok Choi. A novel type of tunable magnetorheological dampers operated by permanent magnets. *Sensors and Actuators A: Physical*, 255:104–117, 2017.

[18] Saikat Dutta and Seung Bok Choi. A nonlinear kinematic and dynamic modeling of Macpherson suspension systems with a magneto-rheological damper. *Smart Materials and Structures*, 25(3):035003, 2016.

[19] Seung Bok Choi, Moo Ho Nam, and Byung Kyu Lee. Vibration control of a MR seat damper for commercial vehicles. *Journal of Intelligent Material Systems and Structures*, 11(12):936–944, 2000.

[20] Seung Bok Choi and Young Min Han. Vibration control of electrorheological seat suspension with human-body model using sliding mode control. *Journal of Sound and Vibration*, 303(1-2):391–404, 2007.

[21] Sy Dzung Nguyen, Wanho Kim, Jhinha Park, and Seung Bok Choi. A new fuzzy sliding mode controller for vibration control systems using integrated-structure smart dampers. *Smart Materials and Structures*, 26(4):045038, 2017.

[22] Saikat Dutta, Sang Min Choi, and Seung Bok Choi. A new adaptive sliding mode control for Macpherson strut suspension system with magneto-rheological damper. *Journal of Intelligent Material Systems and Structures*, 27(20):2795–2809, 2016.

[23] Do Xuan Phu, Seung Bok Choi, Yang Sub Lee, and Moon Sihk Han. Vibration control of a vehicle's seat suspension featuring a magnetorheological damper based on a new adaptive fuzzy sliding-mode controller. *Proceedings of the Institution of Mechanical Engineers, Part D: Journal of Automobile Engineering*, 230(4):437–458, 2016.

[24] Do Kyun Shin, Do Xuan Phu, Sang Min Choi, and Seung Bok Choi. An adaptive fuzzy sliding mode control of magneto-rheological seat suspension with human body model. *Journal of Intelligent Material Systems and Structures*, 27(7):925–934, 2016.

[25] Hasan Omur Ozer, Yuksel Hacioglu, and Nurkan Yagiz. High order sliding mode control with estimation for vehicle active suspensions. *Transactions of the Institute of Measurement and Control*, 40(5):1457–1470, 2018.

[26] GS Paddan and MJ Griffin. Effect of seating on exposures to whole-body vibration in vehicles. *Journal of Sound and Vibration*, 253(1):215–241, 2002.

[27] Huihui Pan, Weichao Sun, Huijun Gao, Tasawar Hayat, and Fuad Alsaadi. Nonlinear tracking control based on extended state observer for vehicle active suspensions with performance constraints. *Mechatronics*, 30:363–370, 2015.

[28] Huihui Pan, Weichao Sun, Xingjian Jing, Huijun Gao, and Jianyong Yao. Adaptive tracking control for active suspension systems with non-ideal actuators. *Journal of Sound and Vibration*, 399:2–20, 2017.

[29] B Rajkumar, P Lakshmi, and S Rajendiran. Vibration control of quarter car integrated seat suspension with driver model for different road profiles using fuzzy based sliding mode controller. In *2015 Seventh International Conference on Advanced Computing (ICoAC)*, pages 1–6. IEEE, 2015.

[30] KA C Cheok, Hong Xing Hu, and NK Loh. Discrete-time frequency-shaping parametric LQ control with application to active seat suspension control. *IEEE Transactions on Industrial Electronics*, 36(3):383–390, 1989.

[31] MP Nagarkar, GJ Vikhe, KR Borole, and VM Nandedkar. Active control of quarter-car suspension system using linear quadratic regulator. *International Journal of Automotive and Mechanical Engineering*, 3(1):364–372, 2011.

[32] Yuping He and John McPhee. Multidisciplinary design optimization of mechatronic vehicles with active suspensions. *Journal of Sound and Vibration*, 283(1-2): 217–241, 2005.

[33] Jaemin Baek, Maolin Jin, and Soohee Han. A new adaptive sliding-mode control scheme for application to robot manipulators. *IEEE Transactions on Industrial Electronics*, 63(6):3628–3637, 2016.

[34] Hongyi Li, Jinyong Yu, Chris Hilton, and Honghai Liu. Adaptive sliding-mode control for nonlinear active suspension vehicle systems using T-S fuzzy approach. *IEEE Transactions on Industrial Electronics*, 60(8):3328–3338, 2012.

[35] I Maciejewski, S Glowinski, and T Krzyzynski. Active control of a seat suspension with the system adaptation to varying load mass. *Mechatronics*, 24(8):1242–1253, 2014.

[36] Huihui Pan, Xingjian Jing, Weichao Sun, and Huijun Gao. A bioinspired dynamics-based adaptive tracking control for nonlinear suspension systems. *IEEE transactions on control systems technology*, 26(3):903–914, 2017.

[37] Sofiane Bououden, Mohammed Chadli, and Hamid Reza Karimi. A robust predictive control design for nonlinear active suspension systems. *Asian Journal of Control*, 18(1):122–132, 2016.

[38] Chao Ge, Yanpen Shi, Ju H Park, and Changchun Hua. Robust H_∞ stabilization for ts fuzzy systems with time-varying delays and memory sampled-data control. *Applied Mathematics and Computation*, 346:500–512, 2019.

[39] Kellie F Oliveira, Manuel Braz César, and José Gonçalves. Fuzzy based control of a vehicle suspension system using a MR damper. In *CONTROLO 2016*, pages 571–581. Springer, 2017.

[40] Donghong Ning, Shuaishuai Sun, Fei Zhang, Haiping Du, Weihua Li, and Bangji Zhang. Disturbance observer based Takagi-Sugeno fuzzy control for an active seat suspension. *Mechanical Systems and Signal Processing*, 93:515–530, 2017.

[41] Shiping Wen, Michael ZQ Chen, Zhigang Zeng, Xinghuo Yu, and Tingwen Huang. Fuzzy control for uncertain vehicle active suspension systems via dynamic sliding-mode approach. *IEEE Transactions on Systems, Man, and Cybernetics: Systems*, 47(1):24–32, 2016.

[42] Redouane Chaibi, Ismail Er Rachid, El Houssaine Tissir, and Abdelaziz Hmamed. Finite-frequency static output feedback H_∞ control of continuous-time T-S fuzzy systems. *Journal of Circuits, Systems and Computers*, 28(02):1950023, 2019.

[43] Abdulaziz Alfadhli, Jocelyn Darling, and Andrew J Hillis. The control of an active seat with vehicle suspension preview information. *Journal of Vibration and Control*, 24(8):1412–1426, 2018.

[44] Weichao Sun, Huijun Gao, and Okyay Kaynak. Finite frequency H_∞ control for vehicle active suspension systems. *IEEE Transactions on Control Systems Technology*, 19(2):416–422, 2010.

[45] Weichao Sun, Zhengli Zhao, and Huijun Gao. Saturated adaptive robust control for active suspension systems. *IEEE Transactions on Industrial Electronics*, 60(9): 3889–3896, 2012.

[46] Donghong Ning, Shuaishuai Sun, Jiawei Zhang, Haiping Du, Weihua Li, and Xu Wang. An active seat suspension design for vibration control of heavy-duty vehicles. *Journal of Low Frequency Noise, Vibration and Active Control*, 35(4): 264–278, 2016.

[47] Zhaowen Xu, Hongye Su, Peng Shi, and Zheng-Guang Wu. Asynchronous H_∞ control of semi-Markov jump linear systems. *Applied Mathematics and Computation*, 349:270–280, 2019.

[48] Xiaobin Gao, Hongru Ren, Feiqi Deng, and Qi Zhou. Observer-based finite-time H_∞ control for uncertain discrete-time nonhomogeneous Markov jump systems. *Journal of the Franklin Institute*, 356(4):1730–1749, 2019.

[49] Oscar Barambones and Patxi Alkorta. Position control of the induction motor using an adaptive sliding-mode controller and observers. *IEEE Transactions on Industrial Electronics*, 61(12):6556–6565, 2014.

[50] Jagat Jyoti Rath, Michael Defoort, Hamid Reza Karimi, and Kalyana Chakravarthy Veluvolu. Output feedback active suspension control with higher order terminal sliding mode. *IEEE Transactions on Industrial Electronics*, 64(2):1392–1403, 2016.

[51] Donghong Ning, Shuaishuai Sun, Lidui Wei, Bangji Zhang, Haiping Du, and Weihua Li. Vibration reduction of seat suspension using observer based terminal sliding mode control with acceleration data fusion. *Mechatronics*, 44:71–83, 2017.

[52] Abdulaziz Alfadhli, Jocelyn Darling, and Andrew J Hillis. The control of an active seat suspension using an optimised fuzzy logic controller, based on preview information from a full vehicle model. *Vibration*, 1(1):3, 2018.

[53] Rudiger Kieneke, Christian Graf, and Jürgen Maas. Active seat suspension with two degrees of freedom for military vehicles. *IFAC Proceedings Volumes*, 46(5): 523–529, 2013.

[54] Xian-Xu Bai, Peng Jiang, and Li-Jun Qian. Integrated semi-active seat suspension for both longitudinal and vertical vibration isolation. *Journal of Intelligent Material Systems and Structures*, 28(8):1036–1049, 2017.

[55] Feng Zhao, Shuzhi Sam Ge, Fangwen Tu, Yechen Qin, and Mingming Dong. Adaptive neural network control for active suspension system with actuator saturation. *IET Control Theory & Applications*, 10(14):1696–1705, 2016.

[56] MM Frechin, SB Arino, and J Fontaine. ACTISEAT: active vehicle seat for acceleration compensation. *Proceedings of the Institution of Mechanical Engineers, Part D: Journal of Automobile Engineering*, 218(9):925–933, 2004.

[57] Shaimaa A Ali, H Metered, AM Bassiuny, and AM Abdel-Ghany. Vibration control of an active seat suspension system integrated pregnant woman body model. Technical report, SAE Technical Paper, DOI: https://doi.org/10.4271/2019-01-0172, 2019.

[58] Igor Maciejewski, Tomasz Krzyzynski, and Henning Meyer. Modeling and vibration control of an active horizontal seat suspension with pneumatic muscles. *Journal of Vibration and Control*, 24(24):5938–5950, 2018.

[59] Jianjun Bai, Renquan Lu, Zhengguang Wu, Ridong Zhang, Xiaodong Zhao, and Anke Xue. Robust control of discrete-time singular systems via integral sliding surface. *Asian Journal of Control*, 20(3):1296–1302, 2018.

[60] Guobao Liu, Shengyuan Xu, Yunliang Wei, Zhidong Qi, and Zhengqiang Zhang. New insight into reachable set estimation for uncertain singular time-delay systems. *Applied Mathematics and Computation*, 320:769–780, 2018.

[61] Hao Zhang, Xiaoyuan Zheng, Huaicheng Yan, Chen Peng, Zhuping Wang, and Qijun Chen. Codesign of event-triggered and distributed H_∞ filtering for active

semi-vehicle suspension systems. *IEEE/ASME Transactions on Mechatronics*, 22 (2):1047–1058, 2017.

[62] Qi Zhou, Deyin Yao, Jiahui Wang, and Chengwei Wu. Robust control of uncertain semi-Markovian jump systems using sliding mode control method. *Applied Mathematics and Computation*, 286:72–87, 2016.

[63] Kangzhi Liu and Yu Yao. *Robust control: theory and applications*. John Wiley & Sons, 2016.

[64] Linchuang Zhang, Hak-Keung Lam, Yonghui Sun, and Hongjing Liang. Fault detection for fuzzy semi-Markov jump systems based on interval type-2 fuzzy approach. *IEEE Transactions on Fuzzy Systems*, DOI: 10.1109/TFUZZ.2019.2936333, 2019.

[65] Linchuang Zhang, Hongjing Liang, Yonghui Sun, and Choon Ki Ahn. Adaptive event-triggered fault detection scheme for semi-Markovian jump systems with output quantization. *IEEE Transactions on Systems, Man, and Cybernetics: Systems*, DOI: 10.1109/TSMC.2019.2912846, 2019.

[66] Peihao Du, Hongjing Liang, Shiyi Zhao, and Choon Ki Ahn. Neural-based decentralized adaptive finite-time control for nonlinear large-scale systems with time-varying output constraints. *IEEE Transactions on Systems, Man, and Cybernetics: Systems*, 2019. doi: 10.1109/TSMC.2019.2918351.

[67] Hongbing Zeng, Yong He, Min Wu, and Jinhua She. Free-matrix-based integral inequality for stability analysis of systems with time-varying delay. *IEEE Trans. Automat. Contr.*, 60(10):2768–2772, 2015.

[68] Laurent El Ghaoui, Francois Oustry, and Mustapha AitRami. A cone complementarity linearization algorithm for static output-feedback and related problems. In *Proceedings of Joint Conference on Control Applications Intelligent Control and Computer Aided Control System Design*, pages 246–251. IEEE, 1996.

[69] Liyi Dai. Singular control systems. *New York*, pages 29–39, 1989.

[70] Guang-Ren Duan. *Analysis and design of descriptor linear systems*, volume 23. Springer Science & Business Media, 2010.

[71] Shengyuan Xu and James Lam. *Robust control and filtering of singular systems*, volume 332. Springer, 2006.

[72] Gang Wang, Mohammed Chadli, Haihong Chen, and Zhijin Zhou. Event-triggered control for active vehicle suspension systems with network-induced delays. *Journal of the Franklin Institute*, 356(1):147–172, 2019.

[73] Hongjing Liang, Linchuang Zhang, Yonghui Sun, and Tingwen Huang. Containment control of semi-Markovian multiagent systems with switching topologies. *IEEE Transactions on Systems, Man, and Cybernetics: Systems*, 2019. doi: 10.1109/TSMC.2019.2946248.

[74] Chen Peng, Hongtao Sun, Mingjin Yang, and Yulong Wang. A survey on security communication and control for smart grids under malicious cyber attacks. *IEEE Transactions on Systems, Man, and Cybernetics: Systems*, 49(8):1554–1569, 2019.

[75] Zhiyang Ju, Hui Zhang, and Ying Tan. Distributed deception attack detection in platoon-based connected vehicle systems. *IEEE Transactions on Vehicular Technology*, 69(5):4609–4620, 2020.

[76] Deyin Yao, Bin Zhang, Panshuo Li, and Hongyi Li. Event-triggered sliding mode control of discrete-time Markov jump systems. *IEEE Transactions on Systems, Man, and Cybernetics: Systems*, 49(10):2016–2025, 2018.

[77] Xiaomeng Li, Qi Zhou, Panshuo Li, Hongyi Li, and Renquan Lu. Event-triggered consensus control for multi-agent systems against false data-injection attacks. *IEEE Transactions on Cybernetics*, 50(5):1856–1866, 2019.

[78] Liang Cao, Hongyi Li, Guowei Dong, and Renquan Lu. Event-triggered control for multiagent systems with sensor faults and input saturation. *IEEE Transactions on Systems, Man, and Cybernetics: Systems*, 2019. doi: 10.1109/TSMC.2019.2938216.

[79] Chen Peng, Jicai Li, and Minrui Fei. Resilient event-triggering H_∞ load frequency control for multi-area power systems with energy-limited DoS attacks. *IEEE Transactions on Power Systems*, 32(5):4110–4118, 2016.

[80] Yanjun Shen, Fengjiao Li, Daoyuan Zhang, Yanwu Wang, and Yungang Liu. Event-triggered output feedback H_∞ control for networked control systems. *International Journal of Robust and Nonlinear Control*, 29(1):166–179, 2019.

[81] Ligang Wu, Yabin Gao, Jianxing Liu, and Hongyi Li. Event-triggered sliding mode control of stochastic systems via output feedback. *Automatica*, 82:79–92, 2017.

[82] Xiaojie Su, Xinxin Liu, and Yongduan Song. Event-triggered sliding-mode control for multi-area power systems. *IEEE Transactions on Industrial Electronics*, 64(8): 6732–6741, 2017.

[83] Abhisek K Behera and Bijnan Bandyopadhyay. Robust sliding mode control: an event-triggering approach. *IEEE Transactions on Circuits and Systems II: Express Briefs*, 64(2):146–150, 2017.

[84] Anton Selivanov and Emilia Fridman. Event-triggered H_∞ control: A switching approach. *IEEE Transactions on Automatic Control*, 61(10):3221–3226, 2016.

[85] Anton Selivanov and Emilia Fridman. A switching approach to event-triggered control. In *Decision and Control (CDC), 2015 IEEE 54th Annual Conference on*, pages 5468–5473. IEEE, 2015.

[86] Hongjing Liang, Xiyue Guo, Yingnan Pan, and Tingwen Huang. Event-triggered fuzzy bipartite tracking control for network systems based on distributed reduced-order observers. *IEEE Transactions on Fuzzy Systems*, 2020. doi: 10.1109/TFUZZ.2020.2982618.

[87] Zhechen Zhu, Yingnan Pan, Qi Zhou, and Changxin Lu. Event-triggered adaptive fuzzy control for stochastic nonlinear systems with unmeasured states and unknown backlash-like hysteresis. *IEEE Transactions on Fuzzy Systems*, 2020. doi: 10.1109/TFUZZ.2020.2973950.

[88] Tae H Lee, Ju H Park, and Shengyuan Xu. Relaxed conditions for stability of time-varying delay systems. *Automatica*, 75:11–15, 2017.

[89] M Agostinacchio, D Ciampa, and S Olita. The vibrations induced by surface irregularities in road pavements–a Matlab approach. *European Transport Research Review*, 6(3):267–275, 2014.

[90] Haiping Du, James Lam, KC Cheung, Weihua Li, and Nong Zhang. Direct voltage control of magnetorheological damper for vehicle suspensions. *Smart Materials and Structures*, 22(10):105016, 2013.

[91] Morteza Moradi and Afef Fekih. Adaptive PID-sliding-mode fault-tolerant control approach for vehicle suspension systems subject to actuator faults. *IEEE Transactions on Vehicular Technology*, 63(3):1041–1054, 2013.

[92] Weichao Sun, Huihui Pan, and Huijun Gao. Filter-based adaptive vibration control for active vehicle suspensions with electrohydraulic actuators. *IEEE Transactions on Vehicular Technology*, 65(6):4619–4626, 2015.

[93] Zehui Mao, Yanhao Zhan, Gang Tao, Bin Jiang, and Xinggang Yan. Sensor fault detection for rail vehicle suspension systems with disturbances and stochastic noises. *IEEE Transactions on Vehicular Technology*, 66(6):4691–4705, 2016.

[94] Chunyu Wei, Yue Cai, Ke Zhang, Zhan Wang, and Wenda Yu. Novel optimal design approach for output-feedback H_∞ control of vehicle active seat-suspension system. *Asian Journal of Control, DOI: 10.1002/asjc.1887*, 2018.

[95] Zhongyang Fei, Xudong Wang, Ming Liu, and Jinyong Yu. Reliable control for vehicle active suspension systems under event-triggered scheme with frequency range limitation. *IEEE Transactions on Systems, Man, and Cybernetics: Systems*, DOI: 10.1109/TSMC.2019.2899942, 2019.

[96] Donghong Ning, Haiping Du, Shuaishuai Sun, Weihua Li, Nong Zhang, and Mingming Dong. A novel electrical variable stiffness device for vehicle seat suspension control with mismatched disturbance compensation. *IEEE/ASME Transactions on Mechatronics*, 24(5), 2019.

[97] Sabreen Gad, Hassan Ahmed Metered, A.M. Bassuiny, and AM Abdel Ghany. Multi-objective genetic algorithm fractional-order PID controller for semi-active magnetorheologically damped seat suspension. *Journal of Vibration and Control*, 23(8):1248–1266, 2017.

[98] Yi Zhang, Shuai Lu, Yalian Yang, and Qiang Guo. Internet-distributed vehicle-in-the-loop simulation for HEVs. *IEEE transactions on Vehicular Technology*, 67(5): 3729–3739, 2018.

[99] Dan Liu and Guanghong Yang. Decentralized event-triggered output feedback control for a class of interconnected large-scale systems. *ISA Transactions*, 93: 156–164, 2019.

[100] Nana Feng, Baowei Wu, Lili Liu, and Yue-E Wang. Exponential stability of output-based event-triggered control for switched singular systems. *Asian Journal of Control*, 2019. doi: 10.1002/asjc.2035.

[101] Jianqiang Yu, Xiaomin Dong, Zonglun Zhang, and Pinggen Chen. A novel scissor-type magnetorheological seat suspension system with self-sustainability. *Journal of Intelligent Material Systems and Structures*, 30(5):665–676, 2019.

[102] Zhiguang Feng, Huayang Zhang, Haiping Du, and Zhengyi Jiang. Admissibilisation of singular interval type-2 Takagi–Sugeno fuzzy systems with time delay. *IET Control Theory & Applications*, 14(8):1022–1032, 2020.

[103] PooGyeon Park, Jeong Wan Ko, and Changki Jeong. Reciprocally convex approach to stability of systems with time-varying delays. *Automatica*, 47(1):235–238, 2011.

[104] Kenan Melemez, Metin Tunay, and Tuna Emir. The role of seat suspension in whole-body vibration affecting skidding tractor operators. *J. Food Agric. Environ*, 11:1211–1215, 2013.

[105] P Velmurugan, LA Kumaraswamidhas, and K Sankaranarayanasamy. Influence of road surfaces on whole body vibration for suspended cabin tractor semitrailer

drivers. *Journal of Low Frequency Noise, Vibration and Active Control*, 31(2): 75–84, 2012.

[106] P Velmurugan, LA Kumaraswamidhas, and K Sankaranarayanasamy. Whole body vibration analysis for drivers of suspended cabin tractor semitrailer. *Experimental Techniques*, 38(2):47–53, 2014.

[107] Ornwipa Thamsuwan, Ryan P Blood, Charlotte Lewis, Patrik W Rynell, and Peter W Johnson. Whole body vibration exposure and seat effective amplitude transmissibility of air suspension seat in different bus designs. In *Proceedings of the Human Factors and Ergonomics Society Annual Meeting*, volume 56, pages 1218–1222. SAGE Publications Sage CA: Los Angeles, CA, 2012.

[108] Ryan P Blood, Michael G Yost, Janice E Camp, and Randal P Ching. Whole-body vibration exposure intervention among professional bus and truck drivers: a laboratory evaluation of seat-suspension designs. *Journal of Occupational and Environmental Hygiene*, 12(6):351–362, 2015.

[109] Per MG Jonsson, Patrik W Rynell, Mats Hagberg, and Peter W Johnson. Comparison of whole-body vibration exposures in buses: effects and interactions of bus and seat design. *Ergonomics*, 58(7):1133–1142, 2015.

[110] Roberto Deboli, Angela Calvo, and Christian Preti. Whole-body vibration: Measurement of horizontal and vertical transmissibility of an agricultural tractor seat. *International Journal of Industrial Ergonomics*, 58:69–78, 2017.

[111] Jeong Ho Kim, Luz S Marin, and Jack T Dennerlein. Evaluation of commercially available seat suspensions to reduce whole body vibration exposures in mining heavy equipment vehicle operators. *Applied ergonomics*, 71:78–86, 2018.

[112] Ryan P Blood, James D Ploger, and Peter W Johnson. Whole body vibration exposures in forklift operators: comparison of a mechanical and air suspension seat. *Ergonomics*, 53(11):1385–1394, 2010.

[113] R Motmans. Reducing whole body vibration in forklift drivers. *Work*, 41 (Supplement 1):2476–2481, 2012.

[114] James L Coyte, David Stirling, Haiping Du, and Montserrat Ros. Seated whole-body vibration analysis, technologies, and modeling: a survey. *IEEE Transactions on Systems, Man, and Cybernetics: Systems*, 46(6):725–739, 2015.

[115] Beibei Yang, Yefa Hu, Haining Fang, and Chunsheng Song. Research on arrangement scheme of magnetic suspension isolator for multi-degree freedom vibration isolation system. *Journal of Industrial Information Integration*, 6:47–55, 2017.

[116] Leanne F Conrad, Michele L Oliver, Robert J Jack, James P Dickey, and Tammy Eger. Quantification of 6-degree-of-freedom chassis whole-body vibration in mobile heavy vehicles used in the steel making industry. *Journal of Low Frequency Noise, Vibration and Active Control*, 31(2):85–104, 2012.

[117] S Aisyah Adam, NA Abdul Jalil, KA Md Razali, and YG Ng. The effects of posture on suspension seat transmissibility during exposure to vertical whole-body vibration. In *Journal of Physics: Conference Series*, volume 1262, pages 012–026. IOP Publishing, 2019.

[118] Bronson Boi Du, Philip L Bigelow, Richard P Wells, Hugh W Davies, Peter Hall, and Peter W Johnson. The impact of different seats and whole-body vibration exposures on truck driver vigilance and discomfort. *Ergonomics*, 61(4):528–537, 2018.

[119] S Aisyah Adam and Nawal A Abdul Jalil. Vertical suspension seat transmissibility and seat values for seated person exposed to whole-body vibration in agricultural tractor preliminary study. *Procedia engineering*, 170:435–442, 2017.

[120] Federica Caffaro, Margherita Micheletti Cremasco, Christian Preti, and Eugenio Cavallo. Ergonomic analysis of the effects of a telehandler's active suspended cab on whole body vibration level and operator comfort. *International Journal of Industrial Ergonomics*, 53:19–26, 2016.

[121] Ryan P Blood, Jack Dennerlein, Charlotte Lewis, Patrik Rynell, and Peter W Johnson. Evaluating whole-body vibration reduction by comparison of active and passive suspension seats in semi-trucks. In *Proceedings of the Human Factors and Ergonomics Society Annual Meeting*, volume 55, pages 1750–1754. SAGE Publications Sage CA: Los Angeles, CA, 2011.